IDENTIFYING OPTIMUM CONDITIONS FOR STABLE WORMHOLES CREATED BY CHELATING AGENTS

BY

ASSAD AHMED ABDALLAH BARRI

A Thesis Presented to the
DEANSHIP OF GRADUATE STUDIES

KING FAHD UNIVERSITY OF PETROLEUM & MINERALS

DHAHRAN, SAUDI ARABIA

In Partial Fulfillment of the
Requirements for the Degree of

MASTER OF SCIENCE

In

PETROLEUM ENGINEERING

MAY 2015

KING FAHD UNIVERSITY OF PETROLEUM & MINERALS

DHAHRAN- 31261, SAUDI ARABIA

DEANSHIP OF GRADUATE STUDIES

This thesis, written by **ASSAD AHMED ABDALLAH BARRI** under the direction of his thesis advisor and approved by his thesis committee, has been presented and accepted by the Dean of Graduate Studies, in partial fulfillment of the requirements for the degree of **MASTER OF SCIENCE IN PETROLEUM ENGINEERING.**

M. Mahmoud

Dr. Mohamed A. Mahmoud
(Advisor)

Dr. Abdulla S. Sultan
Department Chairman

Dr. Abdulla S. Sultan
(Member)

Dr. Salam A. Zummo
Dean of Graduate Studies

Dr. Ibnelwaleed A. Hussein
(Member)

2/6/15

Date

This work is dedicated to my parents, my wife, my daughter and all my extended family

ACKNOWLEDGMENTS

Glory and praise to Allah the Almighty, for every success l made in my life and knowledge been developed throughout my master thesis study and especially my research work.

I would like to acknowledge the scholarship given by King Fahd University of Petroleum and Minerals and giving me this opportunity to pursue and complete my master degree in petroleum engineering. Also l would like to thank King Abdulaziz City for Science and Technology for funding my research work.

My sincere gratitude goes to my thesis advisor Dr. Mohamed A. Mahmoud for allowing me to be part of his research group and for the trust he put on me. I also would like to acknowledge his professional guidance during the course of my thesis work. I would like to extend my thanks to Dr. Ibnelwaleed A. Hussein and Dr. Abdulla S. Sultan for their valuable comments and contribution.

I would like to thank the department of Petroleum Engineering for allowing me to use the department's laboratories and equipment and the help received from laboratory technicians. I would like to express my thanks to the Center for Petroleum and Minerals for the help that l received during my research work.

I wish to express my love to my beloved parents, my wife, and my daughter; for their understanding and endless support and love they have shown throughout my study.

TABLE OF CONTENTS

LIST OF TABLES

LIST OF FIGURES

LIST OF ABBREVIATIONS

AC	:	Austin Chalk
API	:	American petroleum institute
Ca	:	Calcium ion
CDTA	:	1,2-cyclohexanediaminetetraacetic acid
cp	:	Centipoise
CT	:	Computer Tomography
DI	:	Deionized water
DTPA	:	Diethylenetriaminepentaacetic acid
E	:	Young Modulus
EDTA	:	Ethylenediaminetriacetic acid
G	:	Shear Modulus
GLDA	:	L-glutamineacid -, N-diacetic acid
HCl	:	Hydrochloric acid
HEDTA	:	Hydroxyl ethylenediaminetriacetic acid
HEIDA	:	Hydroxyethyliminodiacetic acid
IL	:	Indiana Limestone

K	:	Bulk Modulus
KCl	:	Potassium Chloride
M	:	Molarity
MW	:	Molecular weight
NDp	:	Normalized pressure drop
NMR	:	None magnetic resonance
NPVs	:	Normalized pore volumes
NTA	:	Nitrilotriacetic acid
pH	:	Power of hydrogen
PVs	:	Pore volumes
SW	:	Sea water
WH	:	Wormhole

ABSTRACT

Full Name : [Assad Ahmed Abdallah Barri]

Thesis Title : [Identifying Optimum Conditions for Stable Wormholes Created by Chelating Agents]

Major Field : [Petroleum Engineering]

Date of Degree: [May 2015]

Acidizing of carbonate formations is a common practice to reduce the formation damage near the wellbore. In fact, acid stimulation removes the damage created by the drilling and completion fluids and also creates channels (wormholes) that can bypass the damaged area. In this process, acidic solution is injected to dissolve part of the rock matrix and creates conductive channels that facilitate the flow of hydrocarbons to the wellbore. Recently, researchers investigated the usefulness of chelating agents as stand-alone stimulation fluids to create wormholes in carbonate reservoirs. They showed that chelating agents can effectively be used as stimulation fluids especially in the cases of high temperature and low injection rate situations.

This research targets the use of different types of chelating agents at different formulations as stimulation fluids for carbonate rocks. The optimum pH and concentration values of each solution will be screened to determine the optimum pH and concentration as a base of each solution based on solubility tests. Deionized water and sea water will be used for stimulation fluids preparation. Carbonate rocks will be stimulated using chelating agents such as ethylenediaminetetraacetic acid (EDTA), diethylenetriaminepentaacetic acid (DTPA), and hydroxyethylenediaminetriacetic acid (HEDTA) to investigate their performance in

creating stable and efficient wormholes. The wormholes will be evaluated after stimulation using CT scan, NMR, and acoustic measurements to assess the rock integrity. This study will provide a detailed description to the performance of these chelating agents in creating stable wormholes. Viscosity of chelates will be measured at different temperatures and different amounts of Calcium ions to establish their relation. At the end, wormhole growth propagation with chelating agents will be modeled by matching the actual pressure drop versus the pore volume injected using the existing models to test their applicability, and apply the necessary modifications to the existing models to obtain the best match.

Solubility screening studies showed that DTPA and HEDTA chelating agents were soluble at pH values as low as 2.0 in all chelant concentrations prepared by deionized water and sea water. EDTA was not soluble at pH values less than 5.0 when sea water was used for dilution. None of the studied chelating was found to be suitable as iron control agent to be added to 20% HCl acid when sea water was used for mixing. 5% DTPA and HEDTA chelating agents were found to be good iron control agents for 20% HCl acid. Core flooding studies showed that the optimum injection rate for the chelating agents was in the range of 1.5 – 2.0 cc/m when both minimum chelant volume and minimum experiment time were used in determinations. Studies on the rock elastic properties revealed that chelating agents have negligible effect on relatively strong carbonate rocks such as Indiana Limestone, whereas, less strong rocks such as Austin Chalk can be highly affected by injecting chelating agents.

ملخص الرسالة

الاسم الكامل: أسعد أحمد عبدالله بري

عنوان الرسالة: تحديد الظروف المثلى لتكوين الثقوب الدودية باستعمال المركبات المخلبية

التخصص: هندسة البترول

تاريخ الدرجة العلمية: مايو2015

من المعلوم أن استعمال المركبات الحمضية لانعاش الصخور الكربونية من الامور الشائعة لتقليل الاضرار في المنطقة قرب بئر النفط. في حقيقة الامر ان أستعمال الاحماض يزيل التضررات الناتجة عن سوائل الحفر و سوائل الاكمال, و ايضا تكوين ثقوب وقنوات داخل الصخر الكربوني مما يمكن النفط من عبور تلك الطبقات المتضررة. خلال عملية الانعاش هذه تقوم السوائل الحمضية باذابة جزء من الصخر لتكوين قنوات فعالة تقوم بتسهيل انسياب المواد الهيدروكربونية. حديثا قام الباحثون ببحث مدي فائدة المركبات المخلبية كسوائل انعاش. بعض الابحات اثبتت فاعلية بعض هذه المركبات كسوائل انعاش خصوصا في الظروف ذات درجات الحرارة العالية والتي تتطلب معدلات حقن قليلة لسوائل الانعاش.

هذا البحث يستهدف استخدام مركبات مخلبية مختلفة بتركيبات مختلفة كسوائل انعاش. وسط المحلول الافضل سواء حمضى أو قلوي وتراكيز هذه المحلولات المثلى سيتم البحث عنها على اساس أختبارات الذوبانية. سوف يتم استخدام الماء عديم الايونات وماء البحر لتخضير تلك المركبات. أيضا سيتم أختيار بعض الصخور الكربونية ليتم انعاشها بواسطة تلك المركبات المخلبية لتحديد اداء كل واحد علي حدا في تكوين تلك الثقوب الدودية الفعالة. سيتم تقييم تلك الثقوب بواسطة الاشعة المقطعية, الرنين المغنطيسي, والقياسات الصوتية للتأكد من سلامة وتماسك الصخر بعدعملية الانعاش. ستعطي هذه الدراسة وصفا مفصلا لأداء هذه المركبات المخلبية في تكوين ثقوب وقنوات مثلى. سيتم أيضا قياس كثافة ولزوجة تلك المركبات في درجات حرارة مختلفة ونسب مختلفة من عنصر الكالسيوم المذاب في المحلول. في النهاية, سيتم نمذجة نمو الثقب الدودي عن طريق مطابقة الهبوط الضغطي مع الحجم الذي تم حقنه

داخل الصخر بأستعمال النماذج المتوفرة. سيتم أيضا ادخال التعديلات اللازمة للنماذج المتوفرة حتى يتسنى الحصول علي افضل مطابقة.

التجارب التي اجريت علي المركبات المخلبية فيمايخص الذوبانية خلصت الى ان مركبي DTPA وHEDTA ذائبين في الاوساط الحمضية حتى درجة حموضة 2.0. مركب EDTA غير ذائب في الاوساط الحمضية أقل من 5.0 عندما يتم تحضير المركب بواسطة ماء البحر. لا يوجد واحد من المركبات المخلبية مناسب للاستعمال للتحكم في ايونات الحديد ليتم استخدامه واضافته لحمض الهيدروكلوريك بتركيز 20% عندما يستخدم ماء البحر للخلط. 5% من مركبي DTPA و HEDTA أعطت أفضل النتائج للتحكم بأيونات الحديد عند اضافتها لحمض الهيدروكلوريك بنسبة 20%. دراسات تجارب الانعاش أثبتت أن أفضل معدل حقن في حدود 1.5 الي 2.0 مل/دقيقة بأخذ الحجم الاقل والزمن الاقل بعين الاعتبار. دراسات مرونة الصخر اثبتت أن المركبات المخلبية لها تأثير ضئيل بالنسبة للصخور الصلبة نوعا ما. أما بالنسبة للصخور الاقل صلابة من الممكن أن تتأثر بحقن هذه المركبات

.

CHAPTER 1

INTRODUCTION

1.1 Overview

Formation damage, which occurred because of drilling, completion, and accumulation of fines during production are common problems that cause decline in hydrocarbon productivity. Thus, carbonate rocks are commonly acidized to reduce the formation damage near the wellbore. In this process, an acidic solution is injected into the formation to dissolve some of the rock creating conducting channels called wormholes. These wormholes play as an easy path for the hydrocarbons to the wellbore [1, 2].

1.2 Significance of this Research

There are lot of theoretical and experimental works have been done to understand the wormholing process using different treatment fluids. These experiments showed that various types of dissolution patterns are formed based on the combined effect of acid transport, reaction kinetics, rock mineralogy and rock heterogeneity. As an example, at low injection rates, chemical reaction dominates the other effects; so the whole rock face is dissolved which forms face dissolution pattern. In contrast, the process is convection dominated at high injection rates where acid reaches nearly all parts of the rock, which forms a uniform dissolution pattern. In between of these two extremes, conical, wormhole

and ramified dissolutions are formed. Figure 1.1 shows the different types of dissolution patterns.

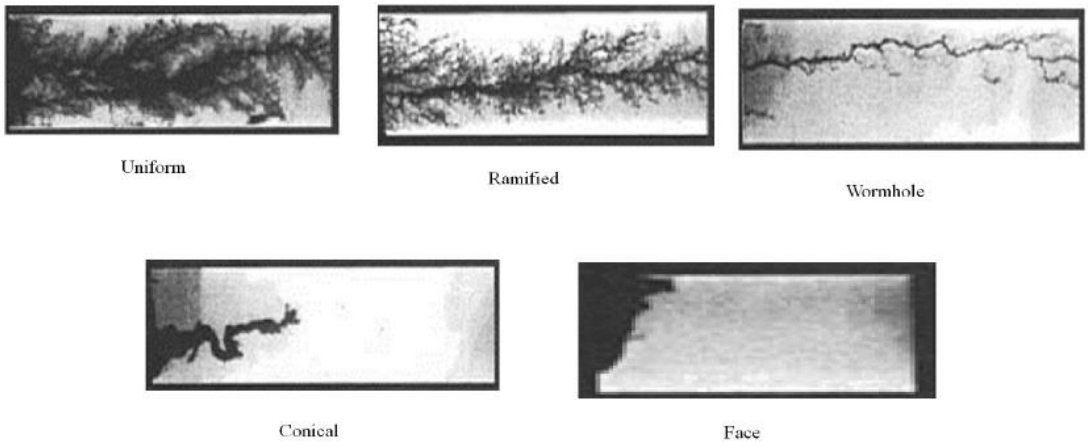

Figure 1.1: Dissolution Pattern

Hydrochloric acid (HCl) is one of the early acids used in carbonate reservoirs acidizing to remove the near wellbore damage. This acid is strong acid that destabilizes the micelles causing precipitations of sludge, which were found a strong function of acid concentration. Also ferric hydroxide precipitation due to steel corrosion was found to be another problem of HCl acid. Formation of these sludges may result on partial or total plugging of formation pores which is difficult to be removed [3]. Many additives should be added in order to eliminate asphaltic sludge precipitations such as corrosion inhibitors, anti-sludge agents and iron control agents.

The major challenges associated with the conventional strong acidic solutions are the corrosive behavior of well tubulars and increase of the reaction rate at high temperature. Addition to that, due to the heterogeneity of some formations, the injected acid will flow into the areas of highly permeable zones which leads to an increase in flow and reaction in that area bypassing the low permeable zones. This action will lead to insufficient

stimulation of the damaged intervals. Also the optimum injection rate is one of the issues for HCl acid stimulation especially in shallow formations that have low fracture pressure.

1.3 Statement of the Problem

Different acidic solutions have been proposed to reduce the problems associated with strong acids. Acid systems based on weak acids, such as formic, acetic, and carboxylic acids have lower hydrogen ions concentration than that of HCl and will have a slower reaction with calcium carbonate [4]**.** The retarded acids were also used to reduce HCl diffusion to the rock surface. An example of these systems is HCl emulsified in oil phase, which reduces diffusion of HCl to the surface of carbonate, and hence allows deep penetration of acid.

Current studies proposed the use of different chelating agents as alternative stimulation fluids in cases where HCl cannot be used. Chelating agents like ethylenediaminetriacetic acid (EDTA), hydroxylethylenediaminetriacetic acid (HEDTA), and L-glutamineacid -, and N-diacetic acid (GLDA) have been recently investigated to stimulate carbonate rocks. These chelating agents have many benefits such as low reaction rate as well as low corrosion.

Matrix treatments of carbonate reservoirs are frequently conducted to remove near wellbore damage and create channels that can improve the productivity of the well. Many laboratory and theoretical researches were done in carbonate rocks to predict the optimum injection rate to maximize stimulation benefits. EDTA and HEDTA chelating agent's solubility and stability with sea water were not deeply investigated. Also their viscosity as function of calcium amount at different temperatures was not studied.

Furthermore, the effect of stimulation with these chelates on the area around the wellbore was not examined.

1.4 Thesis Objective

Objectives of this research are as follow:

1. Identify the compatible pH and optimum concentration for EDTA, HEDTA, and DTPA chelating agents using deionized water and sea water.
2. Measure density and viscosity of chelates as function of temperature and calcium ions in the solution.
3. Perform matrix stimulation treatments using different chelating agent formulations at different conditions and solution concentrations.
4. Identify the effectiveness of using deionized water and sea water-based solutions on creation and propagation of wormholes in carbonate rocks.
5. Examine the effect of rock integrity alterations around the wormholes after stimulation on the overall integrity of the rock.
6. Test the applicability of the existing wormhole propagation models on simulating the results of the current work.

CHAPTER 2

LITERATURE REVIEW

2.1 Acid Stimulation with HCl and HCl-based Fluids

Well stimulation using acid solutions is a common practice to reduce the skin damage and remove the formation damage near the wellbore. Normally acid dissolves part of the rock and creates small channels called wormholes. These channels play as a pathway to facilitate the flow of hydrocarbons to the wellbore [1]. The ability to achieve increase in hydrocarbon productivity is strongly dependent on the radial distance from wellbore to which stimulation fluid reaches. Due to the fact that acids create a dominants channels or wormholes , stimulation effectiveness is controlled by the extent to which these wormholes propagate deep into the formation [5]. HCl acid reaction with carbonate rocks is governed by the following equations:

$$CaCO_{3(s)} + 2H^{+} \rightarrow {Ca^{2+}}_{(aq)} + {CO_2}_{(aq)} + H_2O \quad (2.1)$$

where calcium ions and carbon dioxide gas will be dissolved in the solution.

Studies showed that there is close dependency of the productivity increase with the radius of stimulated area of the formation. For example, for formations not affected by near-wellbore damage but need to increase its productivity, stimulation must reach a distance of order 10 ft from the wellbore to achieve 100% productivity [6]. This gives a light on the fact that enough amount of live acid must penetrate to that distance to make a change in the permeability. In formations affected by damages near the wellbore, that distance is

smaller. Even though, it was recognized that formation damage radius greater than 1 to 3 ft from the wellbore in carbonate formations is generally cannot be removed by HCl acid treatment. This is simply due to the fact that HCl acid is completely consumed before significant penetration is achieved where dissolution rate is rapid.

Experimental studies showed that the various types of dissolution patterns formed based on combined effects of acid propagation, reaction kinetics, and rock heterogeneity [1]. For example, face dissolution pattern formed when injection rate is low where acid reaction with formation dominates the other effects. In contrast, at high injection rate, the process is convection dominated that allows the acid to reach nearly all parts of the rock, which forms a uniform dissolution pattern. In between of these two extremes, conical, wormhole and ramified dissolution are formed. Taylor and Nasr-El-Din in 2007 did experiments on rotating disk to determine the reaction of calcite rocks and HCl acid to determine the reaction rate of HCl acid with calcite rocks [7]. He found that the rate-determining step is the slowest step. Based on that, the reaction will be mass transfer limited when diffusion of the products from and to the rock surface is the slowest step, and surface reaction when the slowest step is surface reaction limited. Also they found that rock minerals have significant effect on acid stimulation especially clay content which can significantly reduce the reaction rate even if the clay concentration is as low as 1 wt.%. Qiu at al. in 2013 and 2014 did studies on the effect of diffusion coefficients of HCl acid when reacted with calcite rocks using rotating disk apparatus as well as core flooding system [8, 9]. They found that the produced CO_2 impacted the diffusion coefficient which found to be much lower at high back pressure than that at low back

pressure at the same concentration. They used these new data for developing a 3D wormholing model to predict wormhole morphology and penetration speed.

Stimulation with HCl acid encounters many problems as discussed by many researchers [10-12]. HCl is very corrosive towards well tubulars and any intervention steel tools such as coiled tubing. Due to the fact that few types of tubulars are made of Cr-13, $Cr_2 O_3$ will act as a thin layer coating the walls of the tubulars as a protective layer. At high temperature reservoirs, acid treatments involved CR-based tubulars are real challenge, so additives such as corrosion inhibitors and corrosion inhibitor intensifiers are required to minimize these problems [13]. Another issue for the strong acids is that formation become brittle upon contact with acids and produces large amounts of fine particles which can cause severe damage rather than improving the well performance [14].

Many researchers studied mixing HCl acid with other fluids to overcome some of the disadvantages of using HCl alone. Nasr-El-din et al. studied HCl/Formic acid formulation to stimulate deep gas wells in Khuff carbonate formations, Saudi Arabia [15]. They conducted lab tests to determine the best HCl/formic acid formulation. A gelled 15 wt.% HCl/9 wt.% Formic acids system was found to be the good formulation in acid fracturing of deep vertical sour gas wells. Field tests resulted in increasing of production by a factor of 2.2 with no operational problems while mixing or injecting the acid.

He and his research group investigated the formation damage occurred when mixing HCl acid with seawater especially in the offshore where fresh water is logistically difficult to be secured for stimulation operations [16]. They concluded that calcium sulphate remains in the core sample when it saturated with seawater, when either HCl is prepared from

seawater or deionized water. But they found that injection with high rates overcome the effect of precipitation due to creation of the wormhole.

The above mentioned problems demonstrated the need of alternative fluids which can combine stimulation ability at low stimulation rates with fluids that are not conductive to asphaltic sludge precipitations or corrosion problems. On top of that, these stimulation fluids need to be environmentally friendly and the flow back fluids can easily be disposed later.

2.2 Organic Acid-Based Solutions

Organic acids such as acetic, citric, formic & lactic acids have been historically used in oil industry as iron-control agents. They are commonly used to prevent iron precipitations in the spent HCl acid and prevent precipitation of ferric hydroxide and iron sulphide [6, 17-20]. During the treatment of the oil and gas wells with mineral acids like HCl, there is high potential of precipitations such as asphaltene sludges. But with the weak reaction of organic acid-based solutions, the amount of these precipitates can be reduced significantly [21]. That is why lot of studies have been done to determine the benefits that can be achieved by using organic acid as a stimulation solution.

Investigation done by Metcalf & Parker in 2005 on acetic acids concluded that at pH ranges between 2.3 to 2.9, dissolution was limited by mass transfer. However, the dissolution rate was lower than the expected [21]. Also it was found that at pH greater than 3.7, the major effect on the dissolution was the surface reaction rate. In their experiments on calcite formations, they concluded that reducing the injection rate of the acetic acid from 20 to 5 ml/mins enhanced the dilution of the carbonate rocks.

T. Huang et al. in 2000 investigated the efficiency of using acetic acid in wormholing core samples from Indiana Limestone cores have 1” size and 6” length at room temperature [22]. These cores have average porosities of 0.16 and permeabilities of 4.8 to 14.5 md. The selected acetic acid concentration was 1.96 N (11.6%) that has pH of 2 and a volumetric dissolving power of 0.036. Their experiments concluded that the optimum injection rate is lower than that of experiments reported by Wang et al. in 1993 with HCl at similar treatment conditions. Also they observed that larger amount of wormholes were created at the optimal flux when compared to HCl. From their experiments they calculated the minimum radius of the wormholes that is sufficient to give a zero skin is estimated to 0.1 mm. But based on their experiments, they preferred to use HCl at low temperature due to its reasonable reaction rate.

Nasr-El-Din et al. studied in their work the use of a chloride-free acids such as acetic and emulsified acetic acid, and later they tested the effectiveness of acetic acid in stimulating carbonate formation of Shu'aiba in Saudi Arabia [23]. Rock tests of this formation indicated that it is mechanically weak, and it can become brittle when contacted by acids, and produces large amount of solids that can cause severe damage. Their lab tests concluded that acetic acid reaction rate with rocks can be reduced by emulsifying the acid in diesel. Also they concluded that both regular and emulsified acetic acids formed narrow and deep wormholes inside core, and hence they resulted in significant increase in the rock permeability. In contrast, field results with emulsified acetic acid were below expectations, mainly because of the weak nature of the formation and production of solids. Regular acetic acid removed the damage in all the treated wells with significant increase in oil production. The field tests showed that acetic acid did not completely

spend in the formations that have temperature of 180^{o} F. Their study concluded that the well productivity was a strong function of the lithofacies distribution of the formation (chalk versus packstone).

Citric and formic acids were introduced as stimulation fluids as an alternative to strong acids to be used in high temperature reservoirs. These acids can also be used in an encapsulated form, which prevents their reaction with bore-hole tubular and formations up to 180^{o} F [7]. The important findings of the lab tests is that the reaction of citric and formic acids with calcite rocks form calcium citrate and calcium formate precipitations that have a significant effect on the effective diffusion coefficient of citric acid especially at high concentrations [24, 25]. Rabie et al. (2011) studied the different reaction regimes of lactic acid in order to understand the reaction kinetics of lactic acid with calcite rocks. They found that at low temperatures, the reaction kinetics was mainly controlled by the kinetics of the surface reaction, whereas, at high temperatures both the mass transfer and the surface reaction influenced the dissolution rate of calcite [26].

Due to the difference in reaction with calcite between organic acids and HCl, models developed for HCl/calcite need to be modified for organic acids. Buijse et al. (2004) presented a new model that can be used for strong and weak acids by introducing a new element of dissociation constant that describes the difference between strong and weak acids. He found that low reactivity of organic acids resulted in deeper penetration; which explained the increase in the etched observed in acid fracturing treatments with organic acids [19].

2.3 Chelating Agent Solutions

Due to the fact that the success of matrix acidizing treatments with HCl acid is limited because of rapid acid spending and low injection rates, researchers have investigated other alternative solutions that combine stimulation ability at low injection rate with fluids that are not conductive to asphaltic sludge precipitation or corrosion. Previously, chelating agents were used to remove formation damages caused by drilling and completion fluids, and also scales such as barium sulphate, barium carbonate, calcium carbonate, etc. from the well tubular and also from the surface facility equipment [27-31].

2.3.1 Evolution of Using Chelating Agents in Well Stimulation

Fredd and Fogler in 1996 were the first researchers who investigated the use of chelating agents as stimulation solutions. They investigated the rate of calcite dissolution at different pH values for different types of chelating agents [32]. They introduced ethylenediaminetetraacetic acid (EDTA) as an alternative fluid which is capable of stimulating calcite formations [12]. EDTA stimulates by means of sequestering the metal components of the calcite rocks. The dissolution mechanism is different from HCl acid in which hydrogen ions are not required. EDTA can make stable chelates with metals such as calcium [12, 33].Figure 2.1 shows the structure of EDTA, which can be represented by H_4Y. Aminopolycarboxylic acids undergo a loss of protons in steps to reach the fully ionized form as shown by equations below:

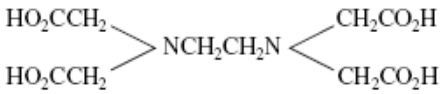

EDTA

Figure 2.1: Chemical Structure of EDTA

$$H_4Y \leftrightarrow H_3Y^{-1} + H^+ \quad (2.2)$$

$$H_3Y \leftrightarrow H_2Y^{-2} + H^+ \quad (2.3)$$

$$H_3Y \leftrightarrow H_1Y^{-3} + H^+ \quad (2.4)$$

$$H_4Y \leftrightarrow Y^{-4} + H^+ \quad (2.5)$$

Fredd and Fogler tested core samples from Indiana limestone and Texas cream chalk in a linear coreflood system. Their laboratory tests were done at room temperature using 0.25M EDTA, and HCl and NaOH were used to adjust the fluid pH. They concluded that EDTA was effective in creating channels in limestone at pH 4-13. They reported also that when increasing injection rate, the number of channels increases. Furthermore, they reported that EDTA is able to create wormholes at low injection rate. Also they observed that trace amounts of sludges to precipitate when oil contacted by EDTA of 6.0 pH due to the ability of EDTA to chelate irons at moderate acidity. They also found that there is no need for corrosion inhibitors for alkaline fluids of EDTA up to 204^o C, and reducing agents are not necessary because EDTA can chelates ferric and ferrous irons a; which can eliminate the need for complex and costly acid additives.

Fredd and Fogler in 1997 extended their works to include other chelating agents of the Aminopolycarboxylic acid group, mainly 1,2-cyclohexanediaminetetraacetic acid

(CDTA) and diethylenetriaminepentaacetic acid (DTPA)[14]. Figure 2.2 shows the chemical structure of CDTA and DTPA. Experiments were performed at room conditions using 0.25M of CDTA, DTPA, EDTA, and 0.5M of HCl acid for comparison. They concluded that CDTA and DTPA have stimulated more efficiently than HCl when injected at low rates. They also observed that the amount of channel branches increase as injection rate increase. Their preliminary rotating disk experiments revealed that the dissolution of calcite by chelating agents is not fully mass transfer limited at 22^{o} C. Also they derived an optimum Damköhler number (which will be discussed later) for all the chelating agents investigated, which is approximately 0.29.

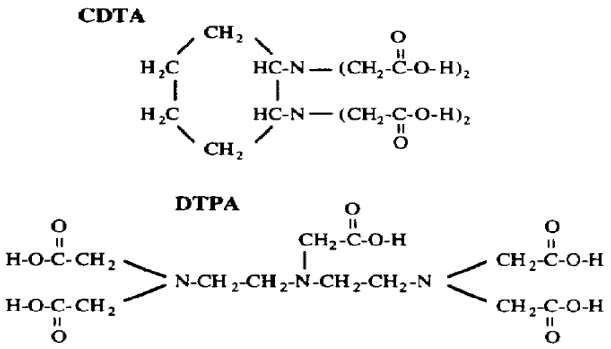

Figure 2.2: Chemical structure of CDTA and DTPA

Frenier et al. in 2001 tested the Hydroxyaminocarboxylic acid (HACA) as stimulation fluid in treating carbonate rocks [11]. They studied hydroxyethylenediaminetriacetic acid (HEDTA) and hydroxyethyliminodiacetic acid (HEIDA) at 150^{o}F. The most significant attribute of these chemicals is the high solubility of the free acids in aqueous solutions. In addition to that, HEIDA is very degradable. Frenier and his group did a core flood experiments in Indiana Limestone rocks. They found that chelating agent formulations based on HACA acids (especially HEDTA) can be formulated into efficient solvents for treating limestone cores, over a wide range of pH values. They observed that dominant

wormholes were formed at temperatures as high as 250^{o}F. Also by using the optimum Damköhler number proposed by Fredd which is 0.29 [34], their predictions of optimum flow rate were close to the observed values of their experiments. The formulated low pH solvents (which include Na_3HEDTA and Na_4HEDTA) appear to be very efficient matrix solutions at high temperatures, and can be inhibited with small amounts of special formulations to produce very low corrosion rates, even at high temperatures.

Husen et al.in 2002 used (EDTA & HEDTA) chelating agent formulations to simulate carbonate and sandstone rocks at high temperature conditions to evaluate the usefulness of these chelates [35]. They found that the reaction rate can be adjusted based on temperature to insure creation of effective wormhole. They reported very low corrosion rates of steel materials; which required less or no corrosion inhibitors. Figure 2.3 shows the chemical structure of the HACA chelating agents

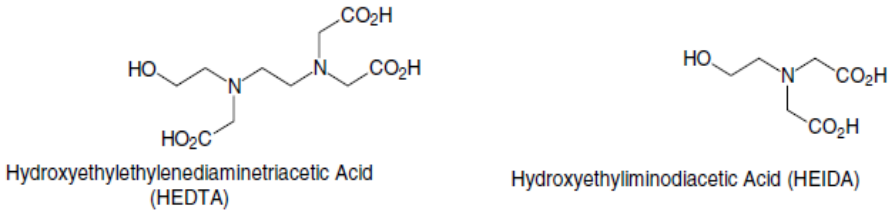

Figure 2.3: Chemical structure of HACA chelating agents

LePage et al. in 2009 studied an environmentally friendly stimulation fluid to be used in high temperature reservoirs [36]. The polyacidic chelate L-glutamic acid, N,N-diacetic acid (GLDA) which is manufactured from L-glutamic acid can dissolve carbonate rocks very effectively, and at the same time has less corrosivity towards the equipment and easy to handle. From an environmental point of view, GLDA is biodegradable and is

made of renewable raw materials - monosodium glutamate, which is less toxic and aquatic toxicity characteristics. Figure 2.4 shows the chemical structure of the GLDA chelating agent.

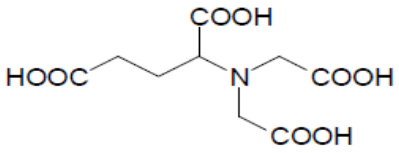

Figure 2.4: Chemical structure of GLDA

LePage et al. conducted a chemical experiments on GLDA as well as EDTA, HEDTA, HEIDA, nirtilotriacetic , Acetic, formic and HCL acids for comparison. Their experiments concluded that GLDA offers high solubility over a wide range of pH and aqueous solutions up to 40%. They found also that the mono sodium salt (pH 3) or free acid (pH 1.5) GLDA offers significant dissolving capacity for calcite. They observed that GLDA is readily biodegradable as compared to other chelating agents.

Mahmoud et al. in 2010 and 2011 conducted comprehensive studies on GLDA chelating agents to define the optimum injection rate for carbonate treatments [4, 33, 37-39]. Indiana limestone and desert pink limestone cores were used in their experiments. Experiments were done at temperatures of 180^{o}, 250^{o} and 300^{o}F. They used GLDA solutions of different pH values (1.7, 3, and 3.8); and de-ionized water was used in preparing the solution to 20% by weight, which was found to be the best concentration of GLDA. Core flooding system was designed to stimulate single and parallel cores. They concluded that GLDA was able to stimulate both parallel and single cores without using diverting agents for permeability up to 6.25 md and temperature up to 200^{o}F. They observed that there was an optimum rate for GLDA to create wormholes at different pH values; and this rate

did not affect by increasing temperature after 180^{o}F. They observed also that increasing the core length decreases the optimum injection rate at the same conditions, but found that it was not a strong function of core length. They found that adding 5% of NaCl to GLDA enhanced its performance during the experiment as less volume of GLDA was required to create a wormhole. They also concluded that as compared to HEDTA and HCL, GLDA performed better at high temperatures, especially at low injection rates as it did not cause face dissolution. Their experiments observed that GLDA was effectively created wormholes in dolomite cores as it chelated both calcium and magnesium.

2.3.2 Effect of Rock Lithology on Stimulation using Chelating Agents

Mahmoud et al. in 2011 did core flood experiments on Limestone and Dolomite rocks to evaluate the effect of lithology of rocks on the GLDA stimulation process [40]. They found a direct relation between the reaction of GLDA and rock lithology as GLDA reacts faster with pure calcite rocks than that have less calcite impurity. Parkinson et al. in 2010 reported a stimulation campaign for carbonate-sandstone formations at different percentages [41]. They did core flooding stimulation experiments with HEDTA chelating agent. Core samples with low and medium percentages of carbonate showed improvement in permeabilities, whereas cores with high carbonate percentages showed evidence of wormholing. Field results confirmed the ability of chelating agents in stimulating such formation types with less corrosion effect. All wells stimulated with chelant based fluids maintained a long-term production results.

2.3.3 Thermal Stability of Chelating Agents

Many researchers examined the stability of chelating agents used in well stimulation at different conditions of temperature [33-38]. Their main objective is to assess the effect of thermal decomposition products on the permeability of carbonate and sandstone rocks. Khatere et al. in 2012 studied the thermal effect on the stability of GLDA, NTA, HEDTA, and EDTA [42]. They concluded that thermal stability is a concern at temperatures greater than 350^{o} F for most of the chelating agents. They found also the decomposition products of the heated chelates are also chelates, which can create damage to the rock due to precipitations. But the overall stimulation process can overcome this damage formed by these precipitations.

2.3.4 Optimum Conditions for Chelating Agent's Injection

Many researches and experiments were done to find the optimum conditions for injecting stimulating fluids for better stimulation results. They found these conditions are function of the rock composition, temperature as well as the pore size. Wang et al. in 1993 found that optimum injection rate varies with rock mineralogy, acid concentration and reaction temperature, but rock mineralogy plays the largest effect on the optimum injection rate [43]. Fredd and Fogler in 1999 extended their researches on the optimum condition by investigating low and medium reaction rate acids as well as strong acids [34]. They reported that the volumes of stimulation fluid to breakthrough and wormhole structures are influenced by the degree of transport/reaction limitations. They also found that there exist an optimum Damköler number at which the minimum number of pore volume required to create an effective wormhole; this number was found to be 0.29 for most of the fluids investigated in their studies as shown in figure 2.5. Mahmoud et al. in 2010 did

extensive studies on an environmentally friendly GLDA chelating agent at different conditions [4]. They confirmed the existence of an optimum injection rate for GLDA at different pH values; which didn't affect by temperature above 180°F to 300°F. They also concluded that creating wormholes are weakly dependent on Damköler number.

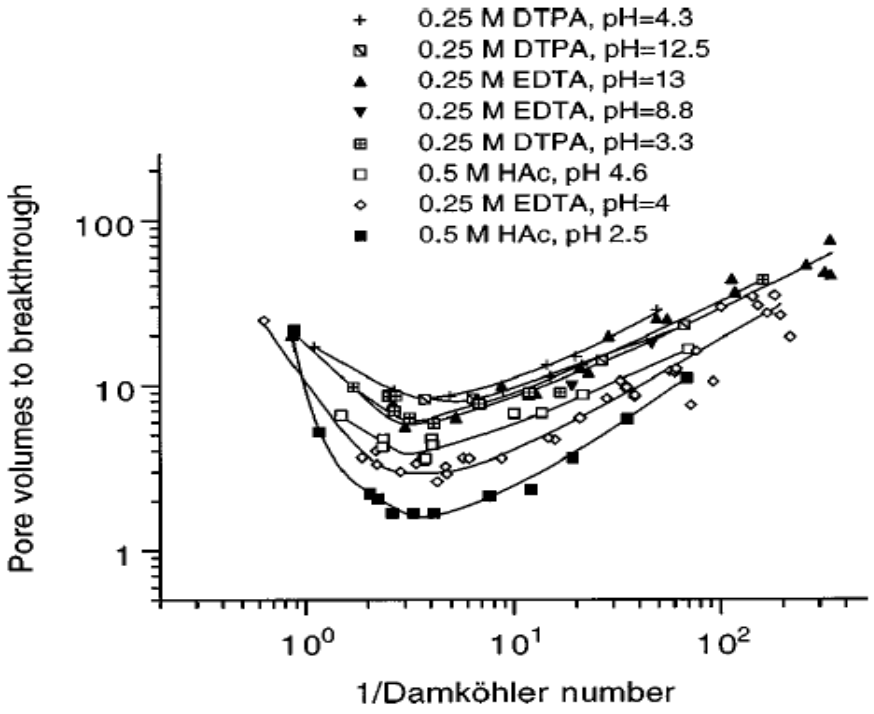

Figure 2.5: Dependency of pore volume at breakthrough to the Damköhler number for different fluids [33]

2.4 Effect of Chelating Agents on the Rock's Mechanical Properties

Rock mechanical properties measurements have become one of the important analysis part in the oil industry for better understanding of rock alterations after well stimulation and EOR operations [44]. Creation of wormholes using stimulation fluids can make changes in the chemical compositions as well as the mechanical properties of the area near the wall of the wormhole. Also stimulation fluids diffusion can further make more changes for the whole area that flushed by these fluids. These changes will be permanent, and at later stages can be areas for well bore failure. That is why the effect of injecting stimulation fluid into the rocks should be examined.

Rock mechanics can be measured using destructive and non-destructive methods. For destructive method, the rock sample will be exposed to stresses. Non-destructive method is done by sending sonic waves through the rock sample, and then elastic properties of the rock can be estimated from the values of sonic velocities. Two types of wave velocities are normally used in elastic properties calculations. Compressional or plastic wave is a wave in which the displacement of the medium is in the same direction as the direction of the travel of the wave. Shear or transverse wave is a wave in which the motion is perpendicular to the direction of wave propagation through the medium. Non-destructive method is the only option in case the same sample needs to be investigated many times, because it will not cause any damage to the sample.

Basic rock mechanical properties have to be determined or estimated using of the above mentioned methods. These properties include compressive and tensile strength, elastic properties such as Young's modulus, shear modulus, bulk modulus and Poisson's ratio

[45]. Rock Young's modulus is the stress needed to compress the solid to shorten in a unit strain, and can be estimated by knowing the elastic waves using the following equation:

$$E = \rho\, v_s^2 \left(\frac{3\, v_p^2 - 4\, v_s^2}{v_p^2 - v_s^2}\right) \tag{2.6}$$

Poisson ratio is the measure of the relativity of the expansion in the lateral directions and compression in the direction which the uni-axial compression applies, and is calculated from elastic waves using the following relation:

$$\upsilon = \frac{v_p^2 - 2\, v_s^2}{2\left(v_p^2 - v_s^2\right)} \tag{2.7}$$

Shear modulus describes how difficult it is to deform a cube of the material under applied shearing force, and it is related to Young's modulus and Poisson ratio by the following equation:

$$G = \frac{E}{2(1-\upsilon)} \tag{2.8}$$

The bulk modulus describes the ratio of the pressure applied to the cube to the amount of volume change that the cube undergoes; and is also related to the Young's modulus and Poisson ratio with the following equation:

$$k = \frac{E}{3(1-2\upsilon)} \tag{2.9}$$

where:

E = Young's modulus.

ρ = Rock density.

vp = Rock compressional or plastic wave velocity.

Vs = Rock transverse or shear wave velocity.

υ = Rock Poisson ratio.

G = Rock shear modulus.

k = Rock bulk modulus.

Many studies have been done to establish the relation between the carbonate rock properties such as permeability, porosity, density, etc. and elastic properties. Results stated that it is not easy to find a straight forward relation. For instance, it is found that rocks with a vp of 4100 m/s can have porosities anywhere between 0.12 and 0.43 [41]. Similar observation was found for the other properties, which make the prediction of mechanical properties based on rock properties difficult. Another research team stated that not only the porosity will affect the acoustic velocities in rock, but also the way these pores were formed an/or whether they were primary or secondary porosities [46]. Nguyen and his group did experiments to evaluate the effect of acid gas injection on carbonate rock's geomechanical properties alterations using the destructive method [47]. Their results showed a weakening of both the elastic properties and the strength of their samples due to the chemical alteration. To the best knowledge of the authors, there are no studies done to evaluate the changes on the rock elastic properties as the stimulation fluid is injected.

2.5 Modeling of Matrix Stimulation Treatments

Because the acid injection rate plays an important role in wormhole formation, several experiments and studies have been conducted to determine the influence of various factors such as temperature, acid concentration, reaction rate, acid diffusion coefficient, length of the core, etc. on the optimum injection rate and the minimum number of pore

volumes required for the breakthrough [16, 48]. Traditionally, most of the matrix acidizing models have under-predicted acid stimulation performance due to under-prediction of wormhole penetration and corresponding completion skin factors in vertical wells [39].

Gong and El-Rabaa in 1999 developed a semi-analytical model to predict the wormhole length and the critical injection rate including all the three acidizing dynamics [49]. Huang et al. in 1999 developed a numerical model to predict the wormhole population density using the pressure field around the wormhole [50]. They combined the above model with the wormhole propagation model developed by Hung et al. in 1989 [51] to determine the volume of acid for a certain distance away from the wellbore. They found that for 15% HCl acid, the model predicted about 12 wormholes/ft. Mohan et al. in 2004 developed a numerical averaged model to describe acid stimulation of calcite rocks [52]. Their 2-D model predictions were quantitatively in good agreement with the experiment data, and captured different dissolution regimes.

Buijse and Glabergen in 2005 developed an empirical wormhole growth model [52].According to their model; the wormhole growth rate can be approximated by:

$$v_{wh} = \frac{v_{i,opt}^{1/3}}{PV_{bt}} v_i^{2/3} \left(1 - exp\left(-4\frac{v_i^2}{v_{i,opt}^2}\right)\right)^2 \tag{2.10}$$

$$v_{i,opt} = \frac{Q_{opt}}{A\emptyset} = \frac{4Q_{opt}}{\pi \emptyset d_{core}^2} \tag{2.11}$$

$$v_i = \frac{Q}{A\emptyset} = \frac{4Q}{\pi \emptyset d_{core}^2} \tag{2.12}$$

where $v_{i.opt}$ is the optimum interstitial velocity, cm/min, Q_{opt} is the optimum injection rate, cm^3/min, A is the cross sectional area, cm^2, ϕ is the porosity, v_i is the interstitial velocity,

cm/min, Q is the injection rate, cm^3/min, d_{core} is the core diameter, cm, and PV_{bt} is the pore volume to breakthrough.

All the current models are based on different parameters and dimensionless numbers such as Peclet and Damköhler numbers. Peclet number (N_{pe}), which is generally defined as the ratio of convective to diffusive flux and can be determined using the equation below [7]:

$$N_{pe} = 2.13\ x\ 10^{-8}\frac{q\sqrt{k}}{2\pi r_w L\phi D_e} \tag{2.13}$$

where, q is the injection rate, gal/min, r_w is the wellbore radius, ft, L is the thickness of the stimulated formation, ft, ϕ is the formation porosity, D_e is the acid diffusivity, cm^2/s. The Damköhler number is the ratio of acid reaction rate at the pore wall to the rate of convective acid transport and can be determined using eq. 2.14 [36]:

$$N_{Da} = \frac{\pi d_{wh} L_{wh} \kappa}{Q} \tag{2.14}$$

where, d_{wh} is the diameter of the wormhole, cm, L_{wh} is the length of the wormhole, cm, κ is the overall dissolution rate constant, cm/s, Q is the injection rate, cm^3/s. Damköhler number can be used to determine the optimum conditions of wormhole creation in carbonate acidizing. The overall dissolution rate constant, κ for different fluids (EDTA, DTPA, acetic acid, etc.) can be determined using Eq. 2.15 [34]:

$$\kappa = \frac{1+\frac{1}{\upsilon K_{eq}}}{\frac{1}{k_{cR}}+\frac{1}{\upsilon K_s}+\frac{1}{\upsilon K_{eq} k_{cP}}} \tag{2.15}$$

Where k_{cR} and k_{cP} are the mass-transfer coefficients for reactants and products, respectively, k_s is the surface reaction rate constant, υ is the stoichiometric ratio of

products to reactants, and K_{eq} is the reaction-equilibrium constant. The mass transfer coefficients for reactants and products can be determined from Levich's solution for laminar injection in a tube as follows [4]:

$$k_{c,i} = \frac{1.86 D_{e,i}^{2/3}}{d_{wh}} \left(\frac{4Q}{\pi L_{wh}} \right)^{1/3} \tag{2.16}$$

where $D_{e,i}$ are the effective diffusion coefficients for reactants and products.

The gravimetric dissolving power (β) of any chelating agent can be determined using the following equation:

$$\beta = \frac{MW_{CaCO_3} \cdot \alpha_{CaCO_3}}{MW_{chelate} \cdot \alpha_{chelate}} \tag{2.17}$$

where MW_{CaCO_3} and α_{CaCO_3} are the molecular weight and the stoichiometric coefficient of calcium carbonate, and $MW_{chelate}$ and $\alpha_{chelate}$ are the molecular weight and stoichiometric coefficient of the chelating agent, respectively.

Mahmoud and Nasr El-Din in 2012 showed that the optimum injection rate using Damköhler number of 0.29 can be determined by [39, 53]:

$$Q_{opt} = 102 L_{wh} D_e \tag{2.18}$$

where; L_{wh} is the wormhole length, cm and De is the diffusion coefficient of the stimulation fluid, cm^2/sec. This equation depends only on the wormhole length and the diffusion coefficient; therefore, it can be used for chelating agents and acids. The optimum flux can be determined using the optimum injection rate and flow area of the core as follows [39]:

$$u_{opt} = \frac{130\, L_{wh} D_e}{\phi d_{core}^2} \tag{2.19}$$

They concluded that equation (2.19) gave a good prediction to the optimum injection rate with maximum error of 14% from the measured optimum injection rate when they used 0.25M DTPA chelating agent at pH 4.3 [39]. Their model can be used as a pre-designed tool for matrix acid treatment before the stimulation job, and then validation can be performed after lab experiments using core flood tests to determine the optimum injection rate.

CHAPTER 3

METHODOLOGY AND EXPERIMENTAL PROCEDURES

3.1 Chelating Agents Preparation and Screening

3.1.1 pH Solubility Screening

A pH meter instrument was used to measure the pH of the solutions to check their solubility in deionized water and sea water. Different chelating solutions with different concentrations were prepared by deionized water and sea water. A compatible pH value was identified for each chelating agent based on its solubility. A pH meter is shown in figure 3.1. Procedures were as follows:

1. Raw chelating agent was diluted by deionized water and sea water to prepare solutions at different concentrations.
2. For each concentration, different solutions at different pH value were prepared. pH range of each concentration was identified.

3.1.2 Density and Viscosity Measurements

Density and viscosity of chelating agents were measured at different temperatures, chelants concentrations and calcium concentrations using density hydrometers from Fischer instrument's company and capillary tube viscometer from Koehler instrument company. Figures 3.2 and 3.3 show the liquid density hydrometer and capillary tube viscometer, respectively.

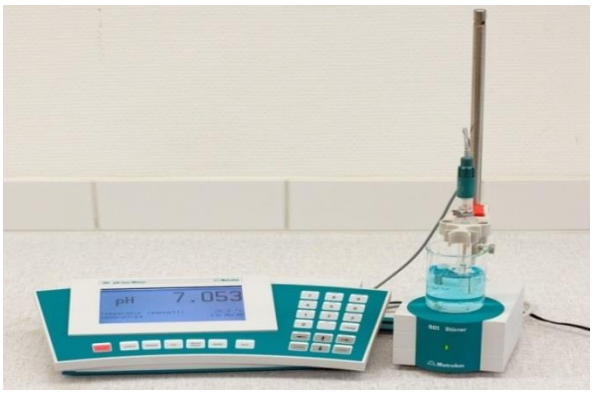

Figure 3.1: pH meter instrument

Figure 3.2: Liquid density hydrometers

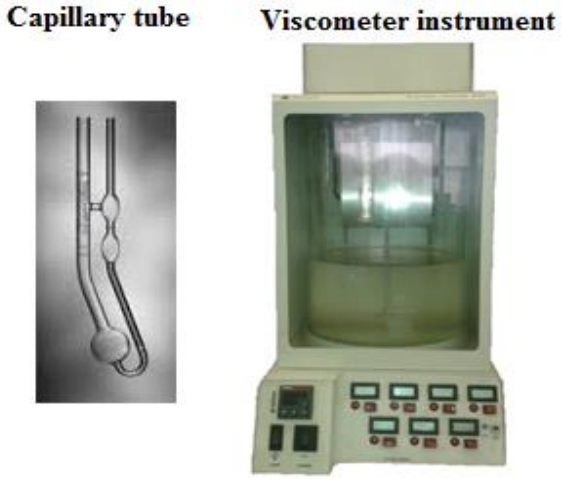

Figure 3.3: Capillary tube viscometer

Measurement procedures were as follows:

1- For any specified chelating agent, the density and viscosity of the solution were measured at different temperatures.
2- Specified concentration of calcium ions were dissolved in the chelating agent, then the density and viscosity were measured at different temperatures.
3- A plot of density and viscosity were plotted versus temperature for each solution.

3.1.3 Interfacial Tension Measurements

Interfacial tension between oil and chelating agent was measured using optical tensiometer from Biolin Scientific Company. Three crudes that have API gravities of 31.18^{o}, 35.6^{o} and 40^{o} were used. Oil droplet was kept in tension with chelating agent for at least 15 minutes to let the reading stabilize. EDTA, HEDTA and GLDA chelating agents were prepared at different concentrations using deionized water for interfacial tension measurements. Figure 3.4 shows the optical tensiometer that was used in this test.

3.2 Core Samples Preparation

A standard carbonate rocks such as Indiana limestone, Austin chalk and pink Desert were used during this research. These rocks have variety of porosity and permeability values. Core sample dimensions were 1.5" in diameter and 2.0 - 6.0" in length. Procedures for core sample preparation were as follows:

1- The core sample was dried first to remove the moisture, and then the weight of the dry core was measured.
2- The core was vacuum saturated using 3% wt. KCl brine, and then the saturated weight was measured.

3- Pore volume and porosity of the core were identified.

4- The core was CT, NMR scanned before stimulation treatments.

5- Core liquid permeability was determined before injecting the chelates by injecting KCl brine at constant rate.

3.3 Core Flooding Experiment Procedure

A core flooding system "AFS-200" from CoreLab^{TM} Company was used for stimulation experiments. The core flooding system has an oven that can heat the core sample up to 300 ^{o}F. Figures 3.5 through 3.9 show the different parts of the core flooding system. The stimulation procedure was as follows:

1- KCl brine and chelating solution were transferred into the specified accumulators.

2- Core sample was inserted into the core holder, and the inlet and outlet of the core holder was tightened against the core sample.

3- Core holder lines were connected to the core flooding system lines.

4- The required temperature was set, and enough time was allowed for the core sample and fluids to be heated up.

5- The required net overburden of 500 psi was applied to insure no flow between the core holder sleeve and the walls of the core sample. A predetermined back-pressure of 1000 psi was also applied to the outlet of the core sample.

6- KCl brine was injected at constant injection rate into the core sample until flow stabilization was reached. Liquid permeability was then estimated using the data of the injection rate and the corresponding pressure drop.

7- After flow stabilization, the chelating solution was injected at specified injection rate, and pressure drop was monitored with time until break-through occurred. Effluents were collected for chemical analysis.

8- Stimulation fluid injection was continued until wormholes were created when pressure drop was almost zero.

9- Stimulation fluid injection was stopped, and KCl brine was injected to flush the core sample from the stimulation fluid.

10- KCl brine injection was stopped and oven was shut down. All the system pressures were released.

11- Core sample was removed from the core holder for further evaluation studies.

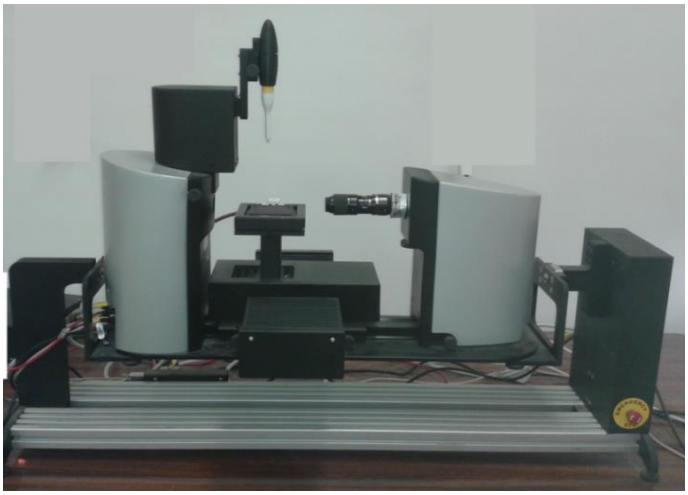

Figure 3.4: Optical tensiometer instrument

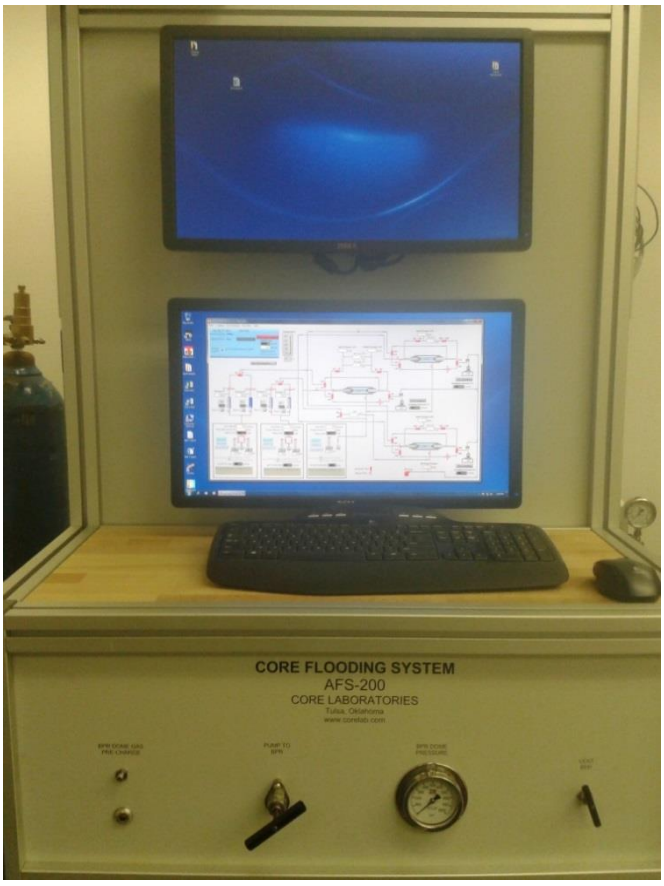

Figure 3.5: Controlling and data monitoring system

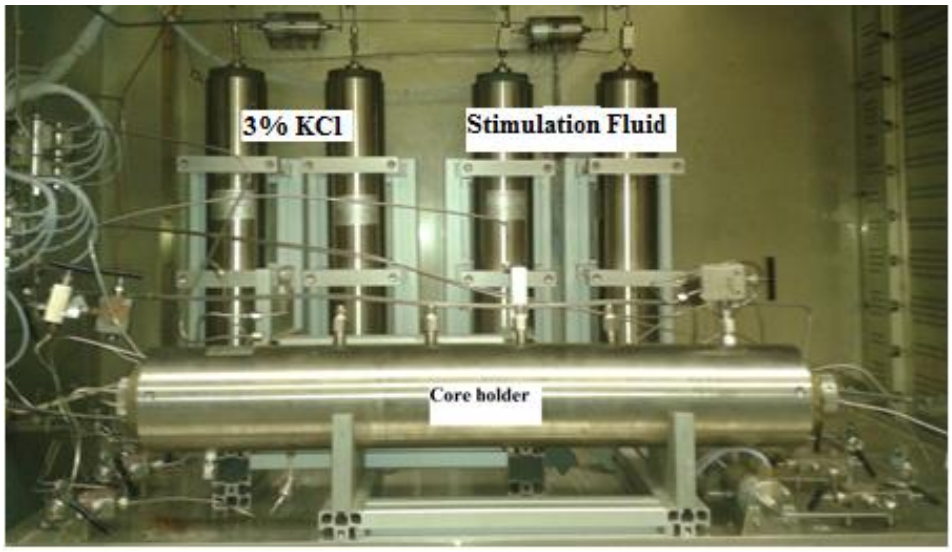

Figure 3.6: Core holder and accumulators

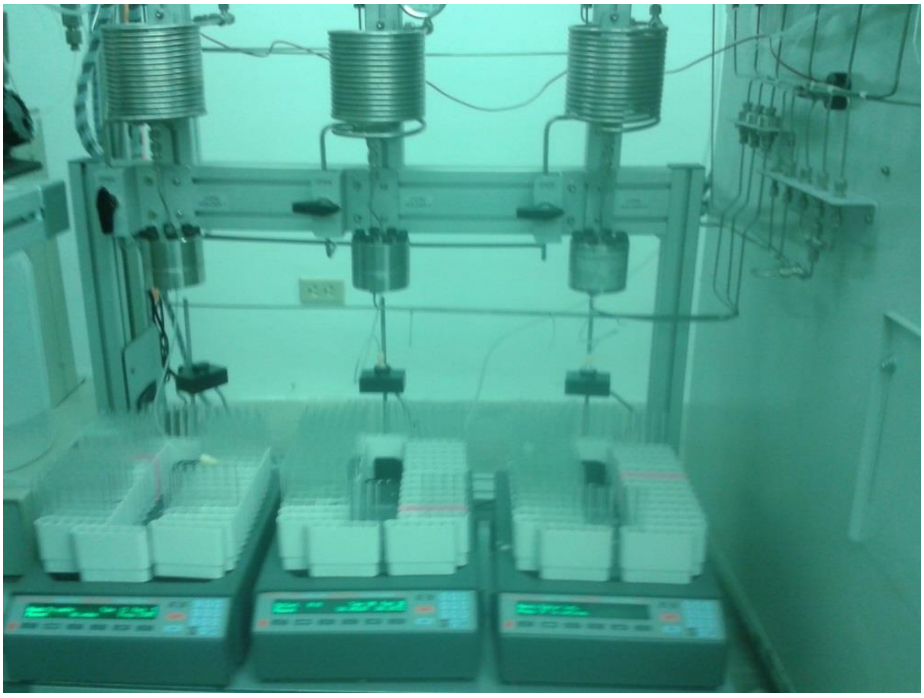

Figure 3.7: Sampling collectors system

Figure 3.8: Transfer pump

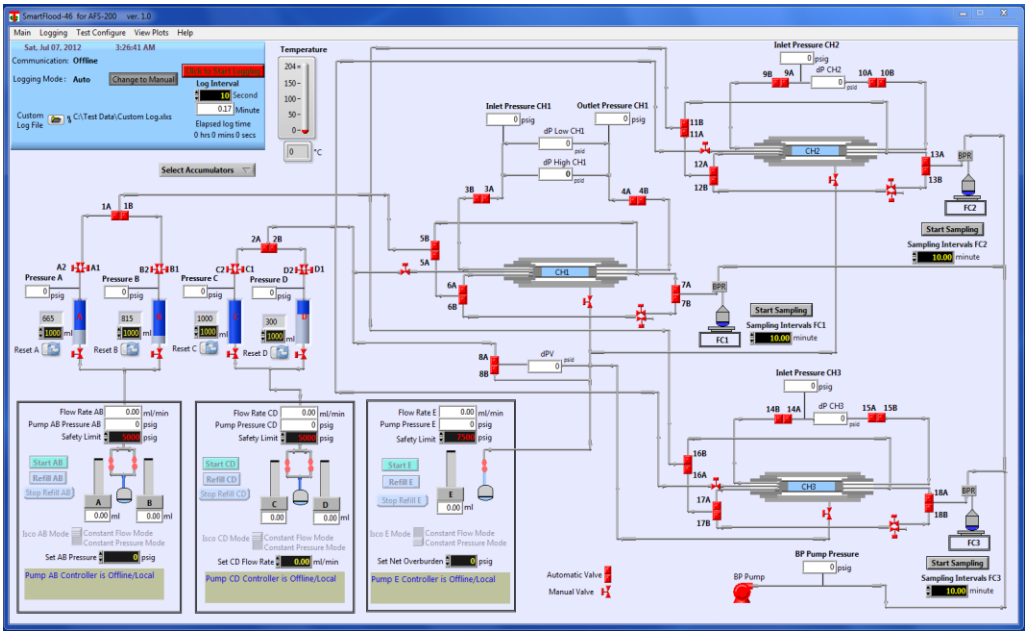

Figure 3.9: Layout of the core flooding software

3.4 Core Sample Post-Stimulation Evaluation

To evaluate the effectiveness of the matrix stimulation with chelating gents, cores need to be scanned before and after the stimulation. The purpose of core scanning is to detect the changes happened to the pores of the core as well as any changes in the mechanical properties of the rock. To do that, the following scanning methods were used:

1. Computed Tomography or CT scan was used to evaluate the diameter and extent of the wormhole inside the core. Figure 3.10 shows the CT scanning instrument.
2. Nuclear Magnetic Resonance or NMR instrument was used to evaluate the changes in pore space of the core sample before and after stimulation. Figure 3.11 shows the NMR instrument.
3. Ultra-sonic velocity measurement system was to evaluate the changes in the rock elastic properties. Figure 3.12 shows the Ultra-sonic velocity measurements instrument.

Figure 3.10: CT scan instrument

Figure 3.11: NMR Instrument

Figure3. 12: Ultra-sonic velocity measurement instrument

CHAPTER 4

SOLUBILITY OF CHELATING AGENTS

4.1 Introduction

Solubility of chelating agents at different pH values and different concentrations in de-ionized water and sea water were not deeply investigated in the literature. That is why it was planned to be conducted for different types of chelating agents. Chelating agents that used in these tests were EDTA, HEDTA, DTPA and GLDA chelating agents. Chelating agent's concentration were estimated based on weight percent, and concentration of the solution were changed using either deionized water or sea water. The pH of the solution was changed using HCl acid and in NaOH pellets. Digital weight indicator as shown in Figure 4.1 was used in measuring the required weight of each solution for concentration calculations. Magnetic stirrer as shown in Figure 4.2 was used to make sure the solution is homogeneous and mixed properly.

HCl acid is frequently used in well stimulation in acid stimulation and also in acid fracturing operations due to its strength in dissolving calcite rocks. The main issue of HCl acid in well stimulation is the corrosion occurred to the tubulars and casing strings during the injection of the acid in the well. Thus, corrosion inhibitors should be used to decrease the corrosion of the tubulars. Ferric ions that dissolved from the tubulars during HCl acid injection can create damages to the carbonate formations when precipitated in the pores of the rocks. Because of that, the dissolved ferric ions need to be in solution in order to be removed later. Chelating agents have good ability to sequester many ions; among them is

the ferric ion. In this study solubility of chelating agents such as GLDA, HEDTA and DTPA as well as organic acids such as acetic and citric acids in HCl acid at different concentrations was investigated. The objective of the study is to find the soluble amount of each fluid separately and mixtures of fluids in a certain HCl acid concentration. Table 4.1 summarizes the information of the chelating agents and HCl acid, acetic and citric acids that were used in this study. Deionized water was used to prepare the specified concentration of each fluid or mixture. Synthetic sea water that has chemical composition similar to Arabian Gulf sea water was used in specific solutions preparation. Table 4.2 shows the chemical composition of the salt of Arabian Gulf Sea.

Table 4.1: Chemical & physical properties of used acids and chelating agents

Solution	Chemical formula	Concentration %wt.	MW gm/mol	pH value	Specific gravity g/cc
HCl acid	HCl	37.0	36.46	0.00	1.19
Acetic acid	$C_2H_4O_2$	99.7	60.05	2.0	1.049
Citric acid	$C_6H_8O_7$	30.0	192.13	1.5	1.124
EDTA	$C_{10}H_{14}N_2Na_2O_8 .2H_2O$	37.0	372.23	7.5	1.22
HEDTA	$C_{10}H_{18}N_2O_7$	41.0	278.26	11.5	1.29
GLDA	$C_9H_{13}NO_8.4Na$	38.0	351.1	11.5	1.26
DTPA	$[(HOOCCH_2)_2NCH_2CH_2]_2 NCH_2COOH$	40.0	393.35	11.5	1.33

Table 4.2: Chemical composition of Arabian Gulf sea water

Substance	Concentration	Concentration
	ppm	g/l
$NaHCO_3$	170	0.17
Na_2SO_4	6,340	6.34
NaCl	41,170	41.17
$CaCl_2$	1,800	1.8
$MgCl_2$	8,270	8.27
Total	57,750	57.75

Figure 4.1: Weight indicator

Figure 4.2: Magnetic stirrer

4.2 Chelating Agents as Stimulation Fluids

To investigate the solubility of each chelating agents at different pH values; different concentrations were prepared from the raw chelating agent. Then from the specified concentration many solutions were prepared representing different solution at different pH values. These solutions were kept in tubes for 24 hours to check the solubility of chelating agents.

4.2.1 Solubility of Chelating Agents in Deionized Water

EDTA-Na_2, HEDTA-Na_3, and DTPA-Na_5 solutions having concentrations of 37%, 41% and 40%; and pH of 7.5, 11.5 and 11.5, respectively were used in this study. Three different solutions of each chelating agent at different concentrations were prepared using deionized water. Figure 4.3 shows the solubility of chelating solutions at different concentrations and different pH values when diluting them by deionized water. From Figure 4.3 it is clear that the solution pH has a big effect on EDTA solubility especially at higher concentrations. For instance, when EDTA concentration diluted to 20% by deionized water, the solution pH should be 6.5 or greater to have a soluble solution. Solution pH does not affect the solubility of HEDTA and DTPA chelating agents as these chelates were soluble at pH values as low as 2 in all concentrations up to 40% by weight. In fact, it was able to prepare solutions from these chelates that have 15% of chelates and 15% HCl acid without any precipitations, and those solutions have pH similar to that of concentrated HCl acid.

4.2.2 Solubility of Chelating Agents in Sea Water

Same chelating agents that were EDTA-Na_2, HEDTA-Na_3, and DTPA-Na_5 having concentration of 37%, 41% and 40%; and pH of 7.5, 11.5 and 11.5, respectively were used in this study. Three different solutions of each chelating agent at different concentrations were prepared using sea water. Figure 4.4 shows the solubility of chelating solutions at different concentrations and different pH values when diluting them by deionized water. From the figure it is clear that solution pH has no effect on the solubility of HEDTA and DTPA chelating agents as they were soluble for all the prepared concentration at pH value as low as 2. EDTA solubility was affected much when sea water was used instead of deionized water. It was not possible to have a soluble solution of EDTA if solution pH is less than 5.4. For EDTA concentrations higher than 20% wt. solution pH must be greater than 7.0 to have soluble solution.

The study also concluded that all the examined chelating agents were soluble in high pH environment with no limitations. All of these chelates were examined pH up to 13 with no precipitations for both cases of deionized water and sea water. From this study, it was clear that only EDTA is not soluble in pH environment as low as 3.0 when prepared by DI-water; and for the case of preparing the solution by sea water, EDTA was soluble only at pH greater than 5.4. So the effect of using sea in preparation was decreasing EDTA solubility especially at high EDTA concentration that forced to change the solution environment from acidic to alkaline environment. Figure 4.5 shows the solubility comparison between the EDTA solutions prepared by deionized water and that prepared by sea water.

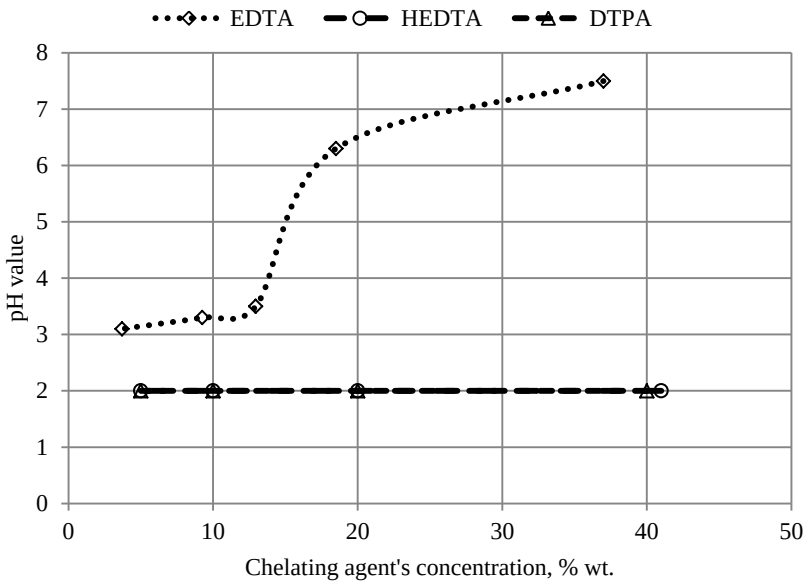

Figure 4.3: Effect of pH on chelating agent's solubility at temperature of 72°F and atmospheric pressure, DI water was used in preparation

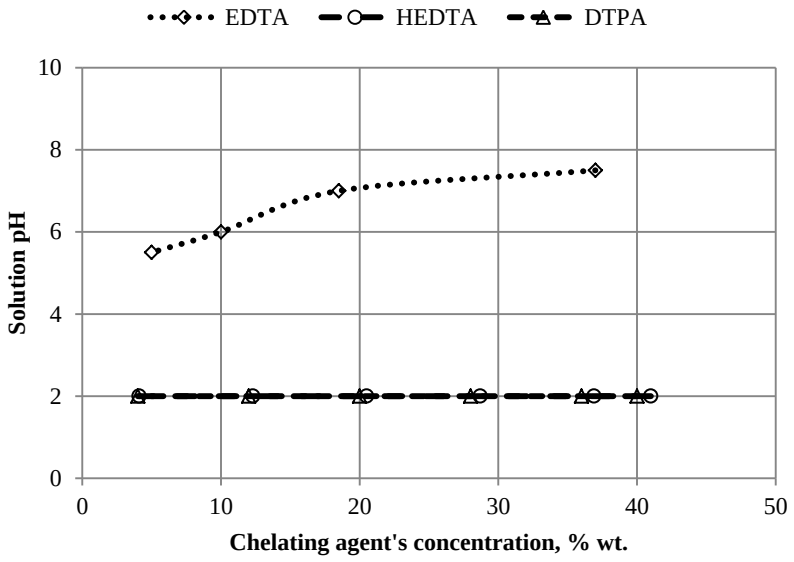

Figure 4.4: Effect of pH on chelating agent's solubility at temperature of 72°F and atmospheric pressure, sea water was used in preparation

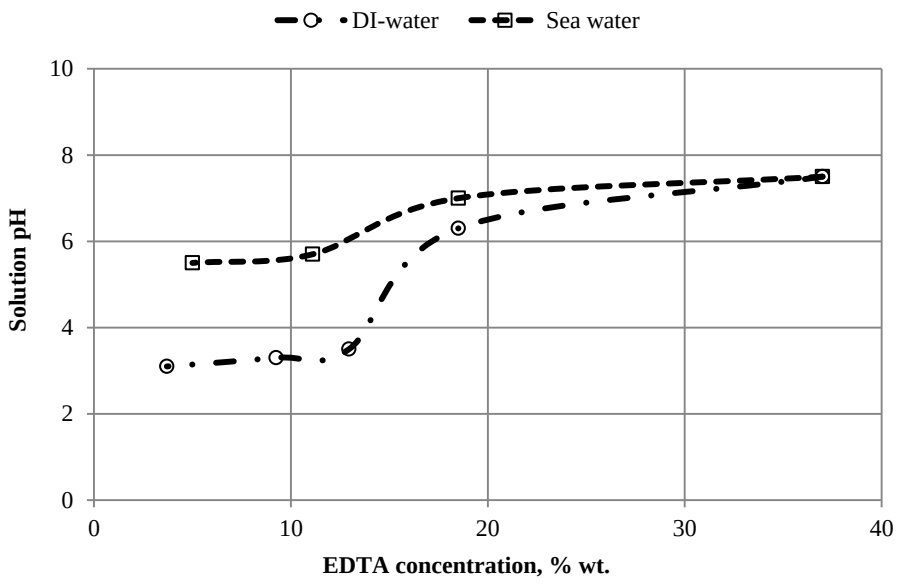

Figure 4.5: EDTA solubility comparison for DI water and sea water at temperature of 72^{o}F and atmospheric pressure

4.3 Chelating Agents as an Iron Control Agent

Due to the fact that iron control problems are frequently encountered while stimulating carbonate formations using strong acids and even weak acids, it is very important to develop an stimulation fluid in such a way that can reduce the damage created by the precipitation of iron compounds [54]. Usually stimulation fluids contain dissolved and entrained oxygen because of the blending. The oxygen in the stimulation fluid immediately oxides the ferrous iron Fe_2 to ferric iron Fe_3. Ferrous iron will remain in the solution for pH as high as 7.5, but the ferric iron will precipitate at a pH as low as 2.5 and completely precipitates at pH of 3.5 [55]. A new laboratory studies done by Taylor et al. in 1998 concluded that ferric compounds can start to precipitate at pH just above 1.0 [56].

Many laboratory studies recommended that it is very important to reduce the amount of ferric compounds in the stimulation fluids before entering the formation to eliminate precipitation of ferric salts especially at high temperature environments. They concluded also that chelating agents such as EDTA, NTA, Iminodiacetic acid (ICA) and DTPA were very effective in stabilizing ferric ions in solution and also reduced the corrosion rate of the tubulars [57-60]. On the other hand, organic acids such as acetic and citric acids were found to be an effective iron control agents. Citric acid was found not effective as an iron control agent at temperatures higher than 200^{o}F [56, 61].

From the above, it was found that chelating agents as well as citric and acetic acids were one of the most effective iron control agents to be added to the HCl acid during stimulation operations. In this study, a solubility screening was done to find out the solubility of HEDTA, GLDA, DTPA, acetic and citric acids in HCl acid at different concentrations.

4.3.1 Solubility of Chelating Agents, Acetic, and Citric Acids in HCl Acid

Solubility of HEDTA, GLDA and DTPA chelating agents as well as acetic and citric acids of different concentrations were examined at HCl acid concentrations of 28%, 20% and 15%. Deionized water and sea water were used to prepare the solutions. Each prepared solution was kept for 48 hours in room condition. Figure 4.6 shows the results of solubility tests done for the above chelating agents and organic acids when diluted by deionized water. For HCl acid concentration less than 20% by weight, all the tested chelating agents were soluble at chelant concentration of 5%. Chelants concentration can be increased as the HCl acid concentration decreased to reach up to15%. DTPA showed better solubility when compared to the other chelants especially at HCl acid concentrations of 20% which HEDTA and GLDA were only soluble at concentrations of 5% and less, whereas DTPA was soluble at concentration of 7.5%. All the tested chelants were not soluble at HCl concentration of 28% wt. Acetic and citric acids were soluble at concentrations up to 10% wt. in all HCl acid concentrations. Figure 4.7 shows the solubility of chelating agents and organic acids when sea water was used for preparing the solutions. All chelates showed similar results except for the case of 20% GLDA which was not soluble in 15% HCl acid. Acetic and citric acids were soluble at concentrations up to10% in all HCl acid concentrations except for acetic acid which was not soluble at any concentration when mixed with 28% HCl acid. From this study, all of the investigated chelates were not suitable as an iron control to be added to 28% HCl when sea water was used in preparation instead of deionized water. For HCl acid concentration of 20%, DTPA was the only chelate that soluble at low concentrations as low as 2.5%. For the case of acetic and citric acids, 10% concentration was used as a

maximum concentration as generally no more than that concentration will be added to the HCl acid as iron control agent.

Mixture of HEDTA and GLDA chelating agents were prepared and mixed with HCl acid at different concentrations to investigate their solubility. The main purpose was to check if there is a difference in solubility conditions than mixing a separate chelate in HCl acid. Results show similar solubility with no big impact. Still there was no solubility of this mixture in high HCl acid concentrations, especially when sea water was used instead of deionized water. Figure 4.8 shows soluble concentrations of these chelates in HCl acid when the solution prepared by deionized water. Figure 4.9 shows an example of the solubility tests done for the case of sea water.

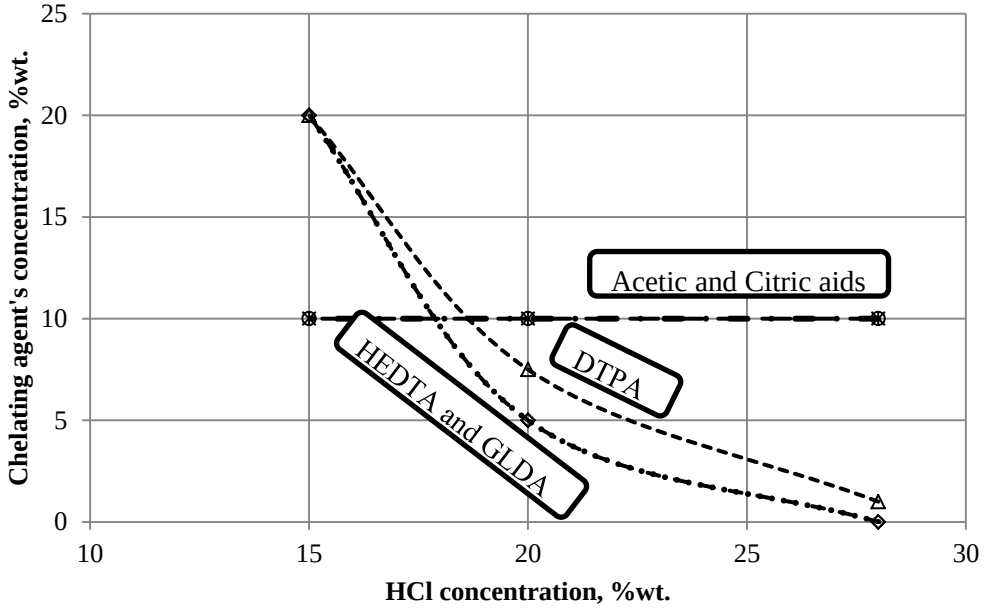

Figure 4.6: Solubility of chelates & organic acids in HCl acid when solutions prepared by DI water at temperature of 72°F and atmospheric pressure

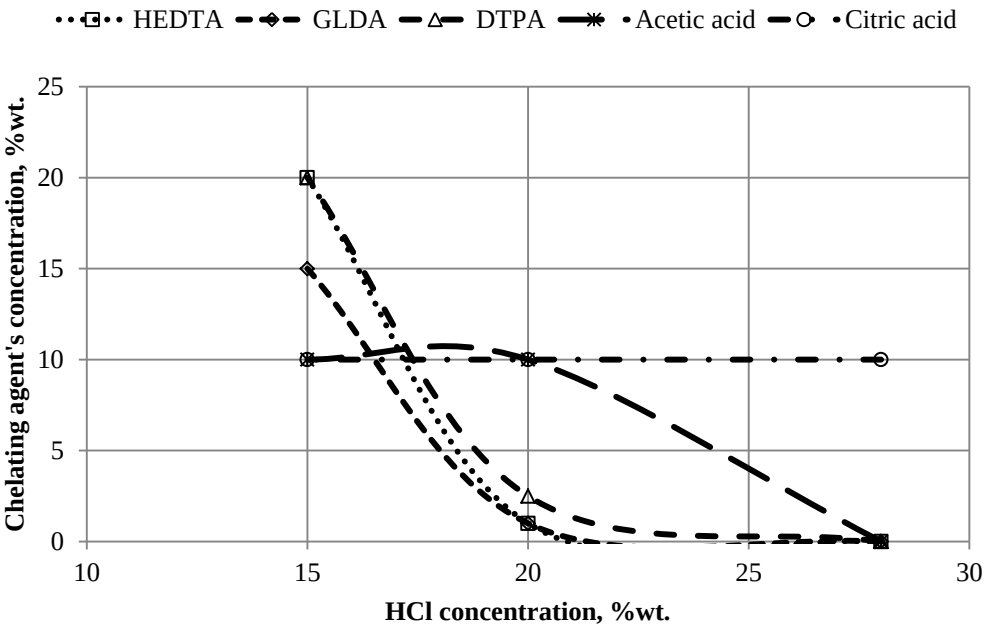

Figure 4.7: Solubility of chelates & organic acids in HCl acid when the solution is prepared by sea water at temperature of 72°F and atmospheric pressure

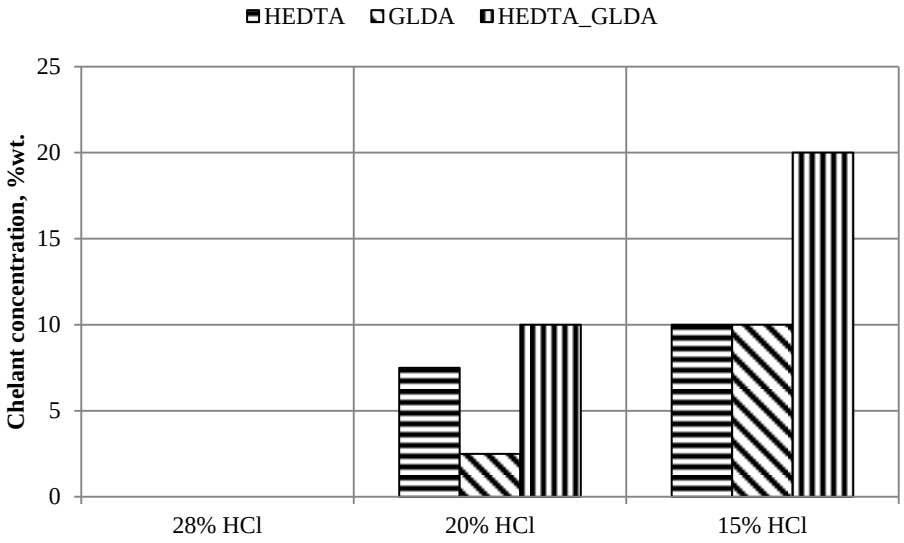

Figure 4.8: Solubility of HEDTA_GLDA mixture in HCl acid when the solutions prepared by DI water at temperature of 72^{o}F and atmospheric pressure

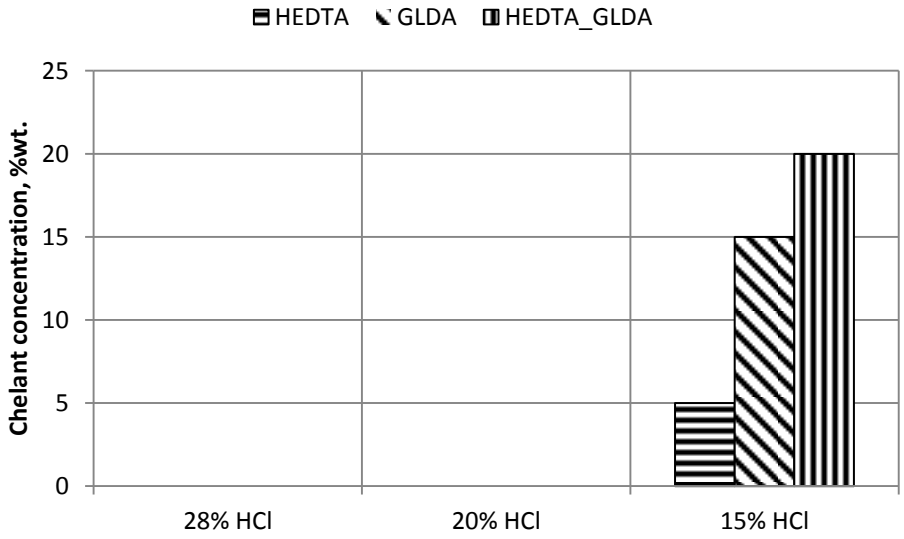

Figure 4.9: Solubility of HEDTA_GLDA mixture in HCl acid when the solutions prepared by sea water at temperature of 72^{o}F and atmospheric pressure

4.3.2 Improving Solubility of Chelating Agents

Acetic and citric acids were used to investigate the ability of improving the solubility of chelating agents in concentrated HCl acid. The focus was on the solutions that have HCl acid concentrations of 20% and 28%. Unfortunately all of the attempts failed to increase the solubility of these chelates. In fact, solubility of these chelates remained as it was after adding 1.0% and 2.5% of acetic and citric acids. Figures 4.10 through 4.12 show some examples of solubility tests by adding acetic/citric acids.

4.3.3 New Formulations for Iron Control Agents

From the screening done for different chelating agents and organic acids mixed with HCl acid at different concentrations, the following formulations were selected to be tested as an iron control agents: 5% HEDTA_20% HCl, 5% GLDA_20% HCl, 5% DTPA_20% HCl and 2.5% acetic acid_2.5% citric acid_20% HCl. A 3000 ppm of ferric ions were added to each of these formulations, and then pH of these solutions was increased in steps to investigate the effectiveness of each iron control agent in keeping ferric ions in solution. All experiments were done at room temperature.

Figures 4.13 through 4.16 show different HCl acid formulations of different concentrations of chelating agents and organic acids as iron control agents. This study showed clearly that 5% of HEDTA and DTPA chelating agents were managed to keep 3000 ppm of ferric ions in solution for pH up to 4.35. Same results were observed for 2.5% acetic acid and 2.5% citric acid which stabilize ferric ions without precipitations for pH up to 4.0. For the case of GLDA chelating agent, brown color precipitations were observed when solution pH was increased to 3.5. This concluded that GLDA can only stabilizes ferric ions at pH environment less than 3.0. Two more experiments were done

for 5% GLDA_20% formulation by adding 1000 ppm and 2000 ppm of ferric ions to investigate the maximum pH before precipitation occurred. For 1000 ppm ferric ions, precipitation occurred when the solution pH was greater than 4.0, and for 2000 ppm ions precipitation occurred when the solution pH increased to 3.4; as can be shown in figures 4.17 and 4.18.

From this study, it was clear that HEDTA and DTPA chelating agents, acetic and citric acids were efficient as iron control agents for HCl acid concentrations up to 20%, as these chemicals successfully kept up to 3000 ppm of ferric ions in solution without any precipitation. GLDA chelating agent has limitations on the amount of ferric ions to be sequestered at pH values greater than 3.0.

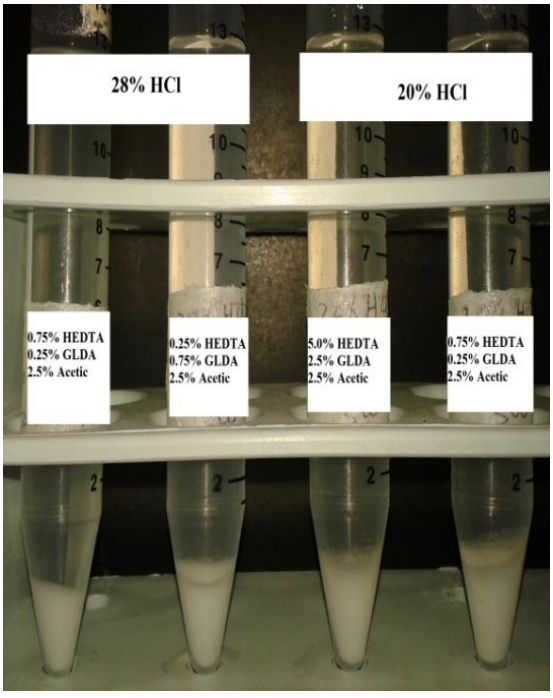

Figure 4.10: Effect of adding acetic acid on solubility of chelating agents at temperature of 72^{o}F

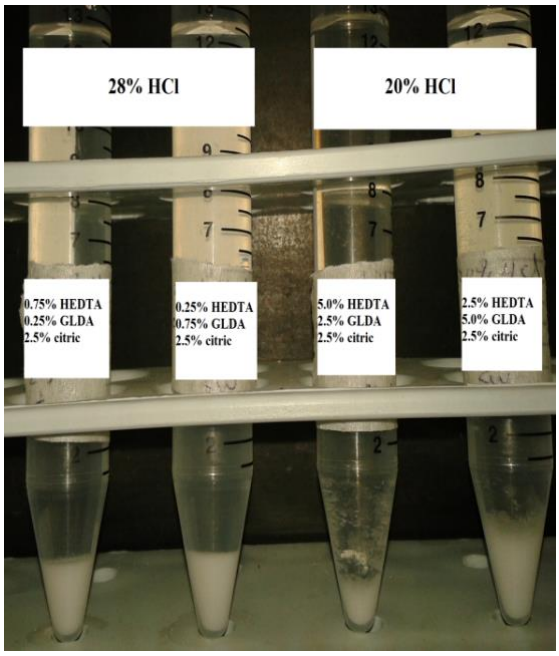

Figure 4.11: Effect of adding citric acid on solubility of chelating agents at temperature of 72^{o}F

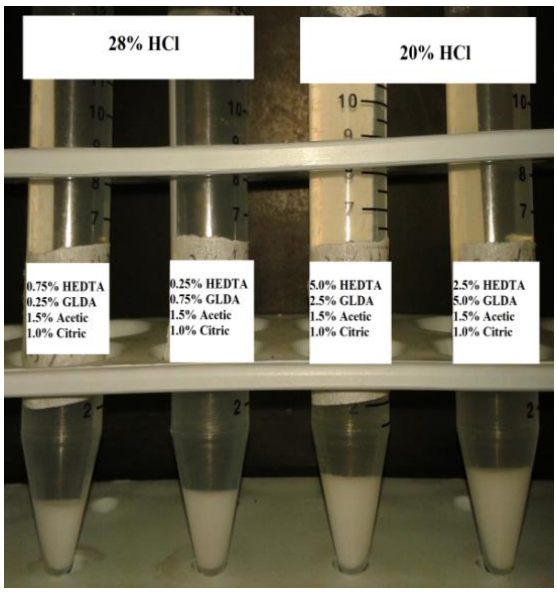

Figure 4.12: Effect of adding acetic and citric acids on solubility of chelating agents at temperature of 72^{o}F

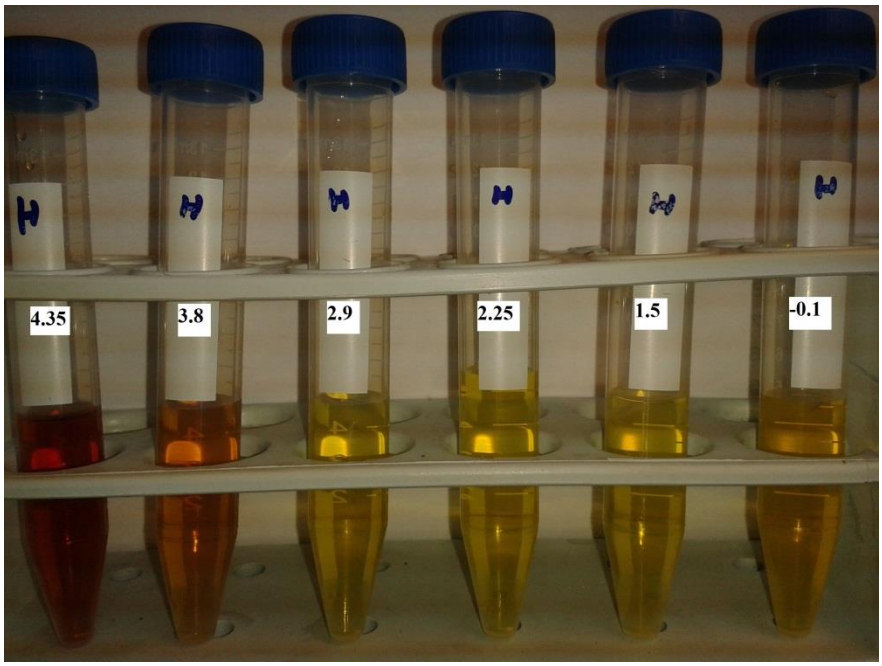

Figure 4.13: 5% HEDTA/20% HCl formulation after adding 3000 ppm ferric ions at different pH at temperature of 72^{o} F

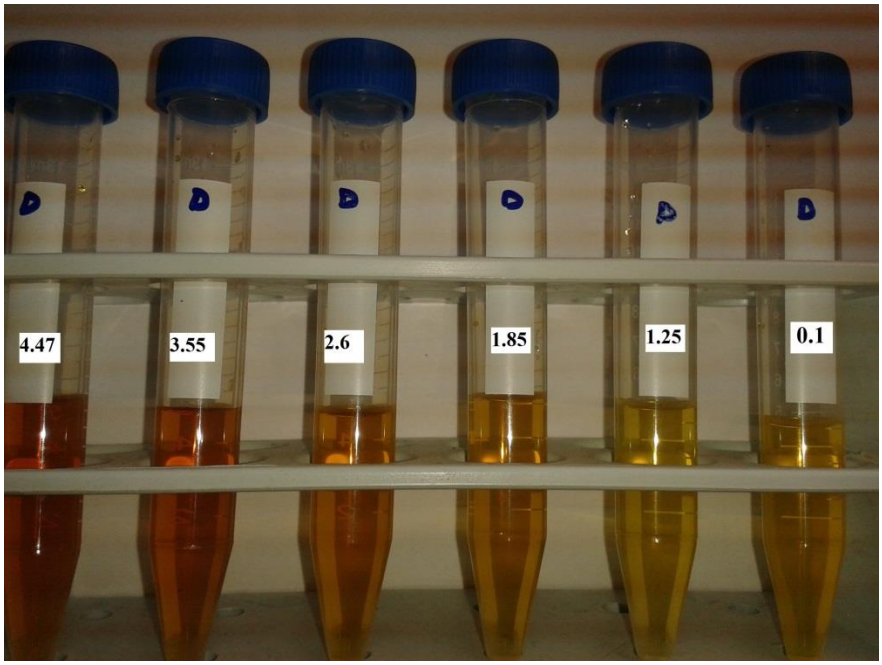

Figure 4.14: 5% DTPA/20% HCl formulation after adding 3000 ppm ferric ions at different pH at temperature of 72^{o} F

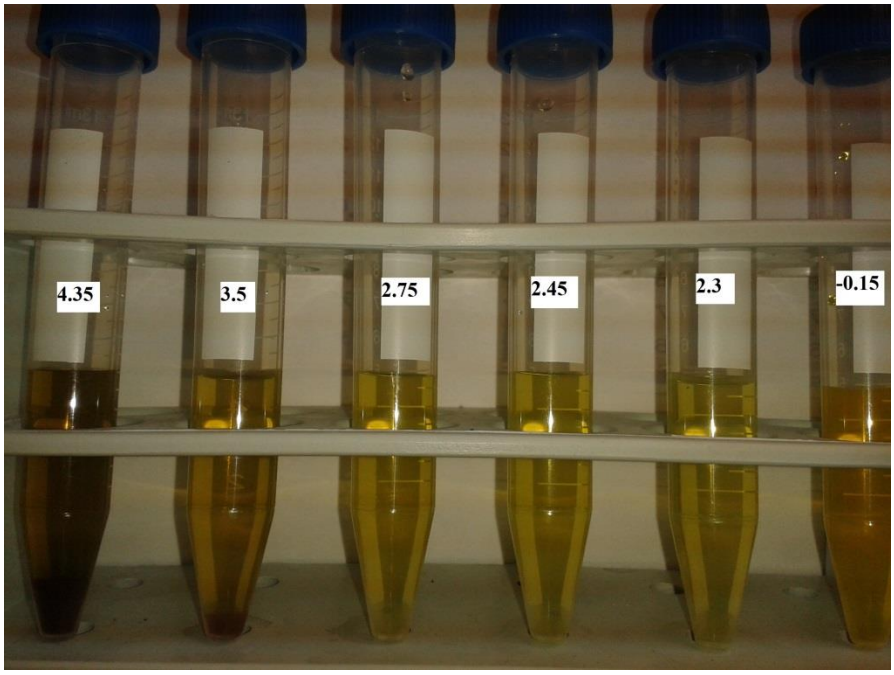

Figure 4.15: 5% GLDA/20% HCl formulation after adding 3000 ppm ferric ions at different pH at temperature of 72^{o} F

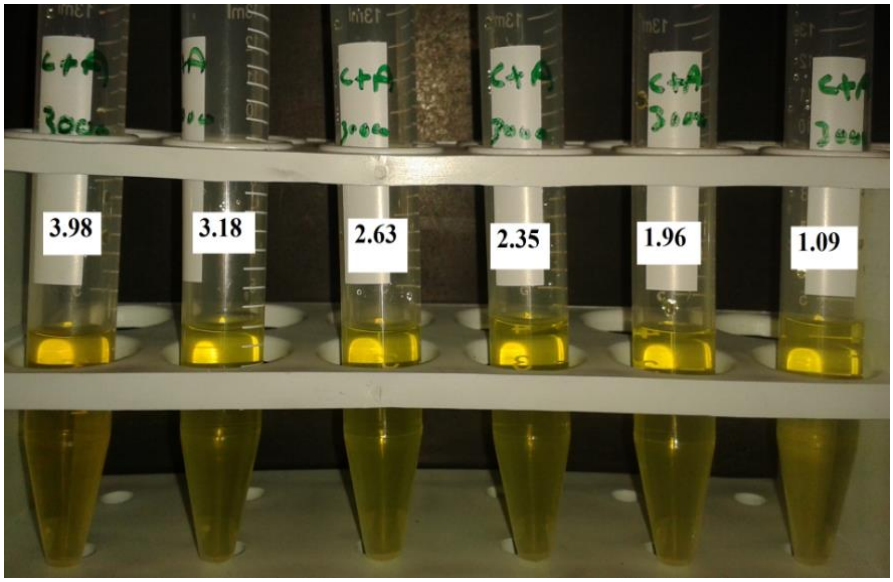

Figure 4.16: 2.5% acetic/2.5% citric/20% HCl formulation after adding 3000 ppm ferric ions at different pH at temperature of 72^{o} F

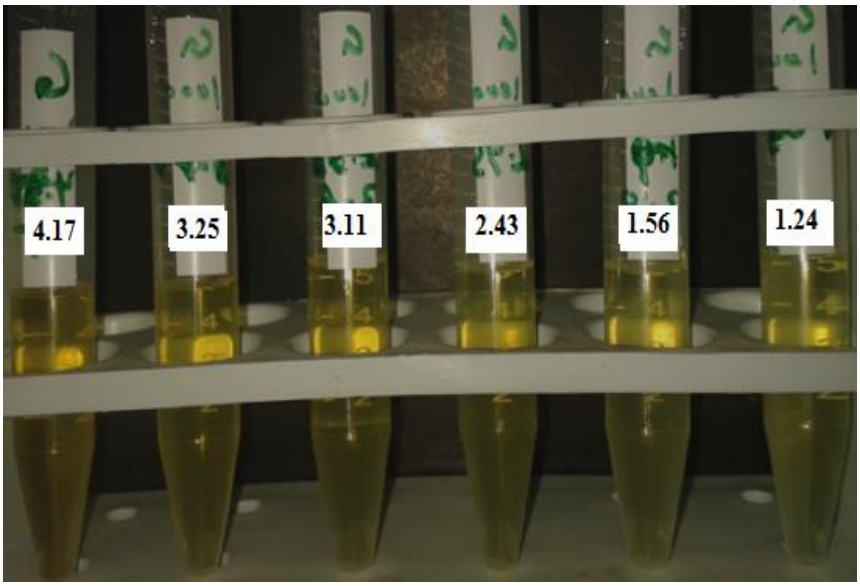

Figure 4.17: 5% GLDA/20% HCl formulation after adding 1000 ppm ferric ions at different pH values at temperature of 72^{o} F

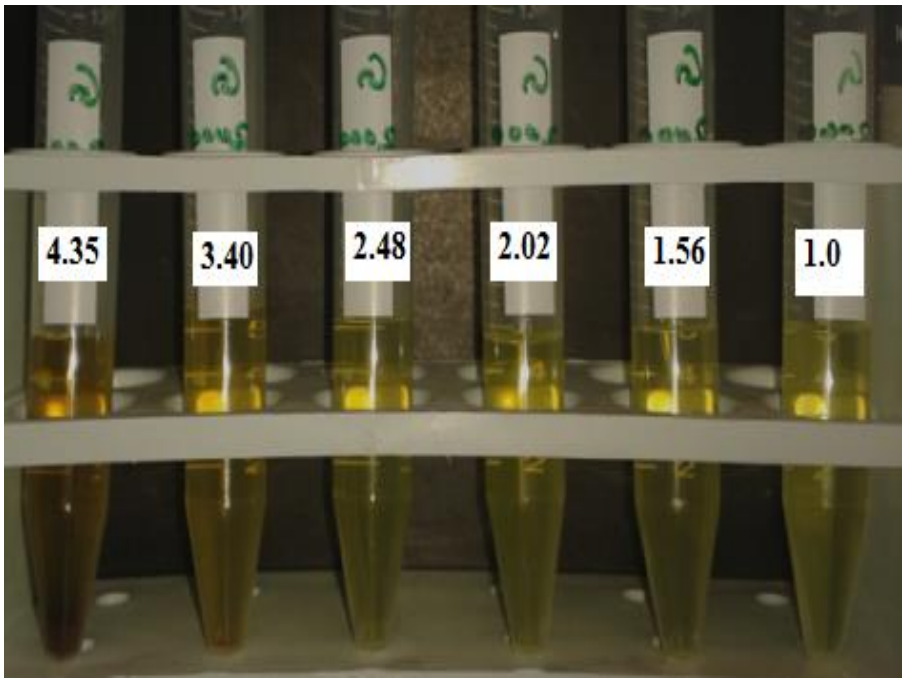

Figure 4.18: 5% GLDA/20% HCl formulation after adding 2000 ppm ferric ions at different pH values at temperature of 72^{o} F

CHAPTER 5

PHYSICAL PROPERTIES OF CHELATING AGENTS

5.1 Introduction

Measuring physical properties of chelating agents such as density, viscosity, and interfacial tension (IFT) is very important for proper understanding of the wormholing mechanism and better modeling. In this part density, viscosity, and IFT were measured at different temperatures and chelant concentrations. EDTA, HEDTA and DTPA chelating agents at different concentrations were studied. Density and viscosity of each chelant were measured after dissolving certain amount of calcium ions in the solution to investigate the effect of the chelated calcium ions on the physical properties of the chelating solutions. Calcium ions in the solution were increased in steps up to 15000 ppm depending on the concentration of the chelating solution. Each chelating solution was stirred for at least 24 hours to insure all the added calcium ions were dissolved, and then the solution was filtered to make sure no any solids or debris in the solution.

5.2 Physical Properties of EDTA

EDTA solutions of different concentrations were prepared using deionized water and sea water at pH of 10. Because pH of EDTA was not able to be reduced to lower values for higher concentrations, only one EDTA solution of 9.25% and 4.5 pH was prepared and tested to see if pH of the solution can have a noticeable effect of the physical properties of the solution at different temperatures.

5.2.1 Effect of Temperature on Density of EDTA

Three EDTA fluids at different concentrations of 18.5%, 9.25% and 3.7% were prepared by deionized water. Density of each solution was measured at different temperatures. Figure 5.1 shows the changes in density with temperature for the above mentioned solutions. From the figure, it was clear that the best equation that represents this relation between density and temperature is polynomial. Based on that, the equation relating the density to the temperature and EDTA concentration was developed as follows:

$$\rho_{EDTA} = -0.00041C_{EDTA}^2 + 0.01466C_{EDTA} - 0.000401\,T + 0.99214 \quad (5.1)$$

where ρ_{EDTA} is density of EDTA in gm/cc, T is temperature in degree F, and C_{EDTA} is concentration of EDTA in wt. %.

Above equation can be used to estimate the EDTA density at any concentration and temperature within average errors of 0.7%.

Figure 5.2 shows the effect of pH on the density of EDTA. The figure claimed that the effect of pH on the density of EDTA is negligible as only a difference of about 0.6% was recorded for the case of 9.25% EDTA.

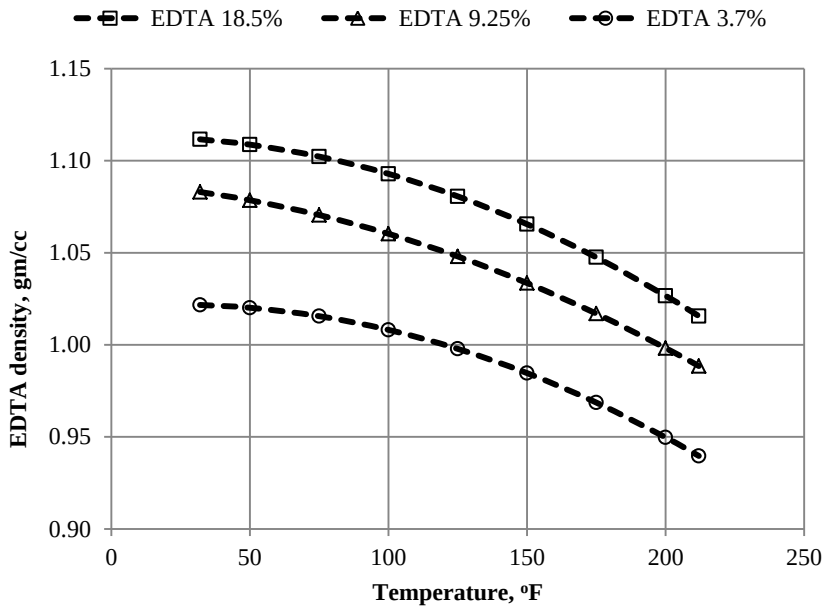

Figure 5.1: EDTA density at different concentrations and temperatures

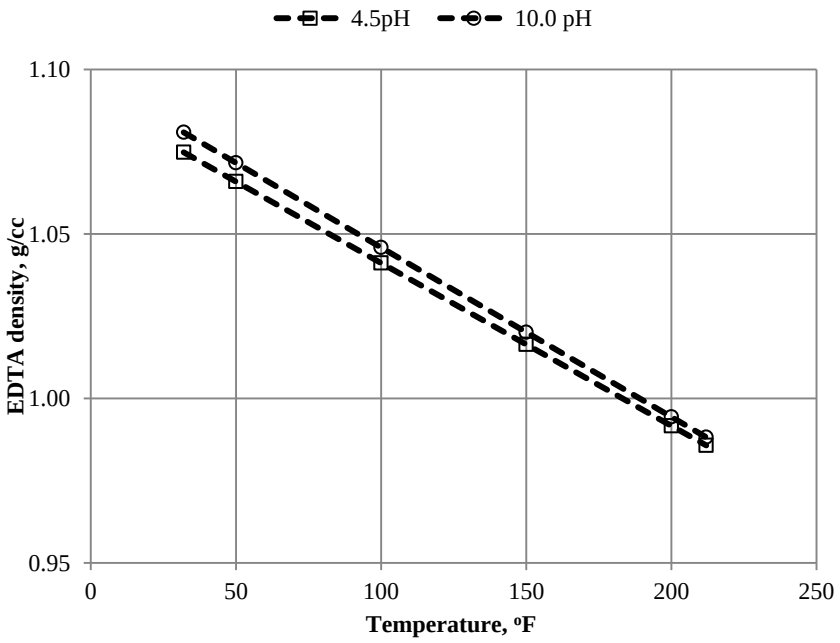

Figure 5.2: Effect of pH on density of 9.25% EDTA

5.2.2 Effect of Calcium Ions on Density of EDTA

Calcium ions were added to a 10.0 pH EDTA at different concentrations to find out the effect of the dissolved calcium on the physical properties. Figures 5.3 to 5.5 show the density of EDTA as the calcium ions were added to the solutions. From these figures, it was clear that the same relation between the density and the temperature was maintained, except the curve was shifted up as the calcium ions were increased in the solution. This shift was expected as the density of each fluid will increase if solid material was dissolved in it. The following equations were developed for the relation between density and calcium ions at different temperature values:

$$\rho_{18.5\%\,EDTA} = 2.6 \times 10^{-6} \times C_{Ca} - 0.000534 \times T + 1.1404 \quad (5.2)$$

$$\rho_{9.25\%\,EDTA} = 9.2 \times 10^{-6} \times C_{Ca} - 0.000492 \times T + 1.0369 \quad (5.3)$$

$$\rho_{3.7\%\,EDTA} = 2.1 \times 10^{-6} \times C_{Ca} - 0.000468 \times T + 1.0497 \quad (5.4)$$

Where $\rho_{18.5\%EDTA}$ is density of 18.5% EDTA in gm/cc, $\rho_{18.5\%EDTA}$ is density of 9.25% EDTA in gm/cc, $\rho_{18.5\%EDTA}$ is density of 3.7% EDTA in gm/cc, and C_{Ca} is calcium concentration in ppm.

The above three equations can be used to estimate the density of EDTA for any specified EDTA concentration and any calcium ions concentrations within an average errors of 0.5%, 1.3% and 0.6%, respectively.

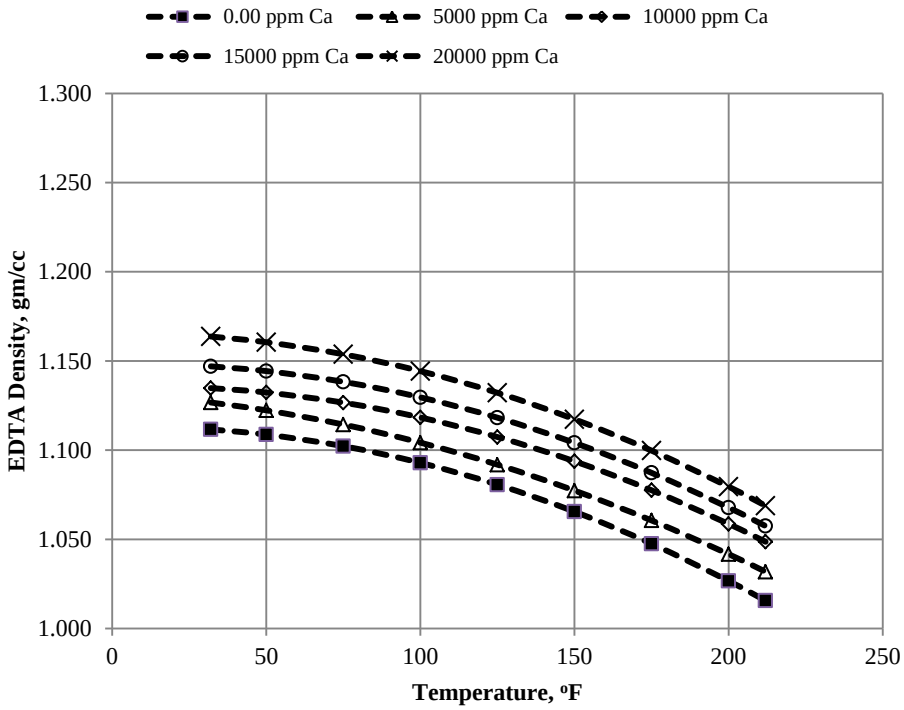

Figure 5.3: Effect of calcium ions on density of 18.5% EDTA

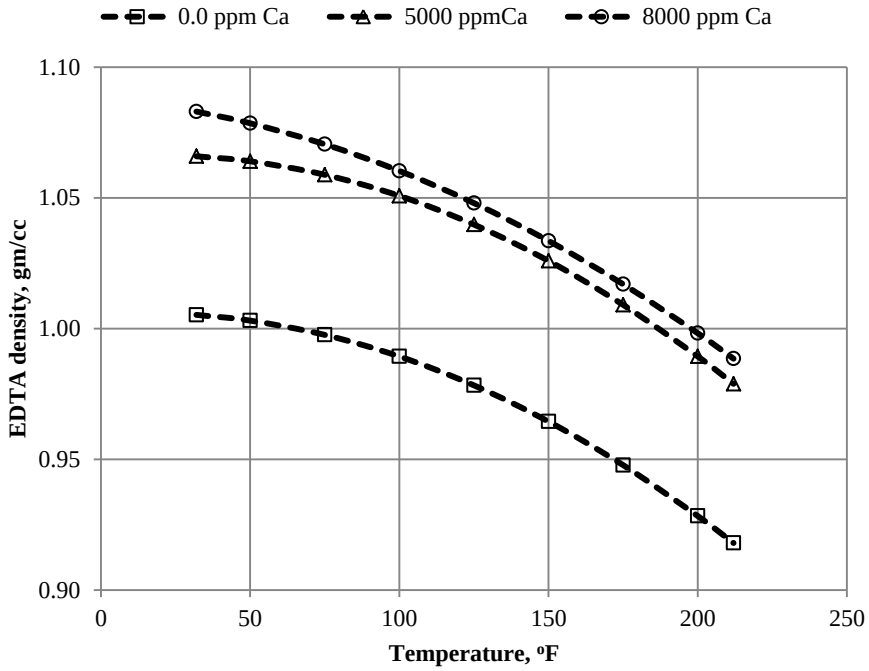

Figure 5.4: Effect of calcium ions on density of 9.25% EDTA

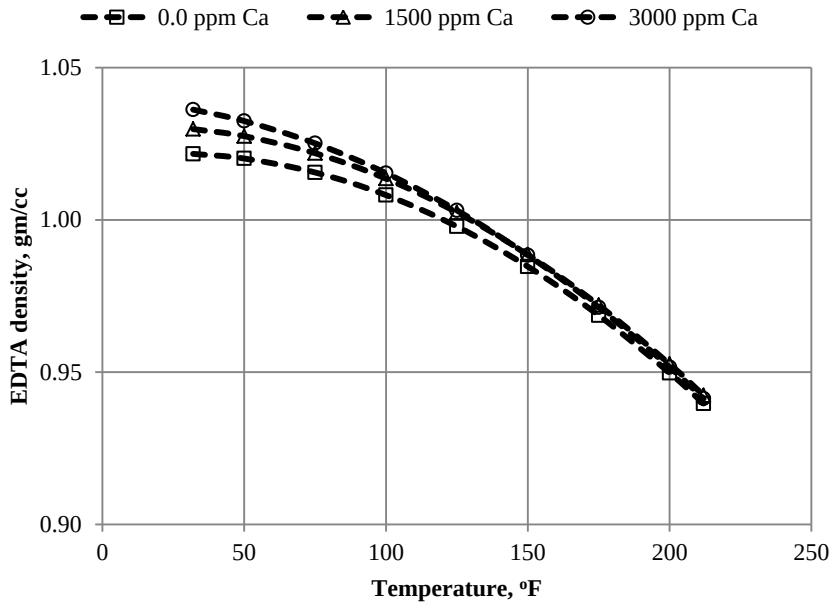

Figure 5.5: Effect of calcium ions on density of 3.7% EDTA

5.2.3 Effect of Temperature on Viscosity of EDTA

Three EDTA fluids at different concentrations of 18.5%, 9.25% and 3.7% were prepared by deionized water. Viscosity of each solution was measured at different temperatures. Figure 5.6 shows the changes in viscosity with temperature for the above mentioned solutions. From the figure, it was clear that the best equation represents this relation between viscosity and temperature is exponential. Based on that, the equation that relating the viscosity to the temperature and EDTA concentration was developed as follows:

$$\mu_{EDTA} = 93.8947 \times T^{-1.1113} \times e^{\left(0.08213 \times C_{EDTA} \times T^{-0.12061}\right)} \quad (5.5)$$

where μ_{EDTA} is viscosity of EDTA in cP.

Above equation can be used to estimate the viscosity of EDTA at any concentration and temperature within average errors of 0.3%.

Figure 5.7 shows the effect of pH on the viscosity of EDTA. The figure showed that the effect of pH on the viscosity of EDTA is noticeable as the difference of about 14.0% was recorded for the case of 9.25% EDTA. But because the viscosity values are generally small at temperature greater than 100^{o}F which is less than 1.0 cp, using one value of viscosity will not create big errors.

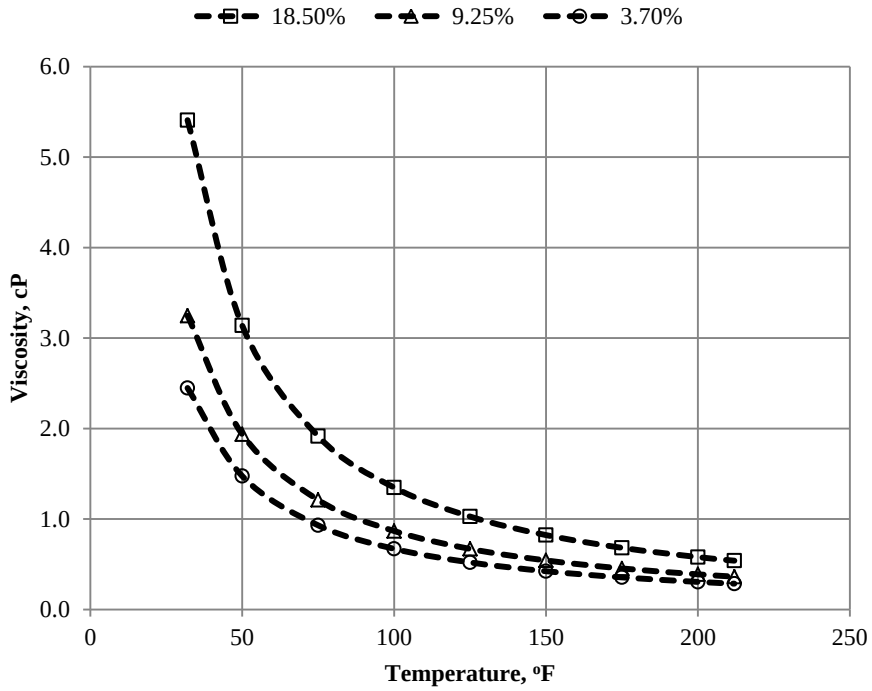

Figure 5.6: EDTA density at different concentrations and temperatures

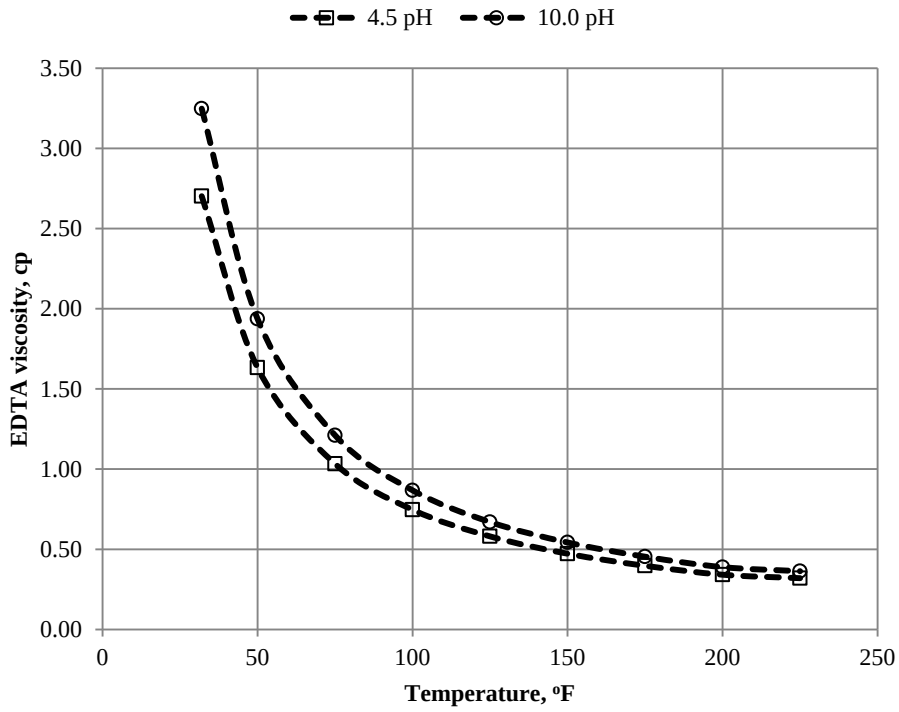

Figure 5.7: Effect of solution pH on viscosity of 9.25% EDTA

5.2.4 Effect of Calcium Ions on Viscosity of EDTA

Calcium ions were added to a 10.0 pH EDTA at different concentrations to find out the effect of the dissolved calcium on the physical properties. Figures 5.8 to 5.10 show the viscosity of EDTA as the calcium ions were added to the solutions. From these figures, it was clear that the same relation between the viscosity and the temperature was maintained, except the curve was shifted up as the calcium ions were increased in the solution. This shift was expected as the viscosity of each fluid will increase if solid material was dissolved in it. The following equations were developed for the relation between viscosity and calcium ions at different temperature values:

$$\mu_{18.5\%\,EDTA} = 362.0691 \times T^{-1.2151} \times e^{0.00002 \times C_{Ca} \times e^{-0.0045 \times T}} \quad (5.6)$$

$$\mu_{9.25\%\,EDTA} = 129.914 \times T^{-1.1124} \times e^{0.000041 \times C_{Ca} \times e^{-0.00935 \times T}} \quad (5.7)$$

$$\mu_{3.7\%\,EDTA} = 125.8347 \times T^{-1.13552} \times e^{0.000129 \times C_{Ca} \times e^{-0.23768 \times T}} \quad (5.8)$$

The above three equations can be used to estimate the viscosity of EDTA for any specified EDTA concentration and any calcium ions concentration within average errors of 0.6%, 0.5% and 0.6%, respectively.

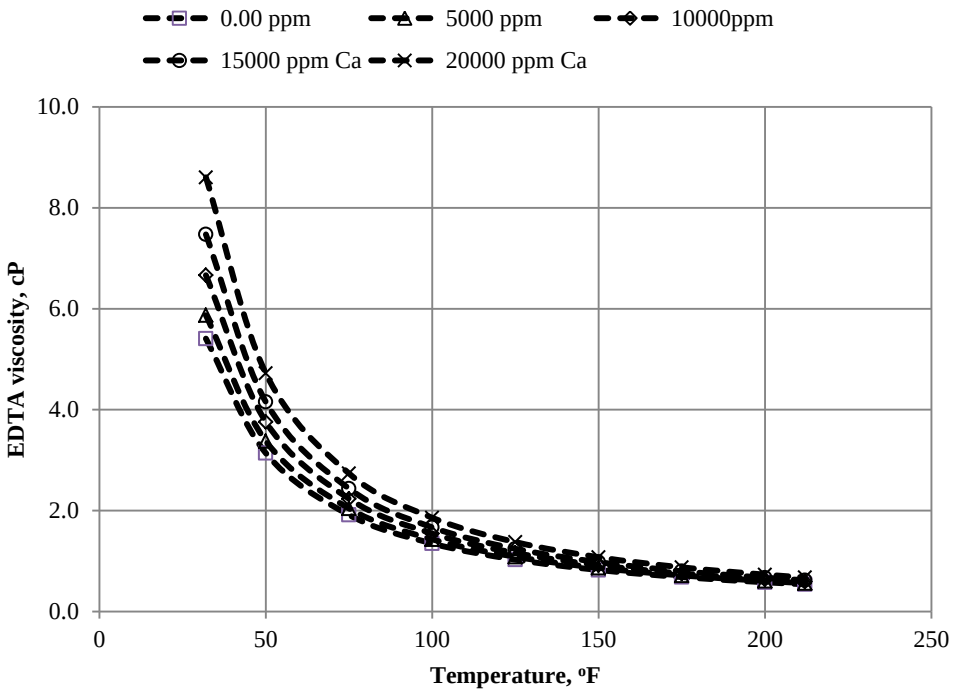

Figure 5.8: Effect of calcium ions on viscosity of 18.5 EDTA

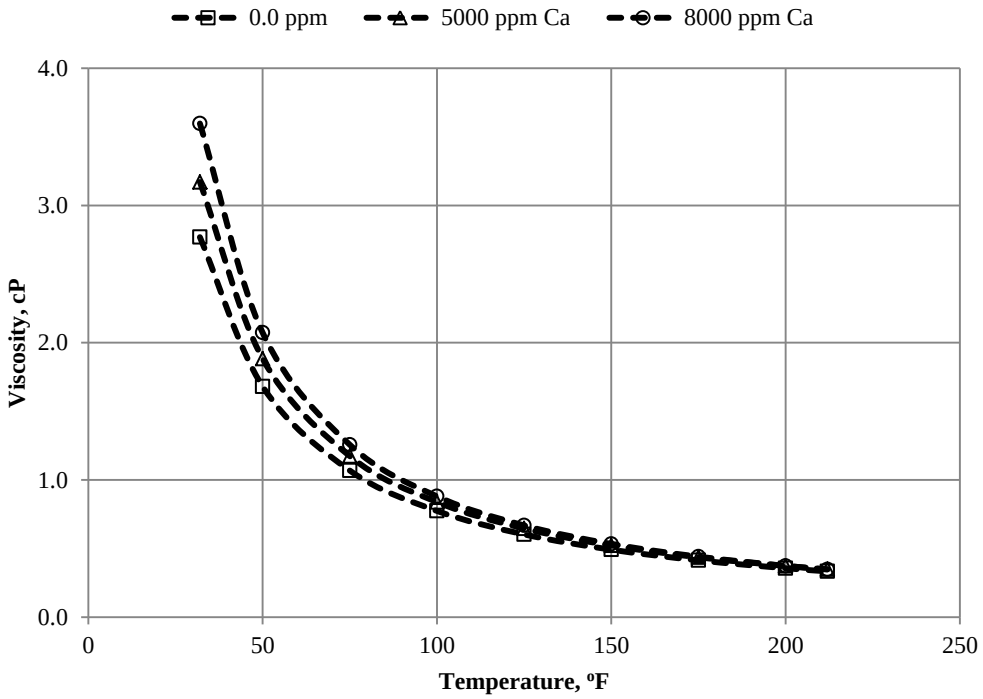

Figure 5.9: Effect of calcium ions on viscosity of 9.25% EDTA

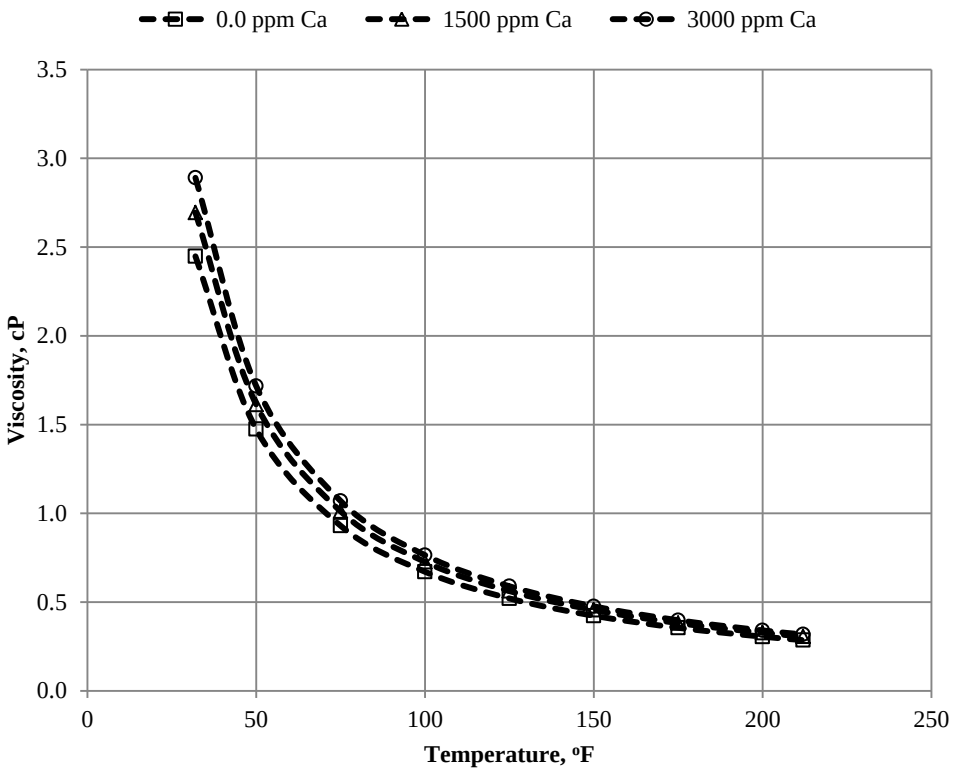

Figure 5.10: Effect of calcium ions on viscosity of 3.7% EDTA

5.3 Physical Properties of DTPA

DTPA solutions at different concentrations and pH of 12.0 were prepared by deionized water and sea water. Density and viscosity of these solutions were measured at different temperature values. Also calcium ions were added to these fluids to figure out the effect of calcium ions on their physical properties.

5.3.1 Effect of Temperature on Density of DTPA

Three DTPA fluids have different concentrations that were 20%, 10% and 4% were prepared using deionized water. Density of each solution was measured at different temperatures. Figure 5.10 shows the changes in density with temperature for the above mentioned solutions. Same relation between density and temperature was obtained, which was following the polynomial relation. The equation that relating the density to the temperature at different DTPA concentration was developed as follows:

$$\rho_{DTPA} = -0.000091 \times \rho_{DTPA}^2 + 0.00862 \times \rho_{DTPA} - 0.000569 \times T + 1.0386 \qquad (5.9)$$

where ρ_{DTPA} is density of DTPA in gm/cc, T is temperature in degree Fahrenheit, and C_{DTPA} is concentration of DTPA in wt. %.

Above equation can be used to estimate the DTPA density at any concentration and temperature within average errors of 0.6%.

Figure 5.12 shows the effect of the solution pH on the density of 10% DTPA solution. It is clear that pH has a negligible effect on the density of the solution as only about 0.7% difference was noticed. In other words, one density value can be used for DTPA solution with same concentration and any pH value.

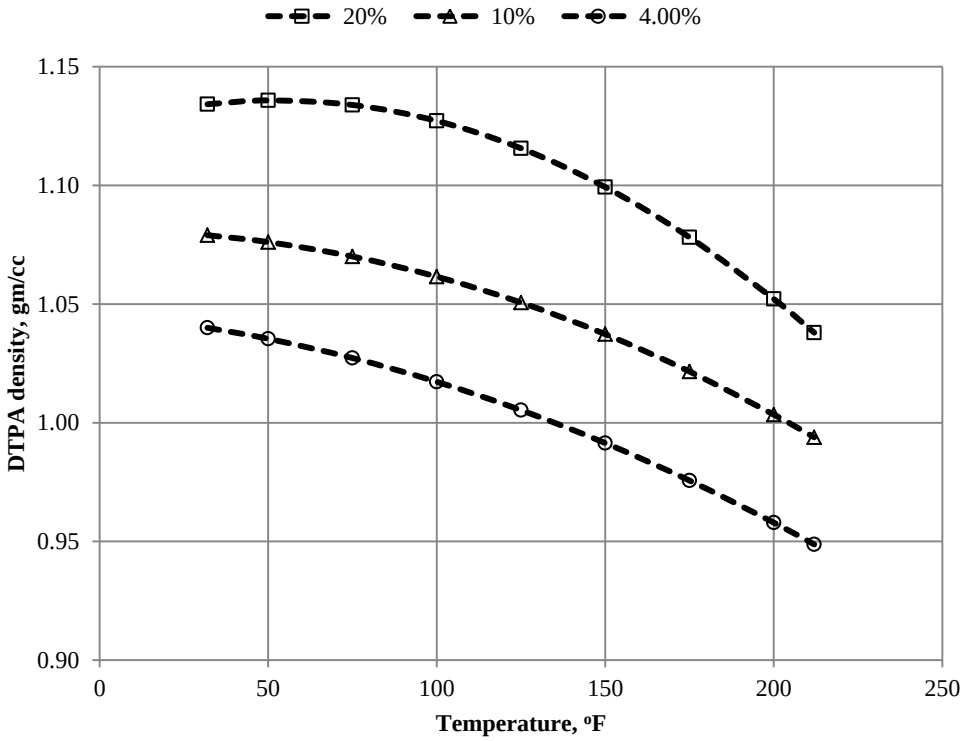

Figure 5.11: Effect of temperature and concentration on density of DTPA

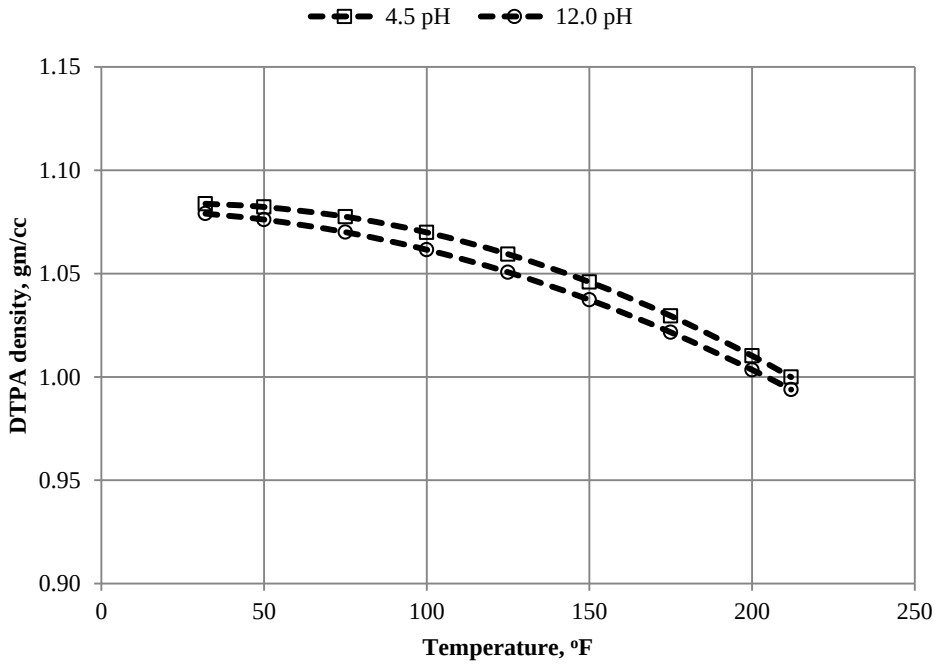

Figure 5.12: Effect of pH on the density of 10.0% DTPA

5.3.2 Effect of Calcium Ions on Density of DTPA

Calcium ions were added to a 12.0 pH DTPA at different concentrations to find out the effect of the dissolved calcium ions on the physical properties. Figures 5.13 to 5.15 show the density of DTPA as the calcium ions were added to the solutions. From these figures, it was clear that the same relation between the density and the temperature was maintained, except the curve was shifted up as the calcium ions were increased in the solution. This shift was expected as the density of each fluid will increase if solid material was dissolved in it. The following equations were developed for the relation between density and calcium ions at different temperature values:

$$\rho_{20\%\,DTPA} = 4.05 \times 10^{-6} C_{Ca} - 0.000534 \times T + 1.1699 \quad (5.10)$$

$$\rho_{10\%\,DTPA} = 3.35 \times 10^{-6} C_{Ca} - 0.000492 \times T + 1.1055 \quad (5.11)$$

$$\rho_{4\%\,DTPA} = 2.03 \times 10^{-6} C_{Ca} - 0.000521 \times T + 1.0653 \quad (5.12)$$

The above three equations can be used to estimate the density of DTPA for any specified concentration and any calcium ions concentration within average errors of about 0.45%.

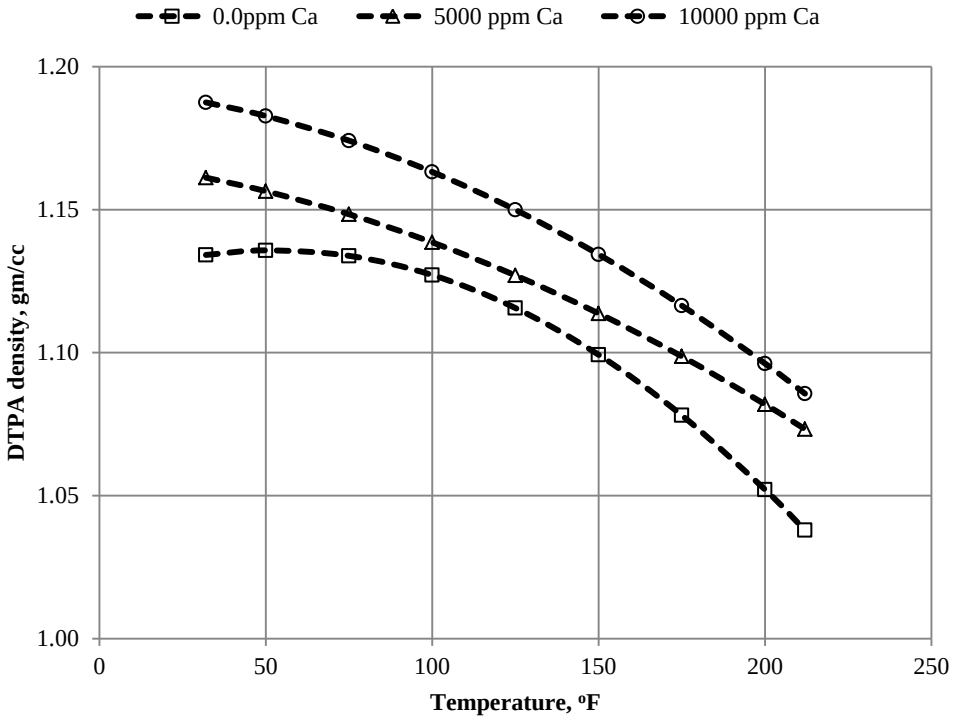

Figure 5.13: Effect of calcium ions on density of 20% DTPA

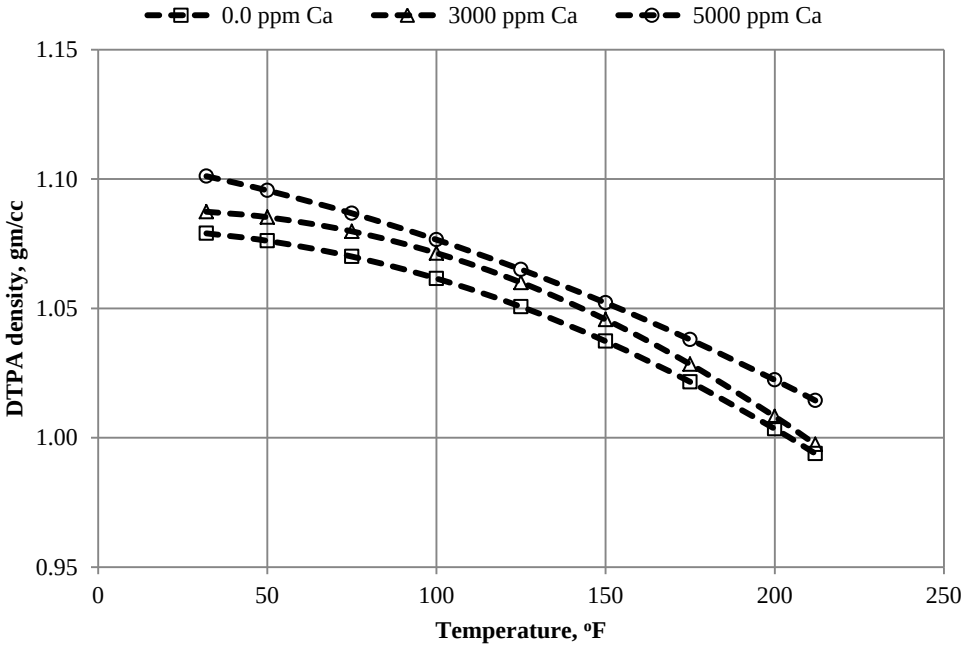

Figure 5.14: Effect of calcium ions on density of 10% DTPA

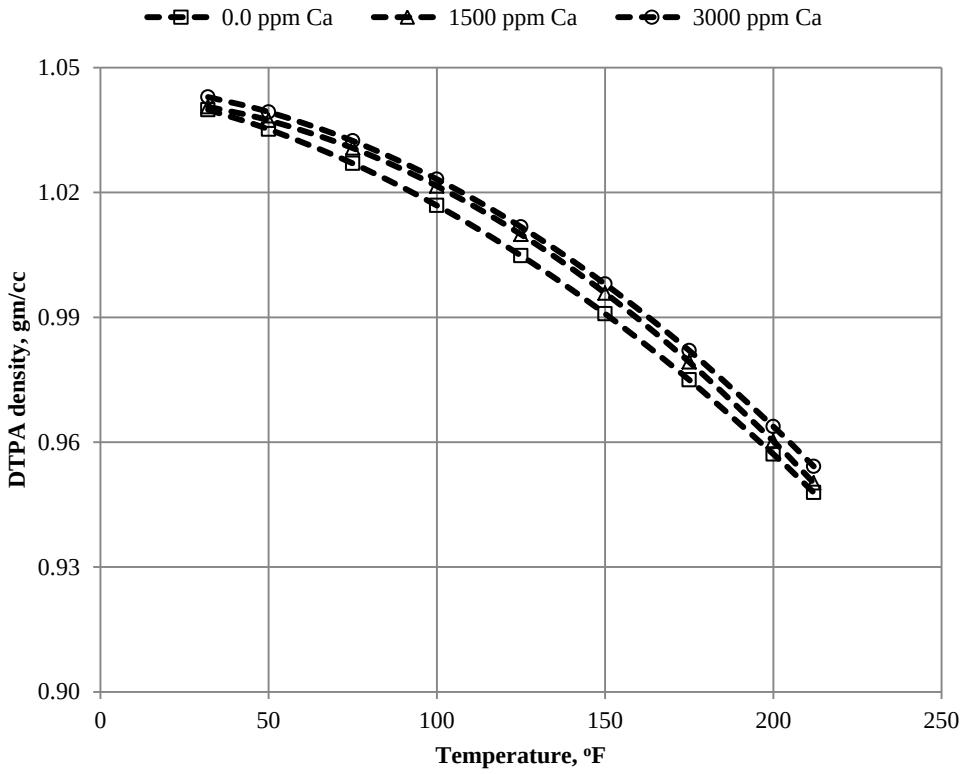

Figure 5.15: Effect of calcium ions on density of 4% DTPA

5.3.3 Effect of Temperature on Viscosity of DTPA

Three DTPA fluids at different concentrations of 20.0%, 10.0% and 4.0% were prepared by deionized water. Viscosity of each solution was measured at different temperatures. Figure 5.16 shows the changes in viscosity with temperature for the above solutions. From the figure, it was clear that the best equation that represents this relation between viscosity and temperature is exponential; as was depicted for EDTA. Based on that, the equation that relating the viscosity to the temperature and DTPA concentration was developed as follows:

$$\mu_{DTPA} = 96.546 \times T^{-1.1180} \times e^{\left(0.1498 \times C_{DTPA} \times T^{-0.1675}\right)} \quad (5.13)$$

where μ_{DTPA} is viscosity of DTPA in cP.

Above equation can be used to estimate the DTPA viscosity at any concentration and temperature within average errors of 3.0%.

Figure 5.17 shows the effect of the solution pH on the viscosity of 10% DTPA solution. It is clear that pH has a small effect on the viscosity of the solution especially at temperatures greater than 100^{o} F. The difference is about 3.5%. In other words, one value of viscosity can still be used for DTPA solution with same concentration and any pH value at temperature higher than 100^{o} F.

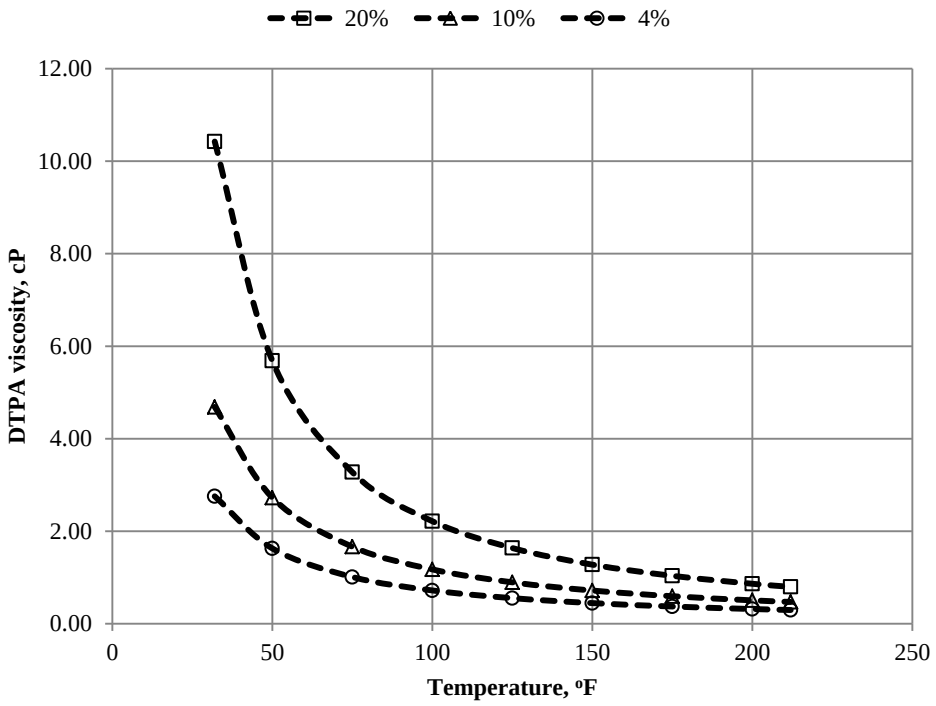

Figure 5.16: Effect of temperature and concentration on viscosity of DTPA

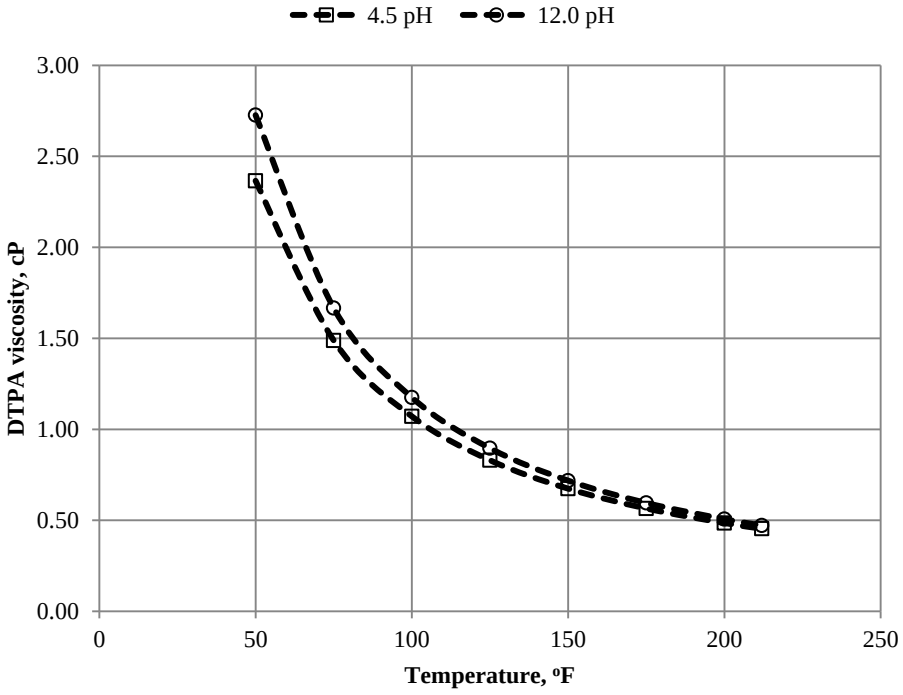

Figure 5.17: Effect of solution pH on viscosity of 10% DTPA

5.3.4 Effect of Calcium Ions on Viscosity of DTPA

Calcium ions were added to a 12.0 pH DTPA at different calcium concentrations to find out the effect of the dissolved calcium on the physical properties. Figures 5.18 to 5.20 show the viscosity of DTPA as the calcium ions were added to the solutions. From these figures, it was clear that the same relation between the viscosity and the temperature was maintained, except the curve was shifted up as the calcium ions are increased in the solution. This shift was expected as the viscosity of each fluid will increase if solid material was dissolved in it. The following equations were developed for the relation between viscosity and calcium ions at different temperature values:

$$\mu_{20\%\,DTPA} = 1131.737 \times T^{-1.3529} \times e^{0.000028 \times C_{Ca} \times e^{-0.00439 \times T}} \quad (5.14)$$

$$\mu_{10\%\,DTPA} = 293.284 \times T^{-1.1994} \times e^{0.000012 \times C_{Ca} \times e^{-0.00273 \times T}} \quad (5.15)$$

$$\mu_{4\%\,DTPA} = 159.053 \times T^{-1.1725} \times e^{-0.0000058 \times C_{Ca}} \quad (5.16)$$

The above three equations can be used to estimate the viscosity of DTPA for the specified DTPA concentrations and any calcium ions concentrations within an average errors of about 1.0%.

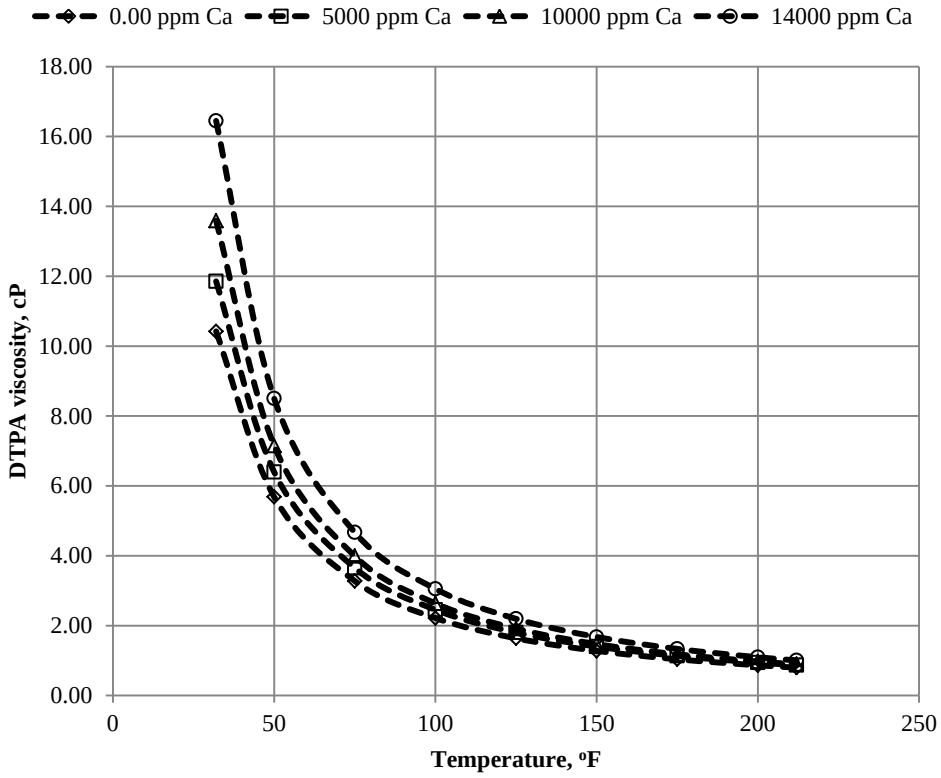

Figure 5.18: Effect of calcium ions on viscosity of 20% DTPA

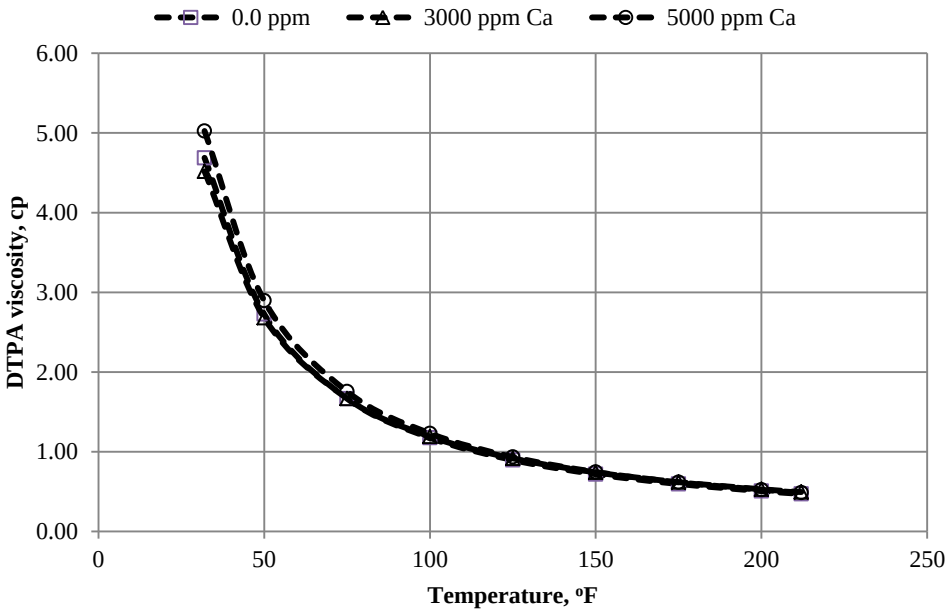

Figure 5.19: Effect of calcium ions on viscosity of 10% DTPA

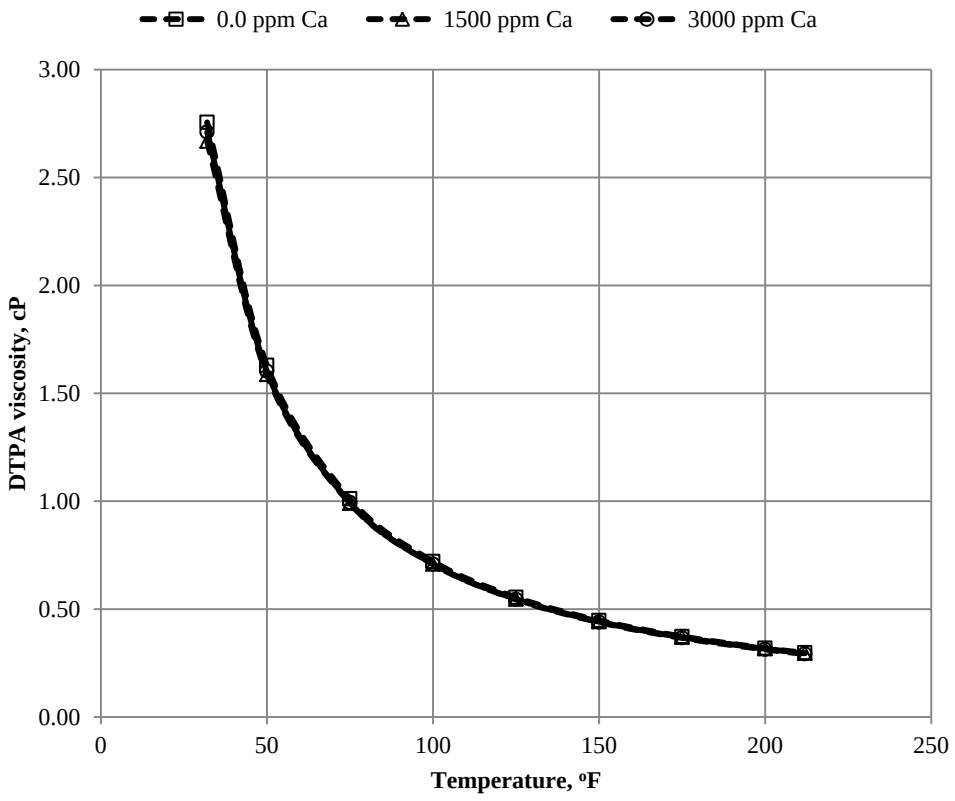

Figure 5.20: Effect of calcium ions on viscosity of 4% DTPA

5.4 Physical Properties of HEDTA

HEDTA solutions at different concentrations were prepared by deionized water and sea water at pH of 4.0. Density and viscosity of these solutions were measured at different temperature values. Also calcium ions were added to these fluids to figure out the effect of calcium ions on the physical properties. HEDTA concentrations of 20%, 15% and 10% were selected to be studied.

5.4.1 Effect of Temperature on Density of HEDTA

Six HEDTA fluids at different concentrations of 20%, 15% and 10% were prepared by deionized water and sea water. Density of each solution was measured at different temperatures. Figures 5.21 and 5.22 show the changes in density with the temperature for the cases of solutions prepared by deionized water and sea water, respectively. Same relation between density and temperature was obtained, which was following the polynomial relation for both cases. The equations relating the density to the temperature at different HEDTA concentration were developed as follows:

$$\rho_{HEDTA\_DI} = 0.0000755\, C_{HEDTA}^2 + 0.00419 C_{HEDTA} - 0.000558\, T + 1.0663 \qquad (5.17)$$

$$\rho_{HEDTA\_SW} = 0.0003890\, C_{HEDTA}^2 - 0.00471 C_{HEDTA} - 0.000455\, T + 1.1401 \qquad (5.18)$$

where ρ_{HEDTA_DI} and ρ_{HEDTA_SW} are the densities of HEDTA prepared by deionized water and sea water in gm/cc, T is temperature in degree Fahrenheit, and C_{HEDTA} is concentration of HEDTA in wt. %.

Above two equations can be used to estimate the HEDTA density at any concentration and temperature within average errors of 0.5%.

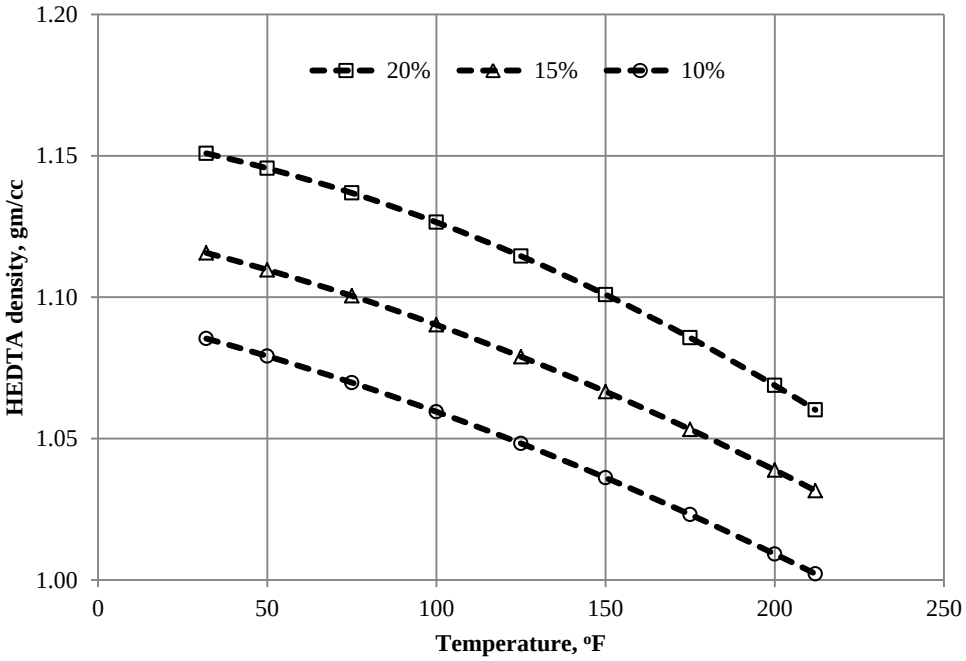

Figure 5.21: Effect of temperature on density of HEDTA prepared by DI water

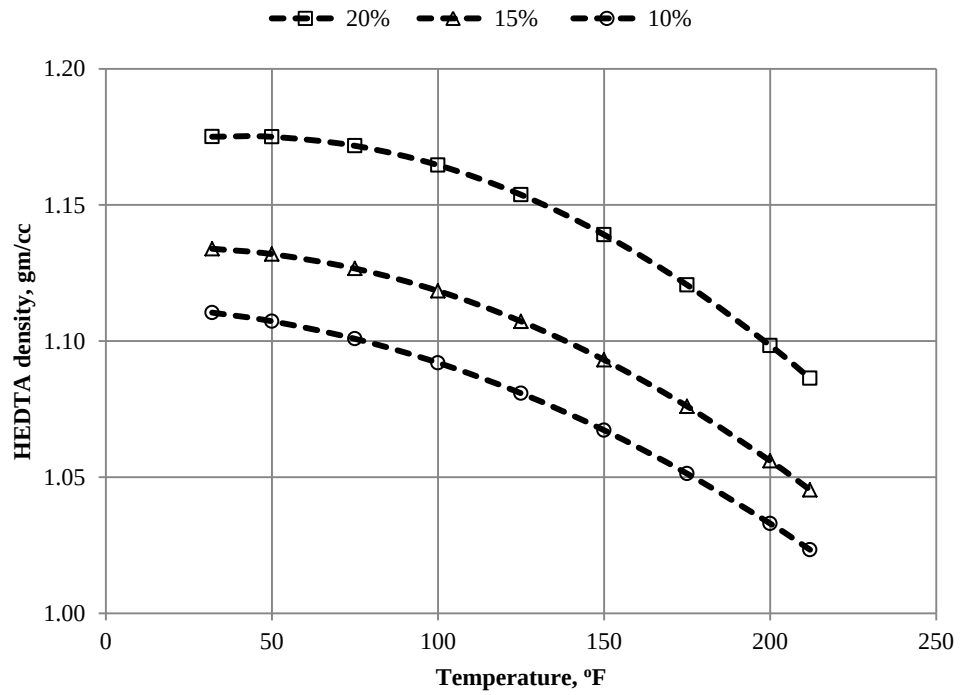

Figure 5.22: Effect of temperature on density of HEDTA prepared by sea water

5.4.2 Effect of Calcium Ions on Density of HEDTA

Calcium ions were added to the previously prepared HEDTA solutions to find out the effect of the dissolved calcium ions on the physical properties. Figures 5.23 to 5.28 show the density of HEDTA as the calcium ions were added to the solutions. From these figures, it was clear that the same relation between the density and the temperature was maintained, except the curve was shifted up as calcium ions were increased in the solution. This shift was expected as the density of each fluid will increase if solid material was dissolved in it. The following equations were developed for the relation between density and calcium ions at different temperature values:

$$\rho_{20\%\,HEDTA\_DI} = (-1.0 \times 10^{-8} \times T + 4.0 \times 10^{-6})C_{Ca} - 0.0005 \times T + 1.174 \quad (5.19)$$

$$\rho_{15\%\,HEDTA\_DI} = (-7.0 \times 10^{-9} \times T + 2.0 \times 10^{-6})C_{Ca} - 0.0004 \times T + 1.133 \quad (5.20)$$

$$\rho_{10\%\,HEDTA\_DI} = (-4.0 \times 10^{-9} \times T + 2.0 \times 10^{-6})C_{Ca} - 0.0005 \times T + 1.105 \quad (5.21)$$

$$\rho_{20\%\,HEDTA\_SW} = (-2.0 \times 10^{-8} \times T + 6.0 \times 10^{-6})C_{Ca} - 0.0007 \times T + 1.231 \quad (5.22)$$

$$\rho_{15\%\,HEDTA\_SW} = (-9.0 \times 10^{-9} \times T + 4.0 \times 10^{-6})C_{Ca} - 0.0005 \times T + 1.162 \quad (5.23)$$

$$\rho_{10\%\,HEDTA\_SW} = (-5.0 \times 10^{-9} \times T + 2.0 \times 10^{-6})C_{Ca} - 0.0005 \times T + 1.137 \quad (5.24)$$

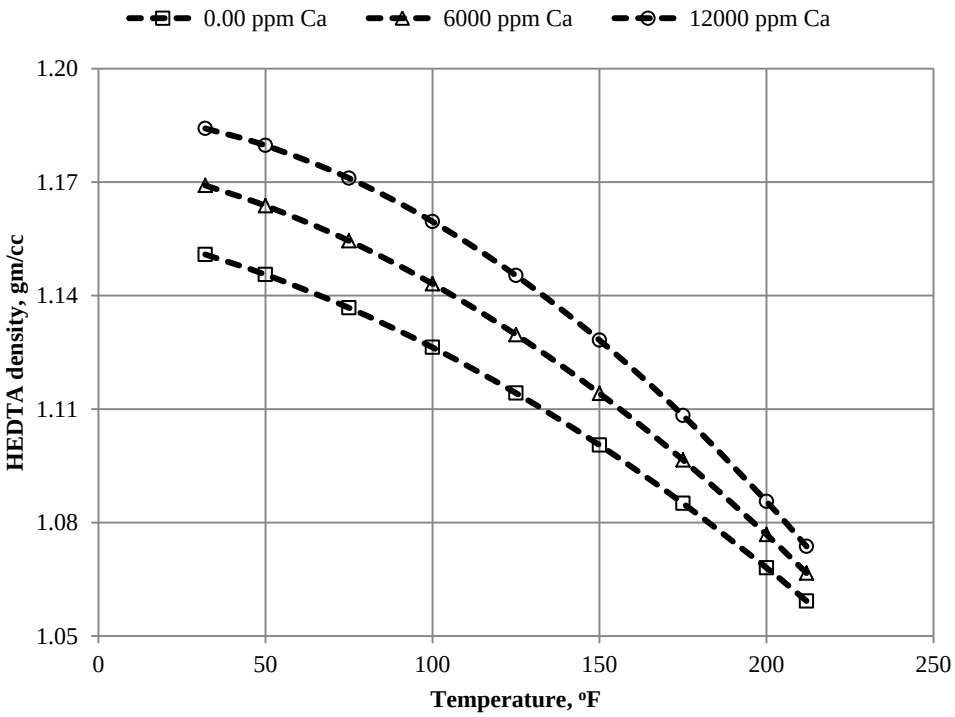

Figure 5.23: Effect of calcium ions on density of 20% HEDTA prepared by DI water

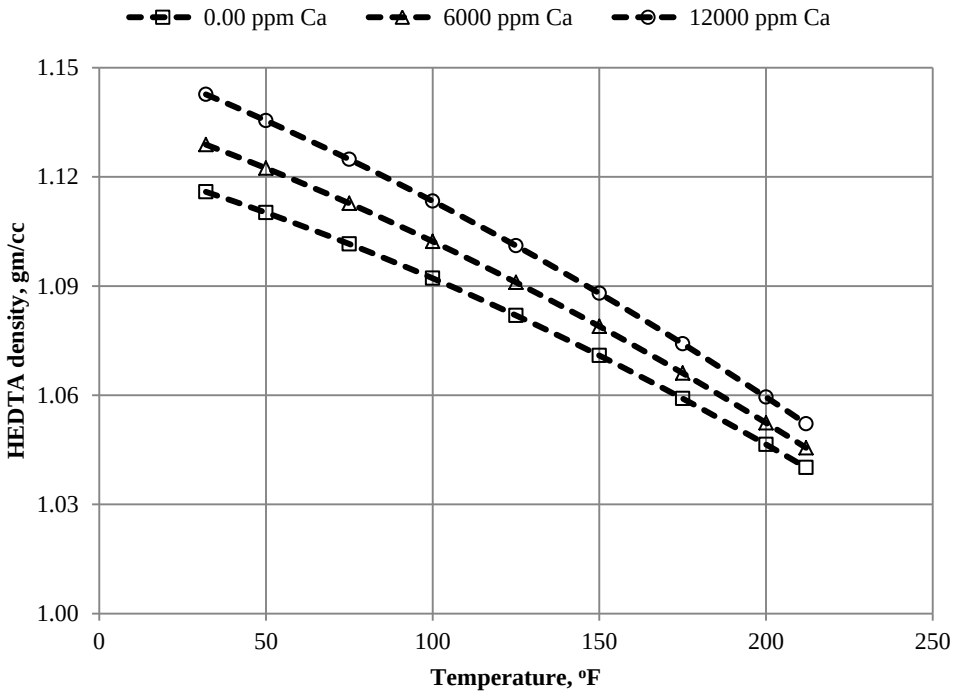

Figure 5.24: Effect of calcium ions on density of 15% HEDTA prepared by DI water

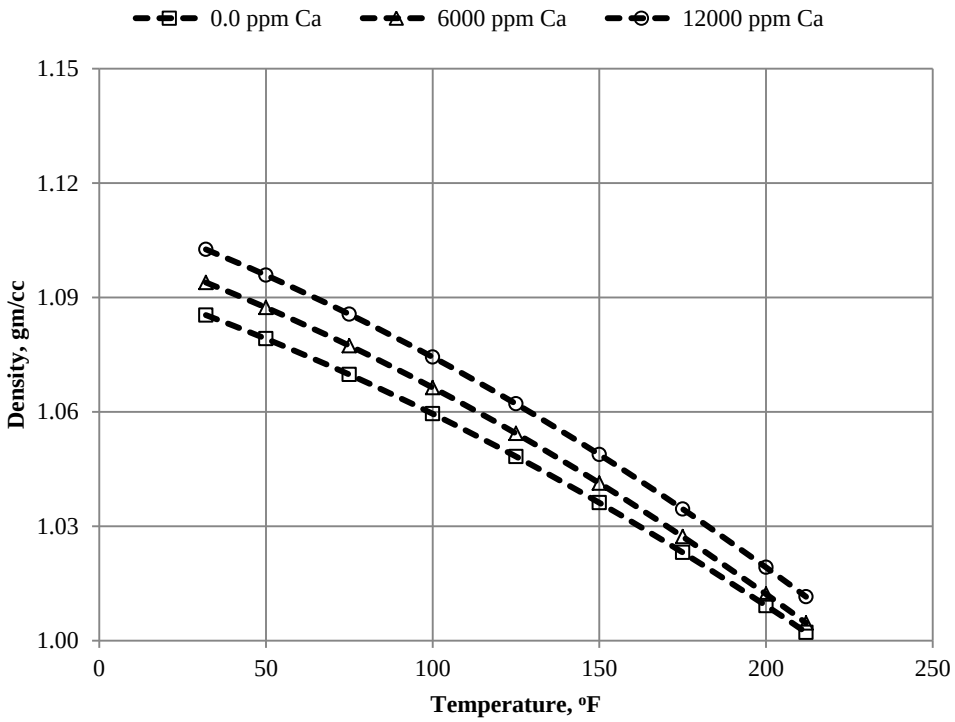

Figure 5.25: Effect of calcium ions on density of 10% HEDTA prepared by DI water

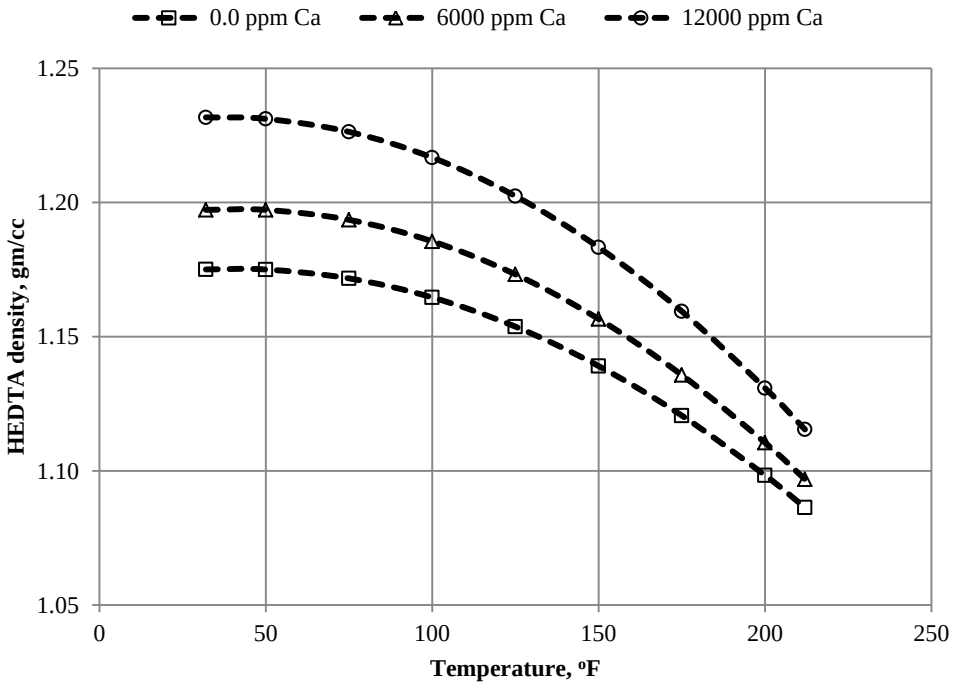

Figure 5.26: Effect of calcium ions on density of 20% HEDTA prepared by sea water

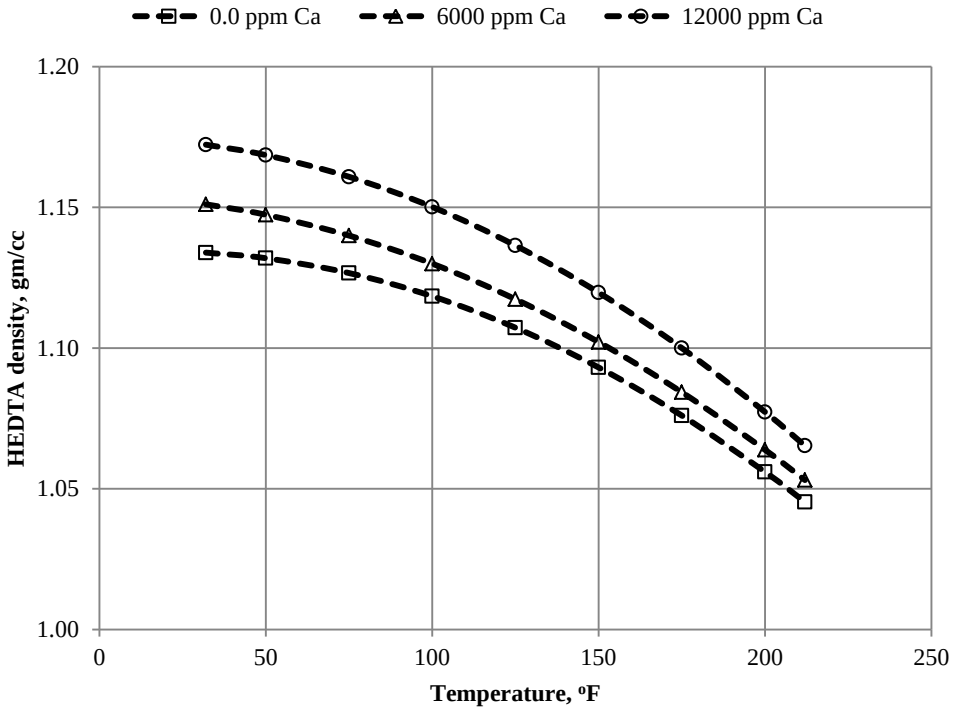

Figure 5.27: Effect of calcium ions on density of 15% HEDTA prepared by sea water

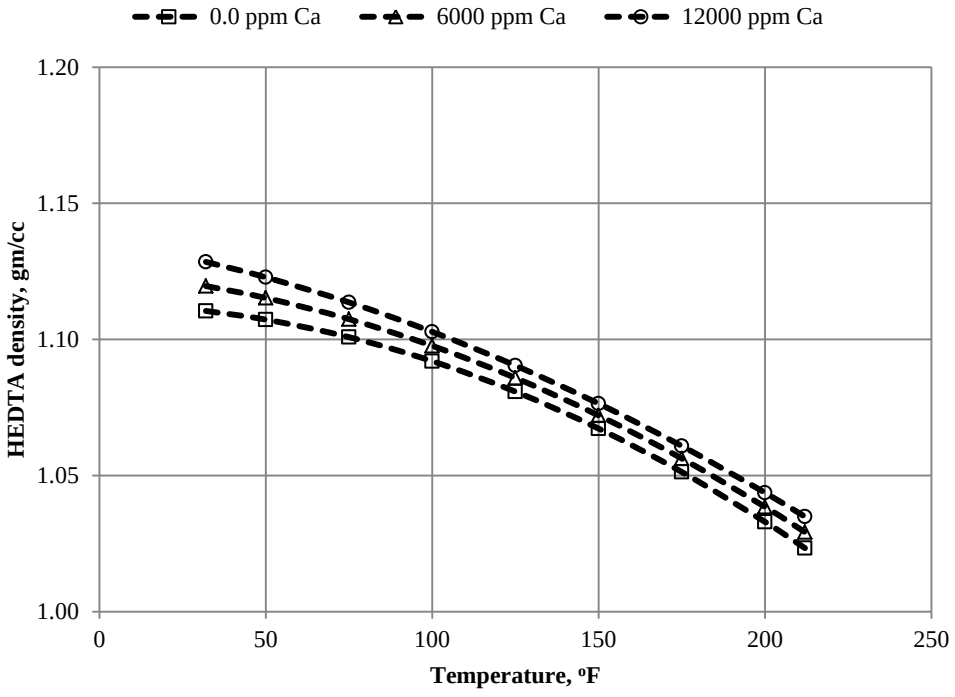

Figure 5.28: Effect of calcium ions on density of 10% HEDTA prepared by sea water

5.4.3 Effect of Temperature on viscosity of HEDTA

Six HEDTA fluids at different concentrations of 20.0%, 15.0% and 10.0% were prepared by deionized water and sea water. Viscosity of each solution was measured at different temperatures. Figures 5.29 and 5.30 show the changes in viscosity with temperature for the above mentioned solutions. From these figures, the relation between viscosity and temperature can be best represented by exponential curve. Based on that, the equations relating the viscosity and the temperature for each HEDTA solution was developed as follows:

$$\mu_{HEDTA\_DI} = 78.789 \times T^{-1.0692} \times e^{\left(0.0684 \times C_{HEDTA}\, T^{-0.0978} \times\right)} \quad (5.25)$$

$$\mu_{HEDTA\_SW} = 30.576 \times T^{-0.8513} \times e^{\left(0.3394 \times C_{HEDTA} \times T^{-0.4326}\right)} \quad (5.26)$$

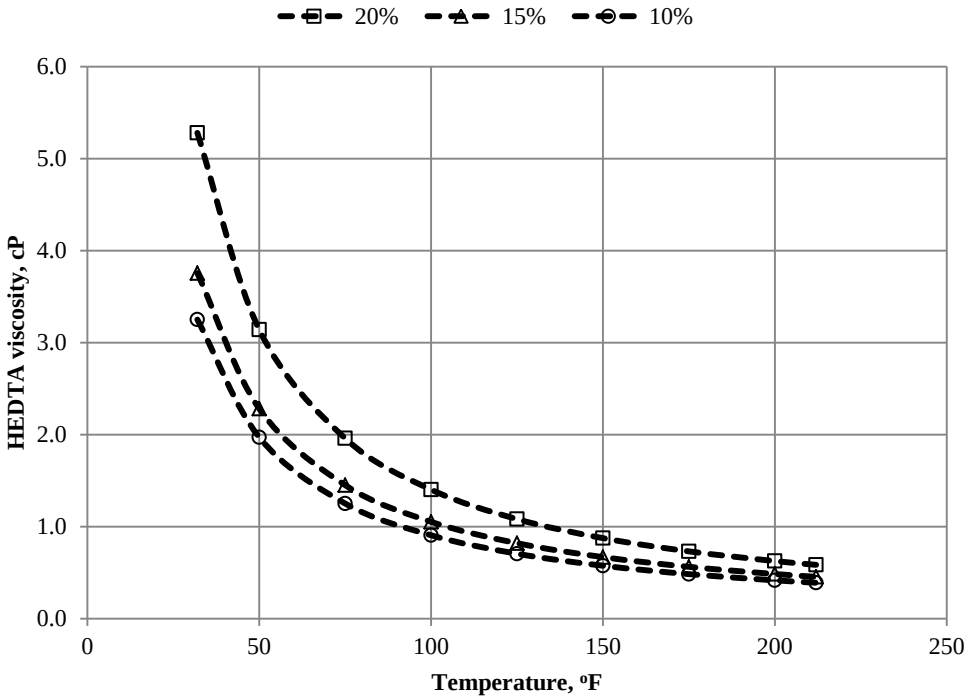

Figure 5.29: Effect of temperature on viscosity of HEDTA prepared by DI water

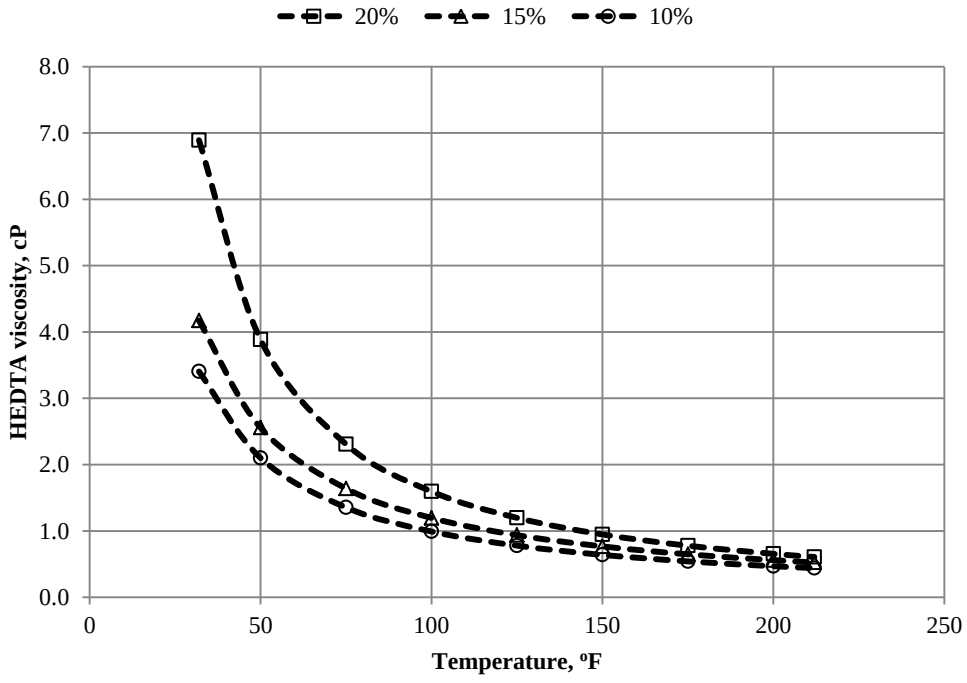

Figure 5.30: Effect of temperature on viscosity of HEDTA prepared by sea water

5.4.4 Effect of Calcium Ions on Viscosity of HEDTA

Calcium ions were added to the previously prepared HEDTA solutions to find out the effect of the dissolved calcium ions on the physical properties. Figures 5.31 to 5.36 show the changes on the viscosity of HEDTA as the calcium ions were added to the solutions. From these figures, it was clear that the same relation between the viscosity and the temperature was maintained, except the curve was shifted up as the calcium ions are increased in the solution. This shift was expected as the viscosity of each fluid will increase if solid material was dissolved in it. The following equations were developed for the relation between viscosity and calcium ions at different temperature values:

$$\mu_{20\%\,HEDTA\_DI} = 300.66 \times T^{-1.1672} \times e^{0.00002 \times C_{Ca} \times e^{-0.00743 \times T}} \quad (5.27)$$

$$\mu_{15\%\,HEDTA\_DI} = 188.04 \times T^{-1.1164} \times e^{0.00003 \times C_{Ca} \times e^{-0.00659 \times T}} \quad (5.28)$$

$$\mu_{10\%\,HEDTA\_DI} = 157.45 \times T^{-1.1204} \times e^{0.00002 \times C_{Ca} \times e^{-0.00164 \times T}} \quad (5.29)$$

$$\mu_{20\%\,HEDTA\_SW} = 585.99 \times T^{-1.2825} \times e^{0.00002 \times C_{Ca} \times e^{-0.00560 \times T}} \quad (5.30)$$

$$\mu_{15\%\,HEDTA\_SW} = 189.31 \times T^{-1.0999} \times e^{0.00003 \times C_{Ca} \times e^{-0.00555 \times T}} \quad (5.31)$$

$$\mu_{10\%\,HEDTA\_SW} = 145.39 \times T^{-1.0824} \times e^{0.00002 \times C_{Ca} \times e^{-0.01027 \times T}} \quad (5.32)$$

The above six equations can be used to estimate the viscosity of HEDTA at specific concentration at a certain temperature and known dissolved calcium concentration with in average errors of about 0.6%.

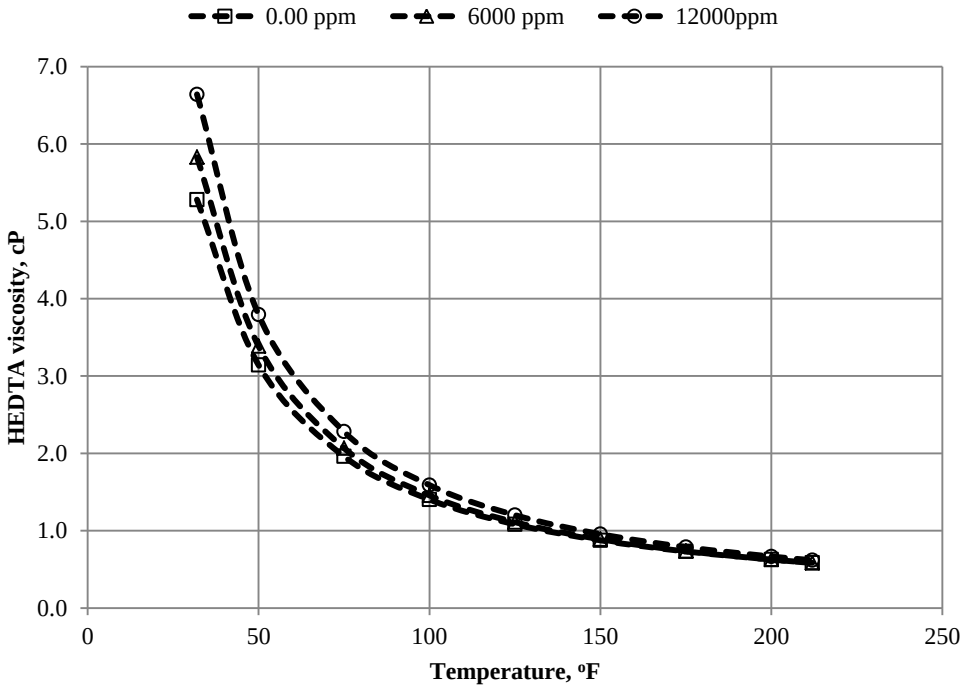

Figure 5.31: Effect of calcium ions on viscosity of 20% HEDTA prepared by DI water

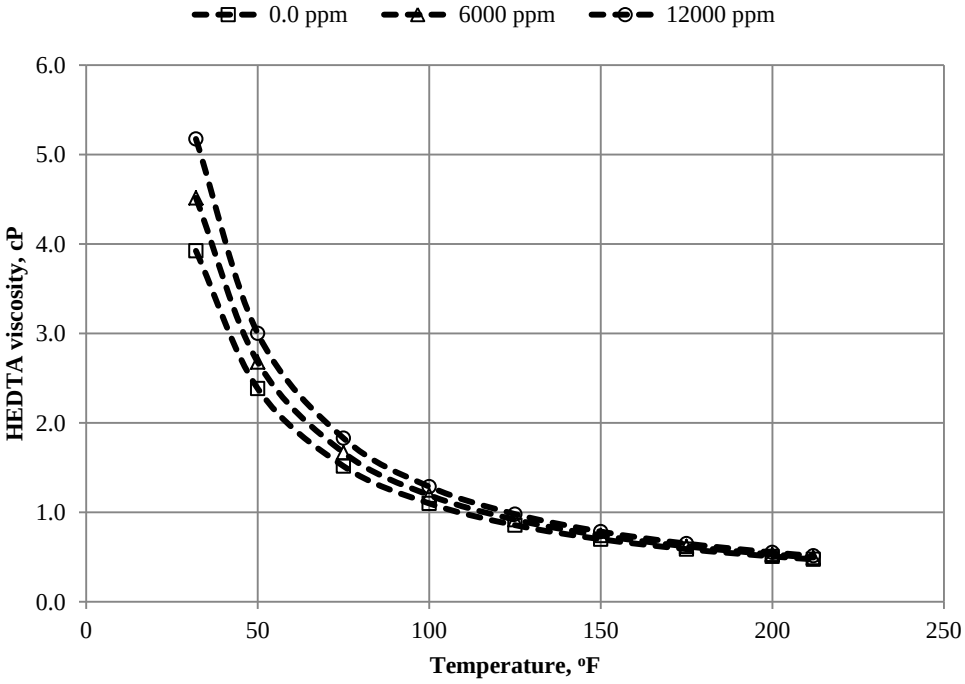

Figure 5.32: Effect of calcium ions on viscosity of 15% HEDTA prepared by DI water

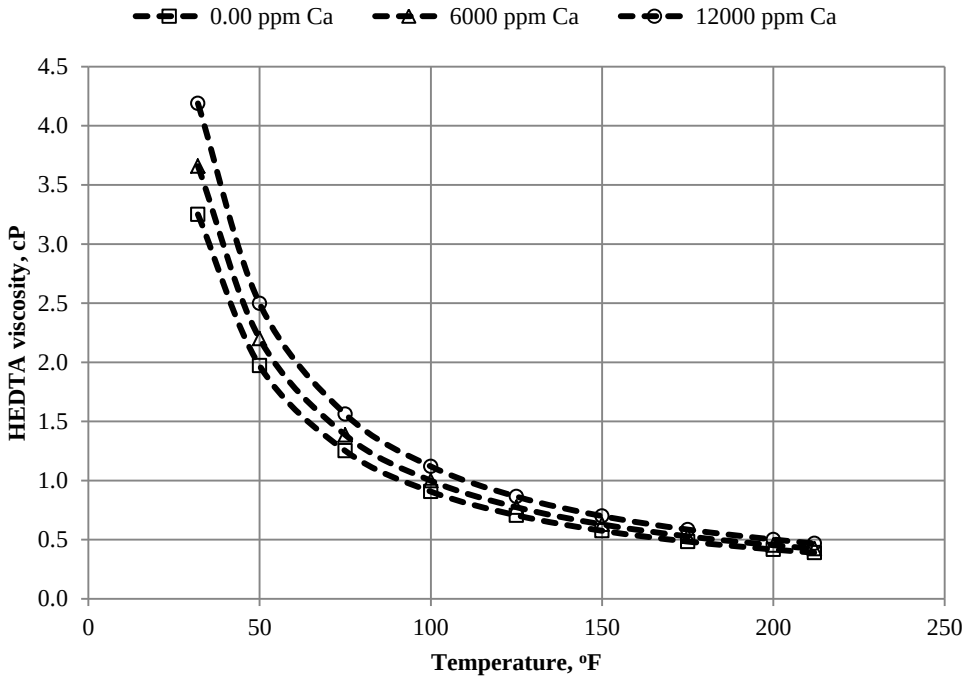

Figure 5.33: Effect of calcium ions on viscosity of 10% HEDTA prepared by DI water

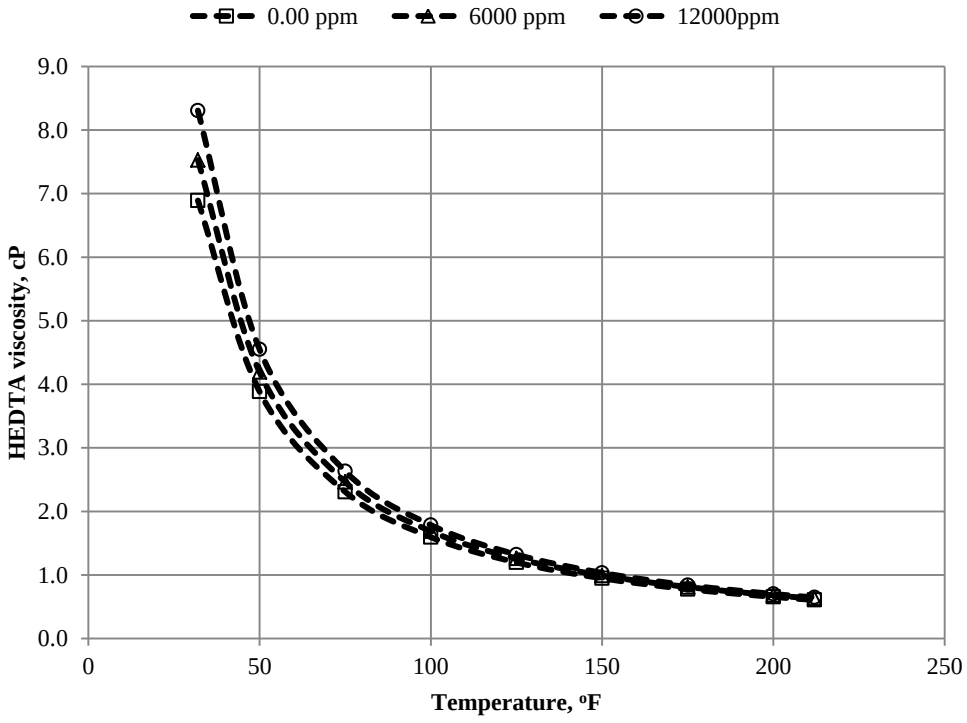

Figure 5.34: Effect of calcium ions on viscosity of 20% HEDTA prepared by sea water

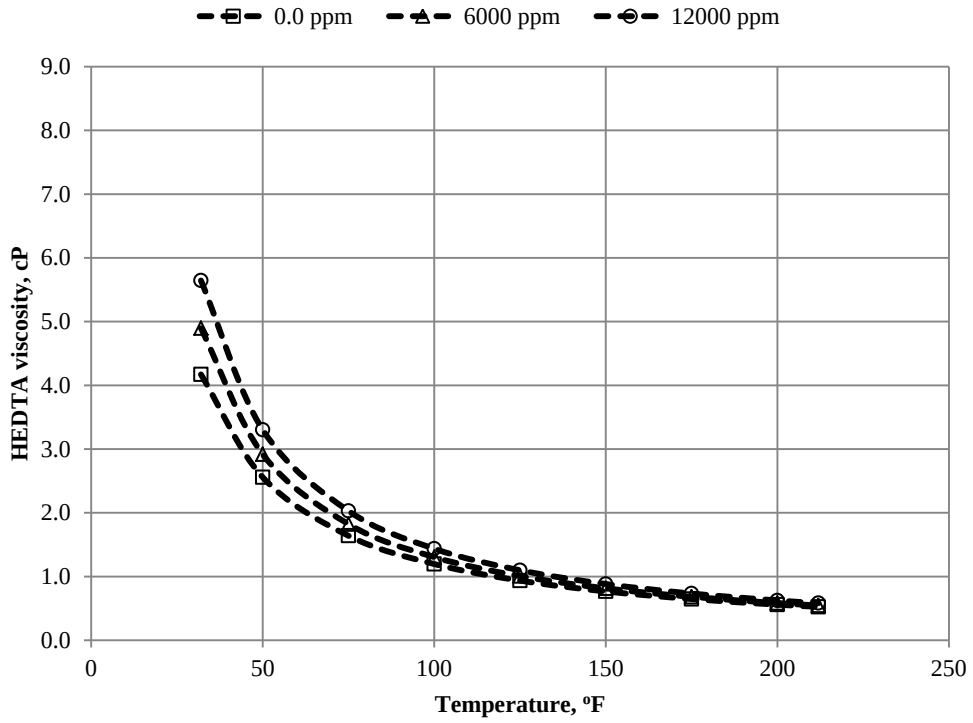

Figure 5.35: Effect of calcium ions on viscosity of 15% HEDTA prepared by sea water

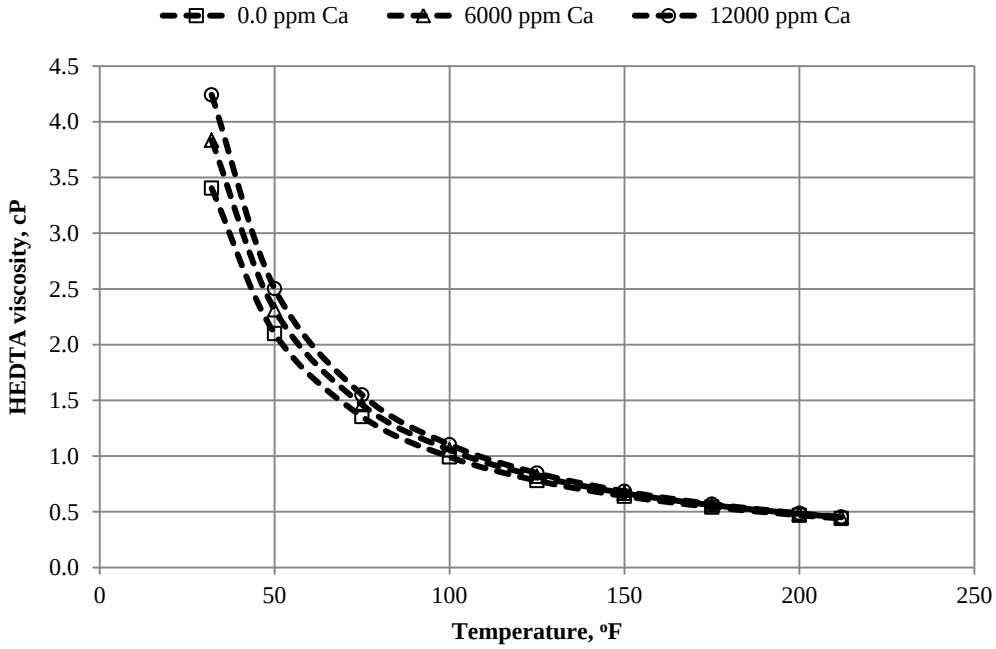

Figure 5.36: Effect of calcium ions on viscosity of 10% HEDTA prepared by sea water

5.5 Interfacial Tension between Oil and Chelating Agents

Interfacial tension between hydrocarbons and chelating agents is important to be studied for many reasons. It gives information on the structure and energy at the oil-chelate or gas-chelate interface. Interfacial tension is very important when stimulating gas wells. Low surface tension between gas and stimulation fluid is required to reduce capillary forces, and hence allow deep penetration inside the reservoir [62].

In this study, effect of concentration of EDTA, HEDTA and GLDA chelating agents on the interfacial tension between them and crude oil was investigated. Interfacial tension between live and spent chelating agents having different concentrations and crude oils of different API gravities were measured at room conditions. Three different concentrations of 20%, 15% and 10% of each chelant, and three crude oils have API gravities of 31.18^{o}, 35.6^{o} and 40.0^{o} were used in this study. Optical tensiometer from Biolin Scientific Company was used to measure the interfacial tension between chelating agents and crude oils. Spent chelating agents were prepared by dissolving 10 grams of calcium carbonate in 50 grams of chelating agents, and then the solution was filtered to remove any solids in the solution. Table 5.1 shows the properties of cheating agents that used in these studies.

Table 5.1: Properties of chelating agents

Chelating Agents	Diluting water	Concentration %	pH value
EDTA	Deionized water	20	8
	Deionized water	15	8
	Deionized water	10	8
HEDTA	Deionized water	20	4
	Deionized water	15	4
	Deionized water	10	4

Chelating Agents	Diluting water	Concentration %	pH value
GLDA	Deionized water	20	4
	Deionized water	15	4
	Deionized water	10	4

5.5.1 Interfacial Tension between Live Chelants and Crude Oils

To investigate the effect of chelant concentration on the interfacial tension between the chelant and crude oil, three measurements were done at three different chelant concentrations. Figure 5.37 shows the effect of EDTA concentration on the interfacial tension of three different crude oils. Figure shows clearly that interfacial tension was increasing with the increase in the EDTA concentration. This increase could be as a result of increasing the amount of chemical solids dissolved in the water, which in turn increase the density and viscosity of the solution that could lead to increase in the interfacial tension. Interfacial tension decreased with the increase in the crude oil API gravity for the same solution due to the increase of the difference in density between the chelant and the crude oil. Interfacial tension for the case of 40^{o} API crude oil for all EDTA concentrations has measurements errors because the oil droplet was very small and it was not stable for enough time as per the recommended practice by the manufacturing company. Similar results were observed for HEDTA and GLDA chelating agents in terms of increasing interfacial tension with the increase in the chelant concentration. Figure 5.38 shows the relation between the interfacial tension of different concentrations of HEDTA and different crude oils. Same trend of increasing interfacial tension with the increase in the HEDTA concentrations was observed, except interfacial tension for 40^{o} API crude oil was slightly greater than that of 35.6^{o} API. Because the difference in

density of these crude oils was not that big, we can conclude that interfacial tension between HEDTA and lighter crude oils can be assumed similar for crude oils having densities in the range 30^o – 40^o API. The difference in the interfacial tension in this range of crude oils was only 2.0 mN/m, which can be considered as small difference. Figure 5.39 shows the relation between the interfacial tension at different concentrations of GLDA and the crude oils. Interfacial tension was experiencing a slight increase as GLDA concentration increase. But in terms of crude oil type, similar trend was observed as for the case of HEDTA where the increase in the crude oil density will tend to decrease the interfacial tension. In general, increasing the chelating agents concentration will tend to increase the interfacial tension, and increasing the API gravity of the crude oil will tend to decrease the interfacial tension. HEDTA was found to have the highest interfacial tension, whereas EDTA has the lowest value for the same chelant concentration and crude oil API gravity.

5.5.2 Interfacial Tension between Spent Chelants and Crude Oils

To investigate the effect of spent chelating agents on the interfacial tension between the chelant and crude oil, three measurements were done at three different chelant concentrations. Spent chelating agents were prepared by adding 10 grams of calcium carbonate to 50 grams of chelant, and then the solution was filtered to insure no solids are suspended in the solution. Unfortunately, no measurements were conducted for HEDTA and GLDA as the screen of the optical tensiometer turned to black when their spent chelant were put in the instrument. Only studies on spent EDTA were conducted at different EDTA concentrations and crude oil gravities. Figure 5.40 shows the effect of concentration of the spent EDTA on the interfacial tension at different crude oil gravities.

Similar trend was observed for the spent EDTA as the interfacial tension tends to increase with the increase of the EDTA concentration, and for the same concentration, interfacial tension will tend to decrease with the increase on the crude oil API gravity. Figure 5.41 shows the comparison between the live and spent EDTA. Figure shows clearly that interfacial tension of the spent EDTA was lower than that of live acid.

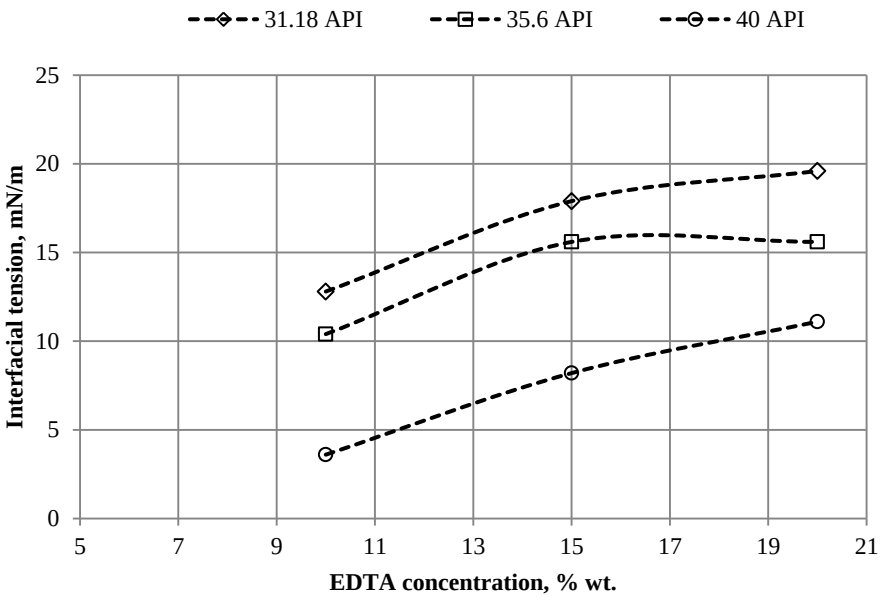

Figure 5.37: Effect of 8.0 pH EDTA concentration on Interfacial tension at temperature of 72^{o}F and atmospheric pressure

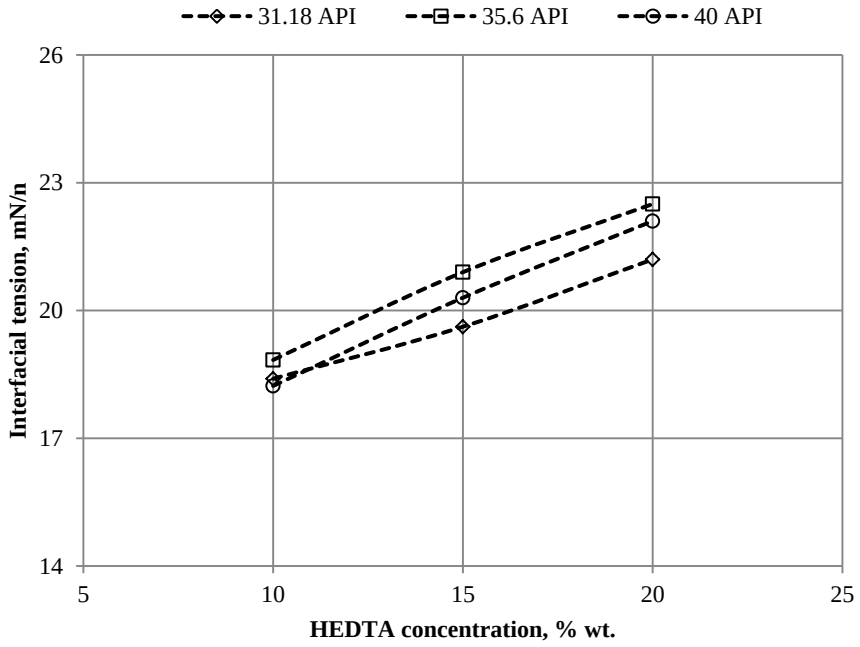

Figure 5.38: Effect of 4.0 pH HEDTA concentration on interfacial tension at temperature of 72^{o}F and atmospheric pressure

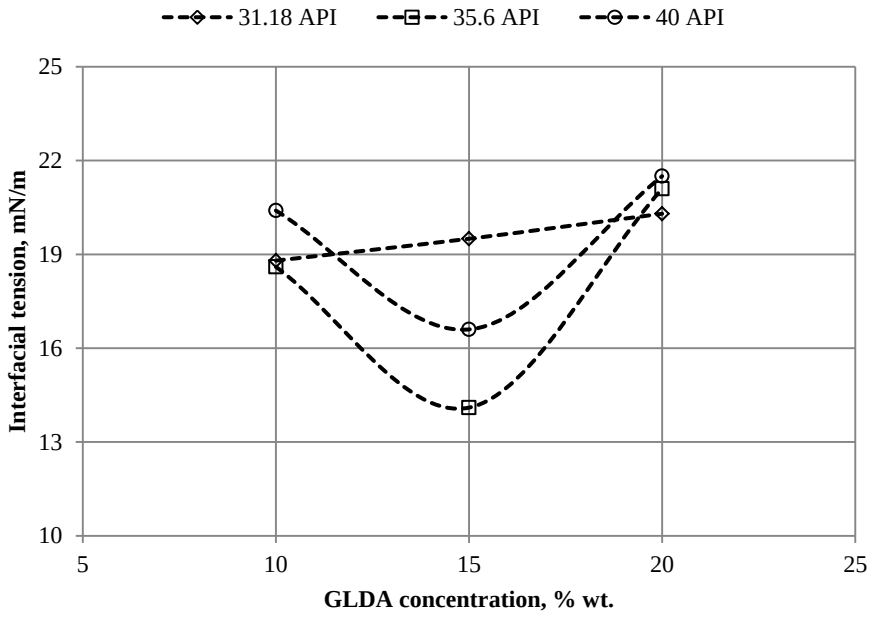

Figure 5.39: Effect of 4.0 pH GLDA concentration on Interfacial tension at temperature of 72^{o}F and atmospheric pressure

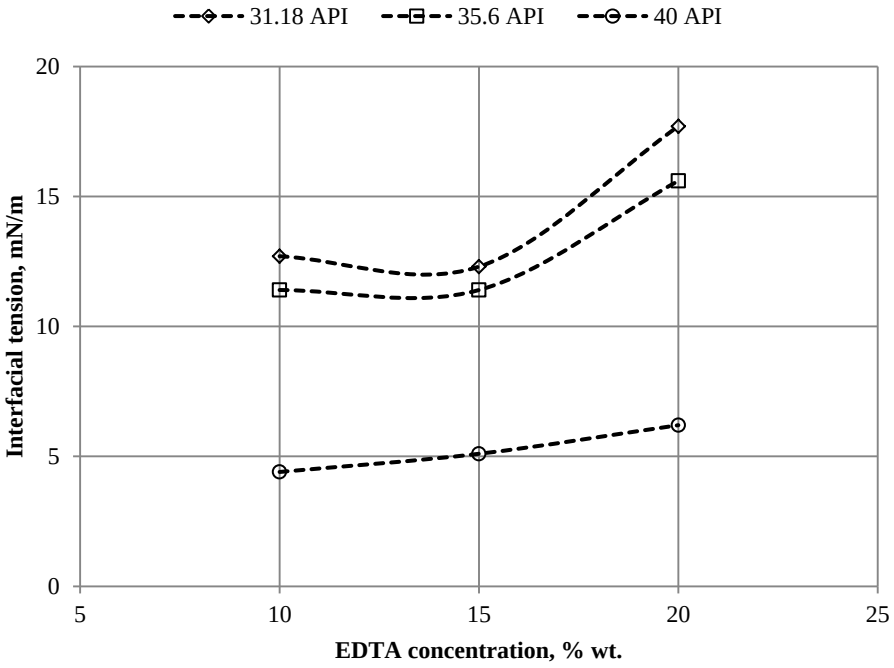

Figure 5. 40: Interfacial tension between 8.0 pH spent EDTA and crude oil at temperature of 72^{o}F and atmospheric pressure

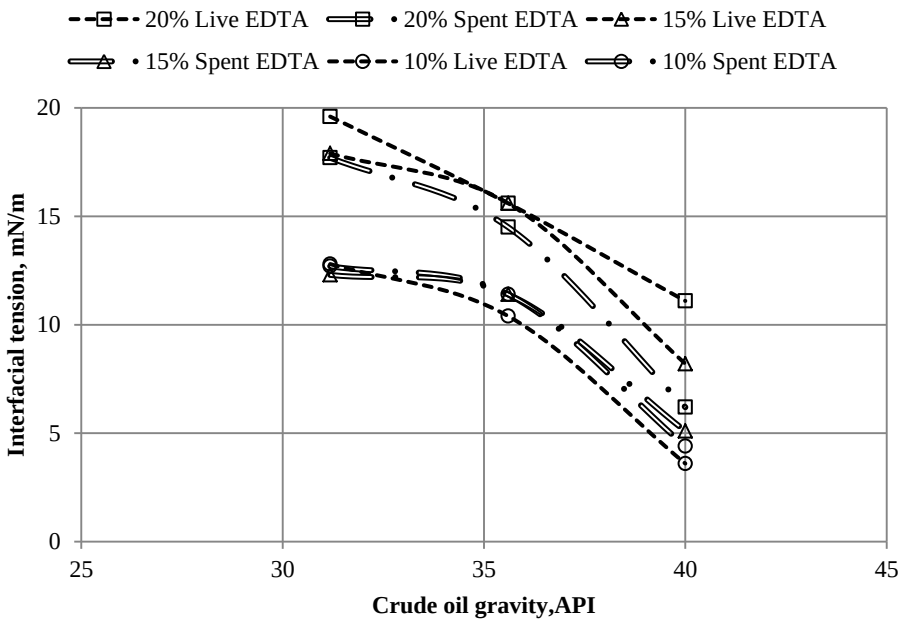

Figure 5.41: Comparisons of interfacial tension of the live and spent EDTA at temperature of 72^{o}F and atmospheric pressure

CHAPTER 6

CORE FLOODING EXPERIMENTS

6.1 Introduction

Core flooding experiments were carried out to investigate the effect of many parameters that influence the matrix treatment of carbonate rocks. These parameters are experiment temperature, injection rate, chelating agent concentration, pH of chelating agent, and water used to prepare the chelating agents. In these experiments, HEDTA, EDTA, and DTPA chelating agents at different concentrations and pH values were used to be injected at different temperatures and injection rates conditions. Deionized water and sea water were used to prepare chelating agents.

6.2 Matrix Stimulation using HEDTA

The main objective of matrix stimulation using HEDTA chelating agents was to find the optimum injection rate, and chelating agent concentration. HEDTA was prepared using sea water; and the pH value was 4.0 for all HEDTA formulations. Another three stimulation experiments were conducted using HEDTA prepared using deionized water to compare the results of both formulations in term of optimum stimulation conditions.

6.2.1 Materials used in the Experiments

Stimulation fluid used in these experiments was prepared using a formulation of HEDTA and synthetic sea water similar to Arabian Gulf sea water. The concentration of the HEDTA was 20% by weight, and the rest was sea water. The pH of HEDTA was

adjusted to be 4.0 by adding HCl to the prepared fluid. The fluid was stirred for at least 6 hours to insure homogeneity of the solution. Indiana Limestone core samples of 3.81 cm size and 15.0 cm long were used in these experiments. Their porosities were varied from 9.4% to 11.0% while permeabilities were varied from 0.33 to 6.56 md. CT scan images showed that all of the core samples were looked homogeneous. Table 5.1 shows the properties and experiments condition for each core sample.

Table 6.1: Core samples properties & experiment conditions- HEDTA formulations

	Core#	**1**	**2**	**3**	**4**	**5**	**6**	**7**	**8**	**9**
Size	cm	3.81	3.81	3.81	3.81	3.81	3.81	3.81	3.81	3.81
Length	cm	14.83	15.20	15.07	14.98	15.33	15.10	14.55	15.16	15.19
Porosity	Fraction	0.10	0.11	0.11	0.10	0.11	0.10	0.11	0.10	0.11
Permeability	md	0.94	3.75	1.29	1.02	1.54	0.33	1.92	0.49	6.56
Pore volume	Fraction	17.37	19.37	19.53	17.17	18.55	16.98	18.35	16.68	18.98
Average CT number	-	2622	2536	2576	2563	2637	2576	2589	2514	2560
Saturated fluid	-	3% KCl	3% KCl	3% KCl	3% KCl	3% KCl	3% KCl	3% KCl	3% KCl	3% KCl
HEDTA Conc.	%	20	20	20	20	20	20	20	20	20
Stimulated fluid's pH		4.0	4.0	4.0	4.0	4.0	4.0	4.0	4.0	4.0
Injection rate		0.5	1.0	2.0	4.0	1.0	2.0	4.0	0.5	1.0
Experiment temperature	^{o} F	250	250	250	250	200	200	200	200	150
Net overburden pressure	psi	500	500	500	500	500	500	500	500	500
Back pressure	psi	1000	1000	1000	1000	1000	1000	1000	1000	1000

Core flooding experiments were run at three different temperatures of 250^{o}, 200^{o}, and 150^{o} F; and four different injection rates of 0.5, 1.0, 2.0 and 4.0 cc/min. The above injection rates were repeated for the temperatures of 200^{o} and 250^{o}F, and then the optimum injection rate was used to conduct one core flooding experiment at temperature

of 150^{o}F. The optimum injection rate was found to be in the range of 0.5 to 1.0 for both temperatures of 200^{o} and 250^{o}F.

6.2.2 Matrix Stimulation at Temperature of 250^{o}F

Four experiments were conducted at 0.5, 1.0, 2.0 and 4.0 cc/min injection rates for Indiana Limestone core samples. The optimum injection rate was found to be 1.0 cc/min and 4.46 PVs was required to create a dominant wormhole throughout the length of the core sample. When similar core sample was injected with 0.5 cc/min, similar results were observed indicating that the optimum injection condition at this temperature were in the range between 0.5 to 1.0 cc/min. Optimum injection rate was selected to be 1.0 cc/min for timing point of view. Dominant and narrow wormholes with small and short branches were created when core samples were injected at 0.5 and 1.0 cc/min. For the case of 2.0 and 4.0 cc/min injection rates, wide wormholes with many branches were created indicating the existence of some sort of ramified pattern of wormholes. Figure 6.1 shows the normalized pressure drop across the core samples versus the pore volumes injected to create the WH. The peak of the pressure drop reached at almost half of the pore volumes needed. Figure 6.2 shows the core CT scan slices for the experiment conducted at temperature of 250^{o}F. These figures show clearly the WHs inside each core sample. Figure 6.3 shows the inlet phases and wormhole paths for the case of 250^{o}F. From this figure it was clear that for the case of optimum injection rates the wormholes were narrow with less number of branches which were short in length. For 2.0 and 4.0 cc/min injection rates, wormhole paths were wide with many branches indicating ramified pattern. Table 6.2 summarizes the results of the experiments conducted at temperature of 250^{o} F.

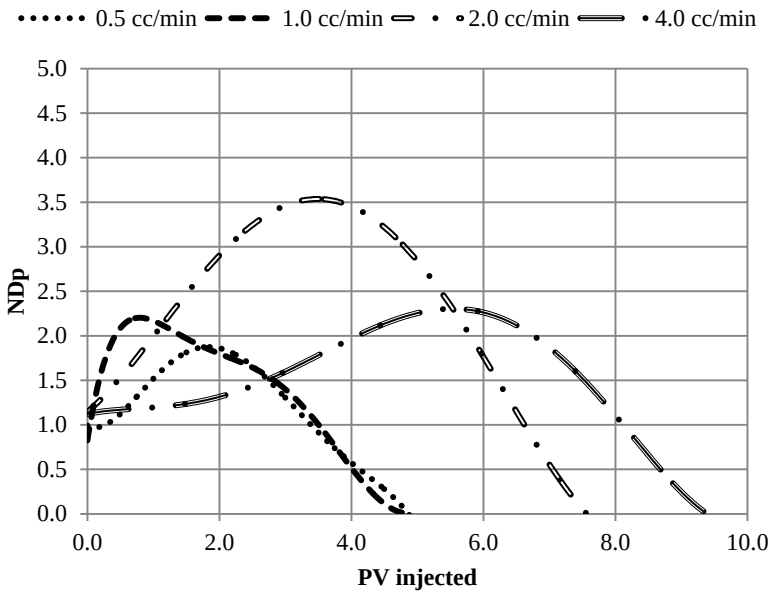

Figure 6.1: Normalized pressure drop versus pore volume injected for experiments conducted at 250^{o}F

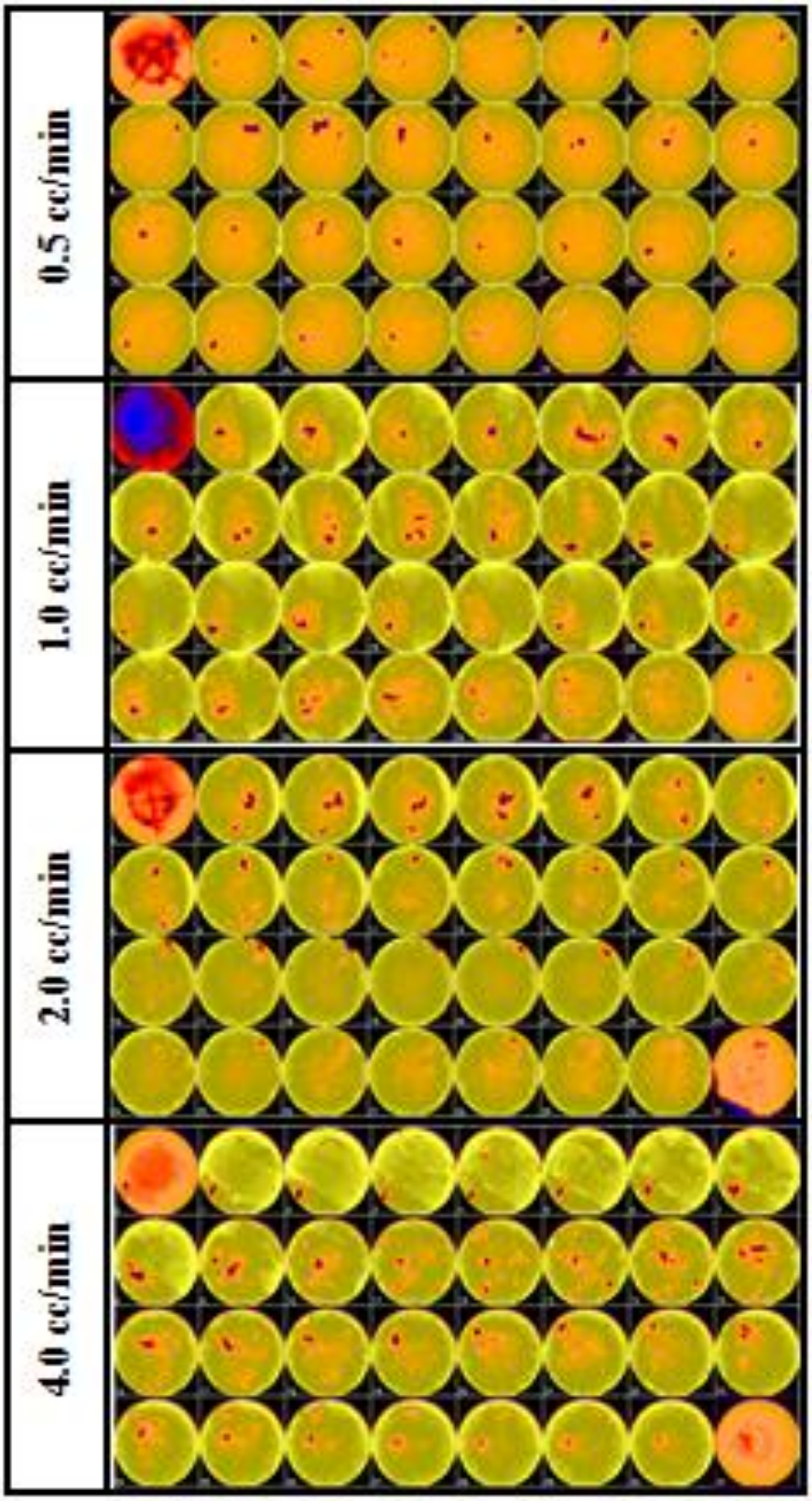

Figure 6.2: CT scan slices show the WH created at temperature of 250°F

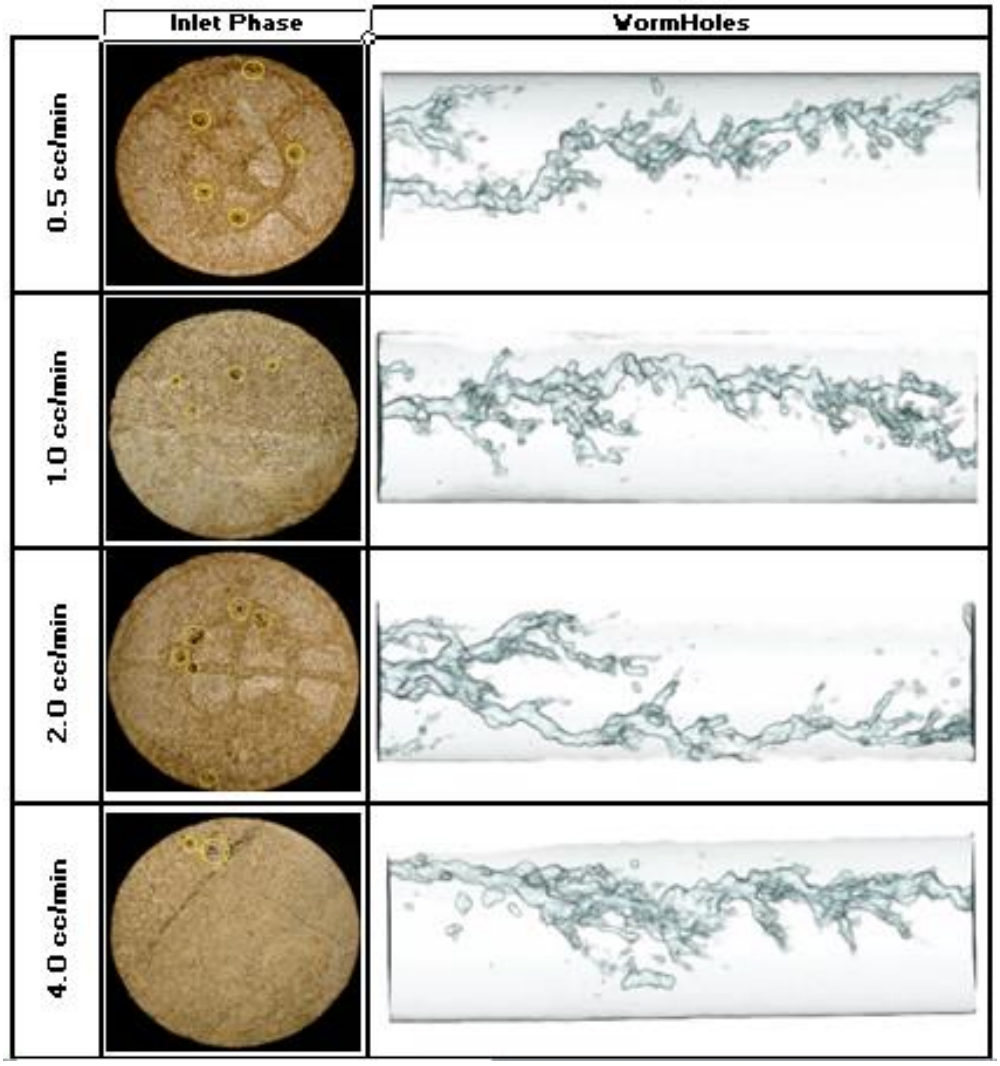

Figure 6.3: Intel phases and wormhole paths for cores stimulated at 250^{o}F

Table 6.2: Results of stimulation experiments conducted at 250°F

	Units	Exp#1	Exp#2	Exp#3	Exp#4
Injection rate	cc/min	0.5	1.0	2.0	4.0
K before	md	0.94	3.75	1.29	1.02
K after	md	195	51	76	76
K increment	Frction	207	14	59	74
PV injected	Fraction	4.40	4.46	7.18	8.70
HEDTA injected	cc	76.4	86.40	140.2	149.4

6.2.3 Matrix Stimulation at Temperature of 200°F

Four experiments were conducted at injection rates of 0.5, 1.0, 2.0 and 4.0 cc/min for Indiana Limestone core samples. The optimum injection rate was found to be 1.0 cc/min and 6.32 PVs was required to create a dominant wormhole throughout the length of the core sample. Similar results were also observed for the injection rate of 0.5 cc/min where it needed around 6.4 PVs to create dominant WHs. This is mainly due to the existence of the optimum injection rate in this range, but the optimum injection rate was selected to be 1.0 cc/min because of timing considerations. These results were in agreement with the results got at temperature of 250°F in terms of the optimum injection rate. For the injection rate of 2.0 cc/min, creation of the wormholes needed about 11.80 PVs due to the dispersion of the fluid in most of core sample pores in addition to the path of the wormhole. The situation was worse for the injection of 4.0 cc/min which required 15.40 PVs to breakthrough, but many branches were formed indicating some sort of ramified wormhole pattern. Figure 6.4 shows the normalized pressure drop versus the pore volumes injected for all the injection rates. This figure showed that the pressure drop reached its peak at almost half of the pore volumes needed to create wormholes for the optimum injection rate, while for the injection rates higher than the optimum rate the peak were reached earlier. Figure 6.5 shows the core CT scan slices for the experiment conducted at temperature of 200°F. Figure 6.6 shows the inlet faces of the core samples

after stimulation; and also the wormhole paths created at different injection rates. Wormhole for the optimum injection rate have small and short branches while for the rates 2.0 and 4.0 cc/min there were many branches which relatively longer than that of the optimum injection rate. Also the areas around the wormholes that affected by the stimulation fluid for the rates of 2.0 and 4.0 cc/min were greater than that for the optimum injection rate which was narrow. Table 6.3 summarizes the results of these experiments. In general, the increase of temperature increases the reaction rate of chelating agents; which was indicated by creating the channels with less pore volumes when comparing the stimulation results of 200^{o}F with the results of 250^{o}F.

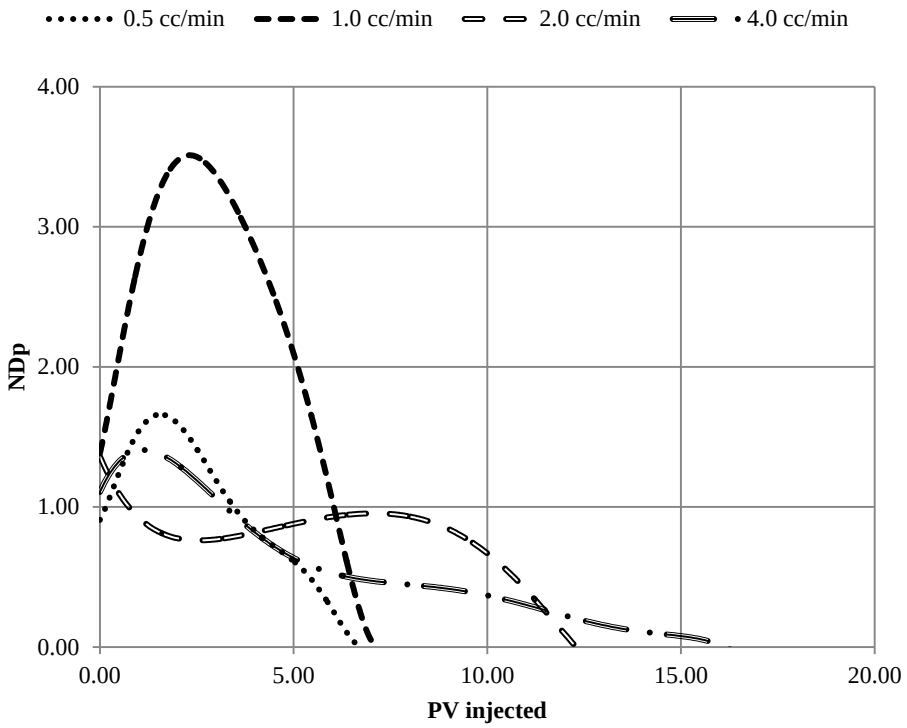

Figure 6.4: Normalized pressure drop versus the pore volume injected for the experiments conducted at 200^{o}F

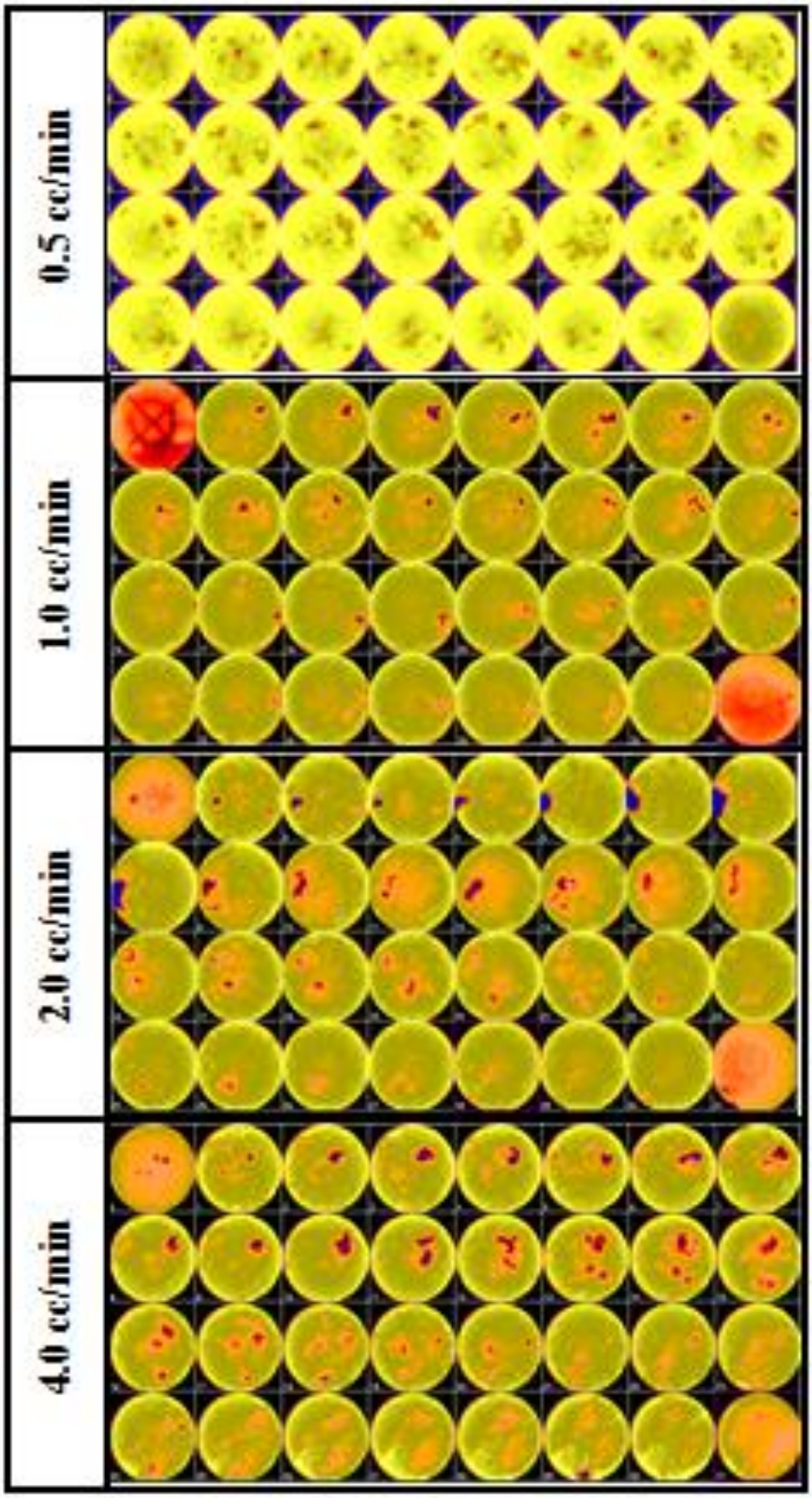

Figure 6.5: CT scan slices show the WH created at temperature of 200^{o} F

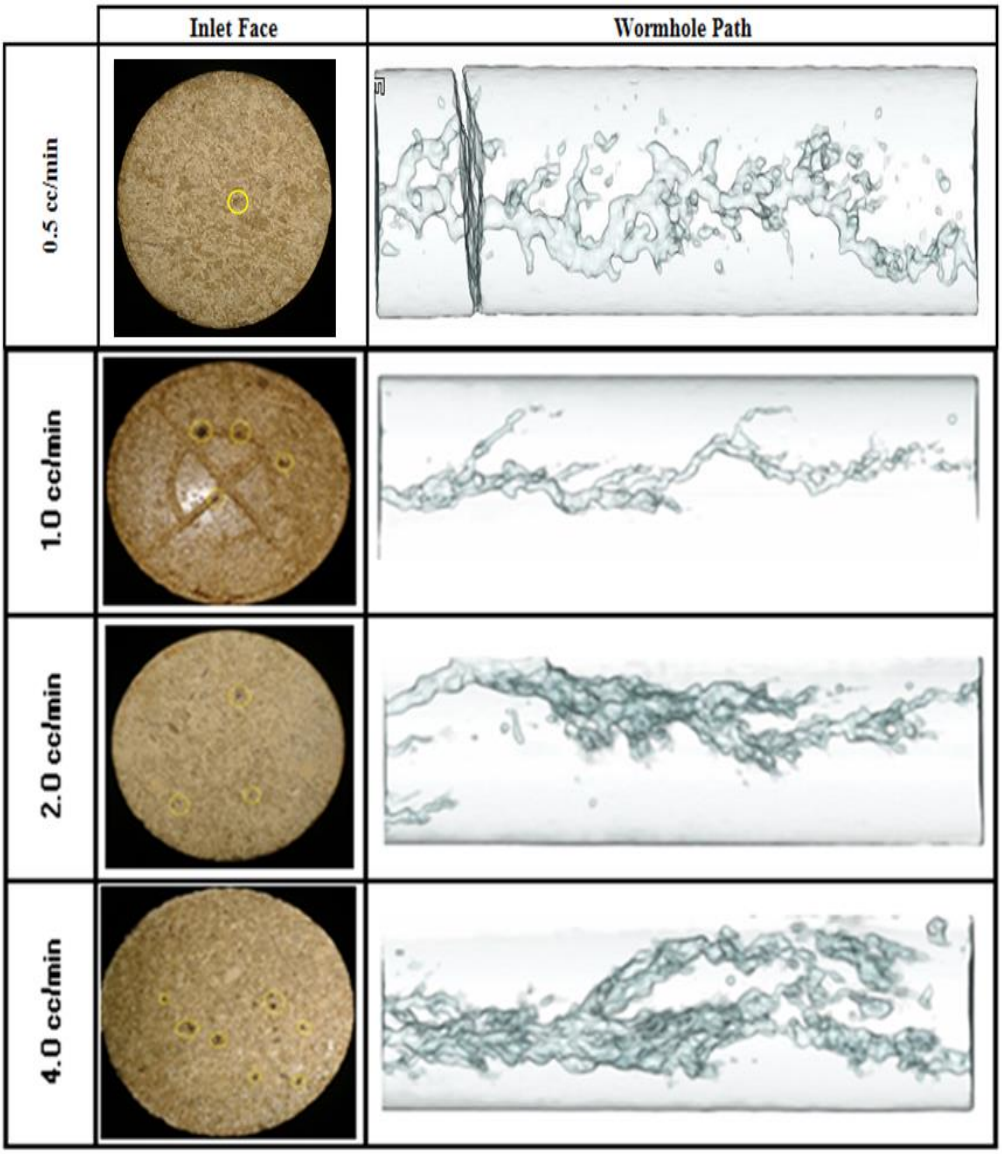

Figure 6.6: Intel phases and wormhole paths for the cores stimulated at 200°F

Table 6.3: Results of stimulation experiments conducted at 200°F

	Units	Exp#1	Exp#2	Exp#3	Exp#4
Injection rate	cc/min	0.5	1.0	2.0	4.0
K before	md	0.49	1.54	0.33	1.92
K after	md	42	51	15	312
K increment	Fraction	85	33	44	163
PV injected	Fraction	6.36	6.32	11.80	15.40
HEDTA injected	cc	106.1	117.2	200.4	282.6

6.2.4 Effect of Injection Rate on Stimulation Process

As illustrated before, the temperature showed a great effect on the pore volume to be injected to reach the breakthrough at any injection rate. Figure 6.7 shows the pore volume required to breakthrough versus the injection rate for temperatures of 200° and 250° F. This figure showed clearly the existence of an optimum injection rate for both temperatures. Also the trend of the relation is similar for both temperature values.

6.2.5 Effect of Temperature on Stimulation Process

To study the effect of experiment's temperature, three experiments were conducted at the optimum injection rate of 1.0 cc/min and three different temperatures that were 150°F, 200°F and 250°F. The aim of this experiment was to determine the required pore volumes to create the wormhole and compare it with the one that observed at the previous temperatures. Creation of dominant wormhole needed about 13.5 PVs of the core sample at temperature of 150°F. This big amount of stimulation fluid required was mainly due to low temperature which tends to weaken the reaction rate of HEDTA with the carbonate rocks. Figure 6.8 shows the normalized pressure drop versus the pore volume injected for at the three different temperatures. The figure showed clearly that the stimulation start directly reacting with the calcite rock and there was no peak in the pressure drop curve for the temperature of 150°F as compared to that of temperatures of 200° and 250°F. Also

the trend was almost linear with no curvature. The figure also concluded that as the temperature decreased, more stimulation fluid should be injected to create the dominant WH. For example, at temperature of 150^{o}F a dominant WH required about 13.5 PVs to be created as compared to 4.46 PVs required for the case of 250^{o}F. Figure 6.9 represents CT slices of the core samples that stimulated at different temperatures, which clearly confirm the creation of dominant WH at the optimum injection rate. Figure 6.10 shows the inlet faces and the WH paths for the core samples stimulated at same injection rate and different temperatures. The figure shows clearly the creation of dominant WH with fewer WH branches for all the investigated temperatures. Figure 6.11 shows the effect of temperature on the pore volume to break-through at the optimum injection rate of 1.0/m. The figure claims that at temperatures higher than 200^{o}F, the effect of temperature is not that big as compared to temperature as low as 150^{o}F or even lower, which the pore volume required is increasing sharply. Table 6.4 shows the results of the experiments conducted at the optimum injection rate and different temperatures.

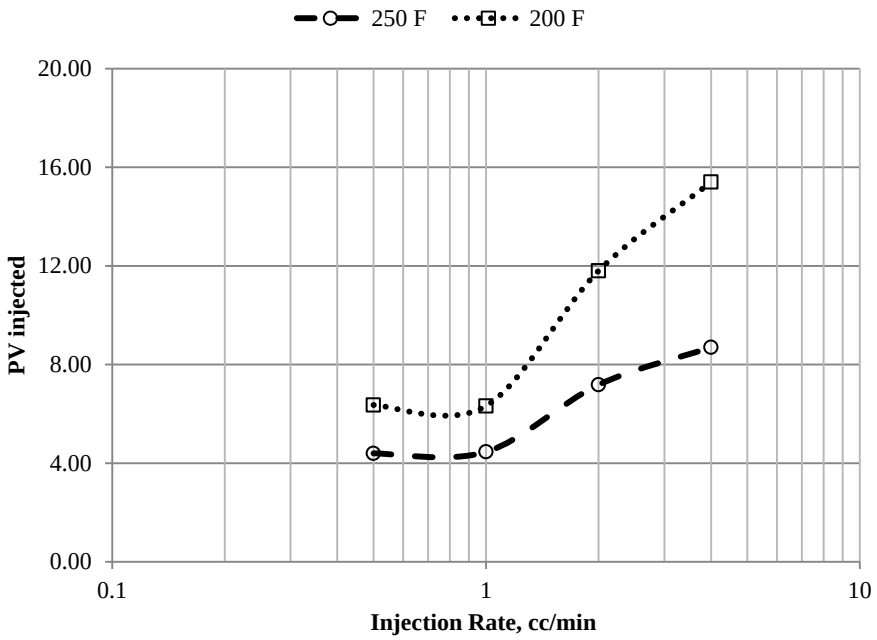

Figure 6.7: Effect of the injection rate on the stimulation process at different temperatures

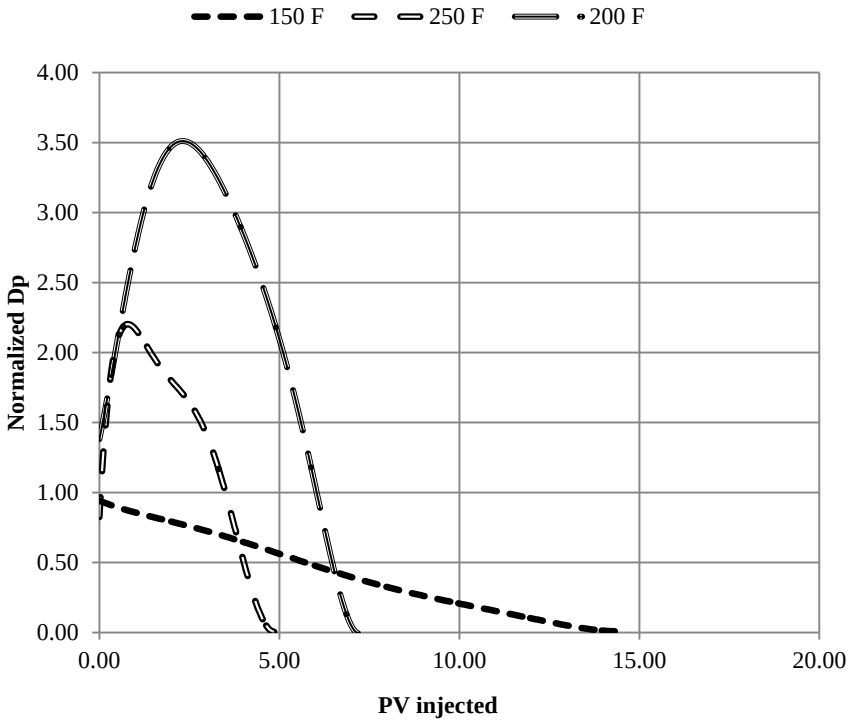

Figure 6.8: Comparison of the PVs injected at three different temperatures

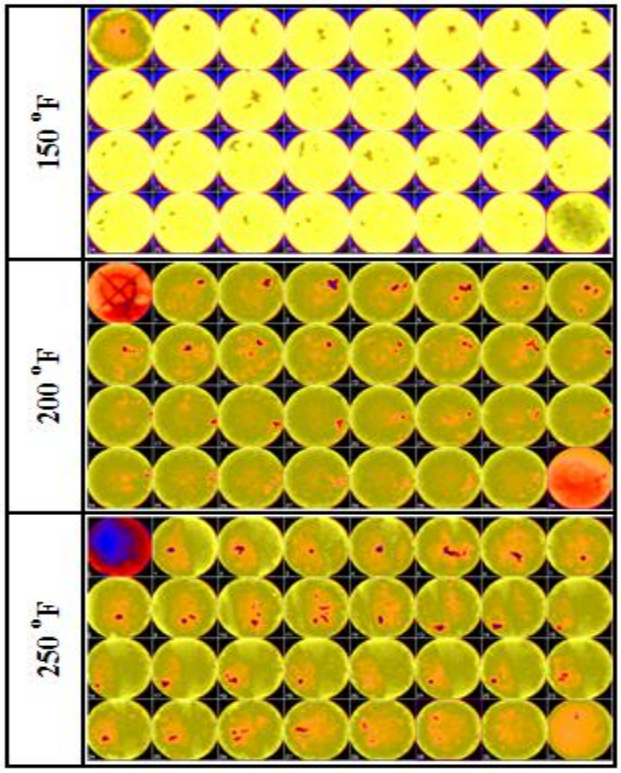

Figure 6.9: CT scans of core samples stimulated at different temperatures

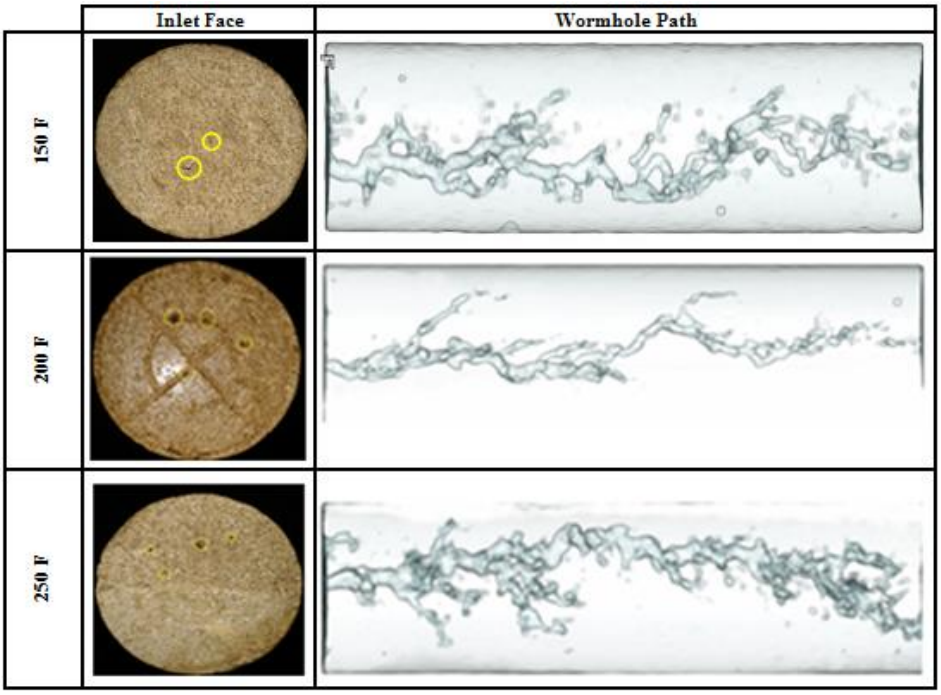

Figure 6.10: Inlet faces and WH paths of core samples stimulated at different temperatures

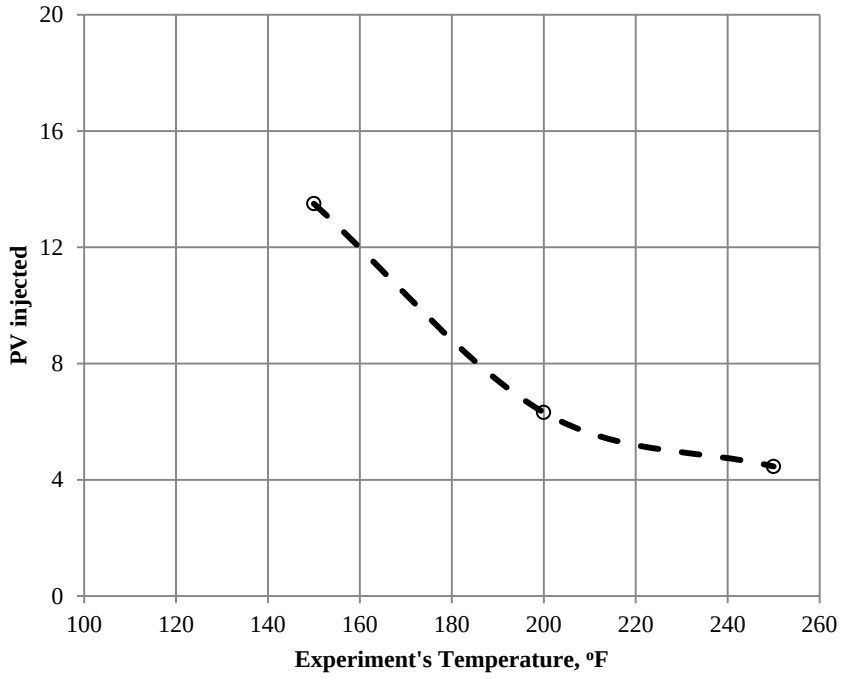

Figure 6.11: Effect of temperature on the PV to breakthrough using 20% HEDTA prepared by SW

Table 6.4: Results of stimulation experiments conducted at different temperatures

	Units	Exp#1	Exp#2	Exp#3
Injection rate	cc/min	1.0	1.0	1.0
Temperature	^{o}F	150	200	250
K before	md	6.6	1.54	0.94
K after	md	118	51	195
K increment	Fraction	18	33	207
PV injected	Fraction	13.5	6.32	4.40
HEDTA injected	cc	256	117.2	76.4

6.2.6 Effect of HEDTA Concentration on Stimulation Process

To study the effect of HEDTA concentration on the stimulation process, three stimulation experiments were conducted at temperature of 250^{o}F, injection rate of 1.0 cc/m and three different HEDTA concentrations that were 10%, 15%, and 20% by weight. Figure 6.12 shows the normalized pressure drop versus the pore volume injected for the experiments conducted at different HEDTA concentrations. Based on the results of these experiments, higher concentrations of HEDTA fluids required lower amount of stimulation fluid to create optimum WHs. As the HEDTA concentration decrease, the volume required to breakthrough will increase. Figure 6.13 shows the relation between the HEDTA concentration and the volume required to create WHs. This figure shows the decreasing trend of pore volumes required with the increase of HEDTA concentration. Figures 6.14 and 6.15 show the CT slices, inlet and outlet of the core samples stimulated at different HEDTA concentrations, which clearly showed the creation of single and dominant WH. Table 6.5 summarizes the results of the experiments conducted at temperature of 250^{o}F, injection rate of 1.0 cc/m and different HEDTA concentrations.

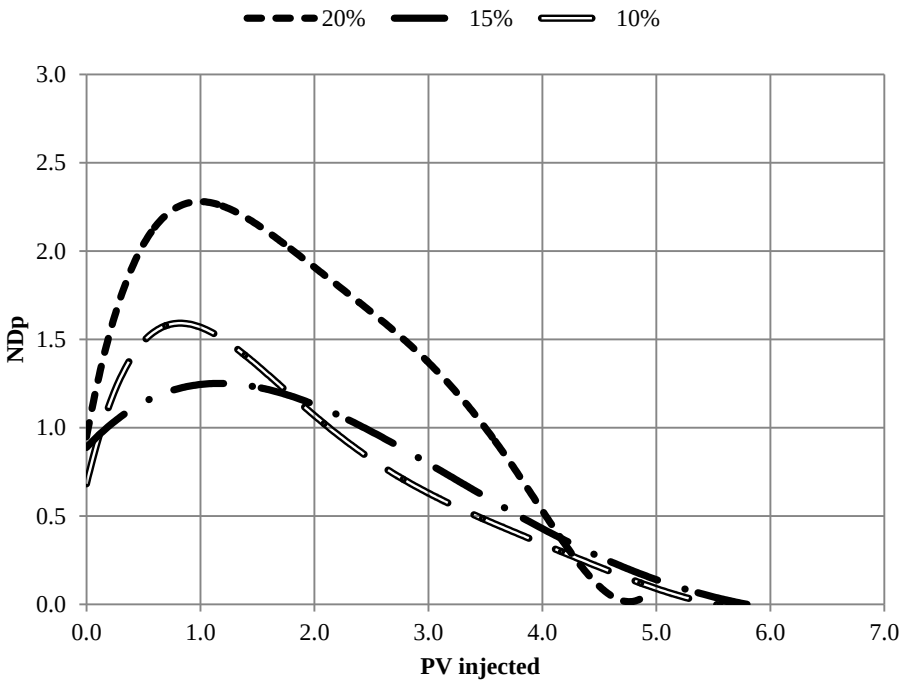

Figure 6.12: Normalized pressure drop versus PV injected for experiments conducted at different HEDTA concentrations and temperature of 250^{o}F

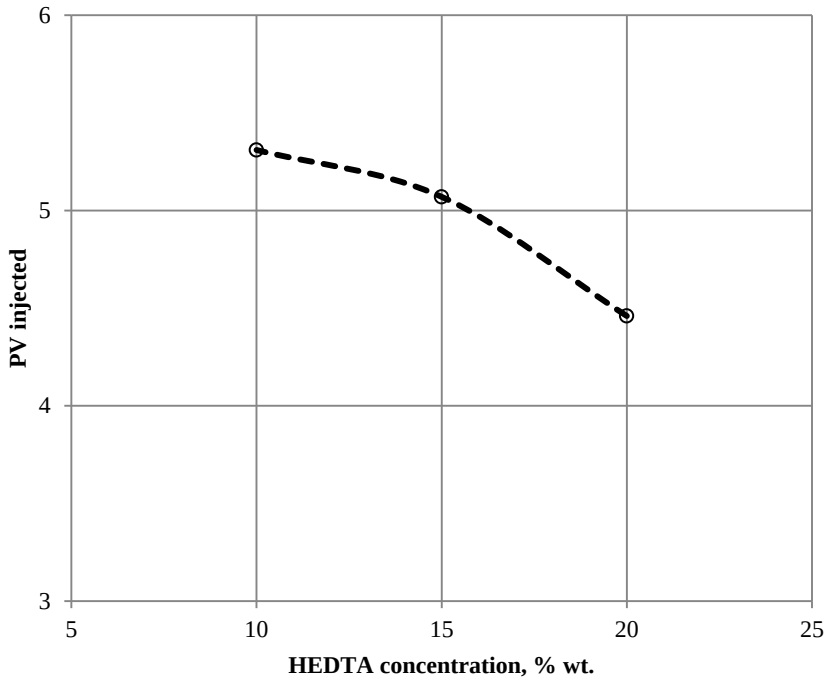

Figure 6.13: Effect of HEDTA concentration on the PV required to breakthrough at temperature of 250^{o}F

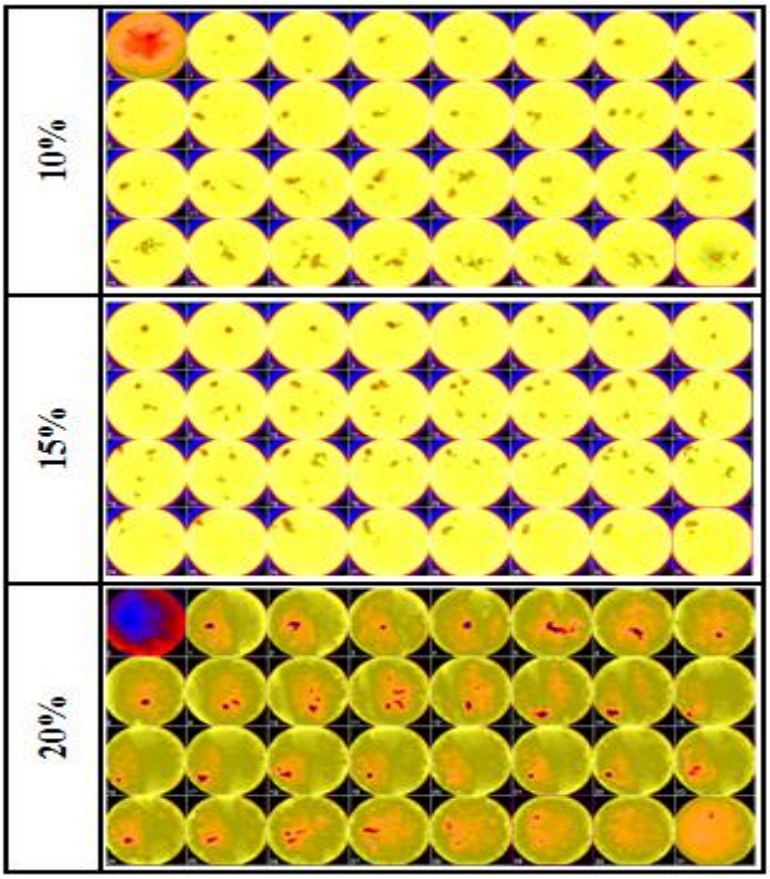

Figure 6.14: CT scan of the core samples stimulated at different HEDTA concentrations and temperature of 250°F

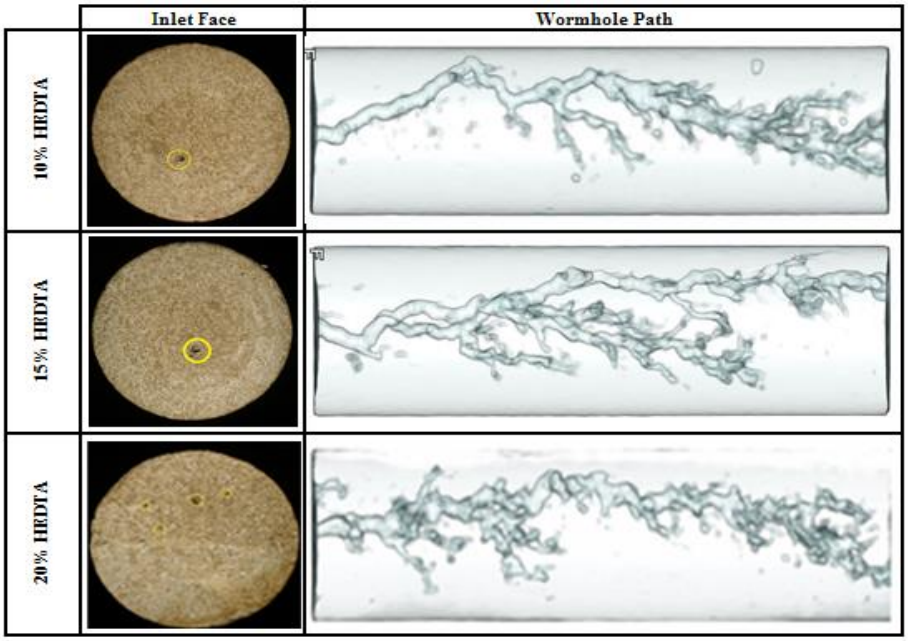

Figure 6.15: Inlet faces and WH paths for core samples stimulated at different HEDTA concentrations and temperature of 250°F

Table 6. 5: Results of stimulation experiments conducted at different temperature

	Units	Exp#1	Exp#2	Exp#3
Injection rate	cc/min	1.0	1.0	1.0
Concentration	% wt.	10	15	20
K before	md	0.70	0.52	0.94
K after	md	1266	1266	195
K increment	Fraction	1811	2440	207
PV injected	Fraction	5.31	5.07	4.40
HEDTA injected	cc	87.3	88.6	76.4

6.2.7 Effect of Mixing HEDTA with Sea Water

To investigate the effect of mixing HEDTA with sea water instead of deionized water, three stimulation experiments were conducted by using 4.0 pH, 20% HEDTA prepared by deionized water. The experiments were conducted using three different injection rates that were 0.5, 1.0, and 4.0 cc/m. Figure 6.16 shows normalized pressure drop versus the pore volume injected for the three core samples stimulated using 20% HEDTA prepared by deionized water at temperature of 250^{o} F. Figure 6.17 shows the comparison between the experiment results of the stimulation conducted using 4.0 pH, 20% HEDTA prepared by deionized water and sea water. The performance of the fluid prepared by sea water was similar to that prepared by deionized water with slight differences in terms of ore volume required to break through. In general, experiments conducted with HEDTA prepared by deionized water consumed small amount of fluid to create WH as compared to that prepared by sea water. Even at low rates, the chelating agent will not totally be consumed to create the WHs. And because sea water has relatively small amounts of ions such as calcium and magnesium, HEDTA will not lose much of its chelation power. Figure 6.18 and 6.19 show the CT scan, inlet faces, and WH paths for the core samples stimulated using 4.0 pH, 20% HEDTA prepared by deionized water. Table 6.6 summarizes the results of the experiments conducted using the above mentioned stimulation fluid at different injection rates.

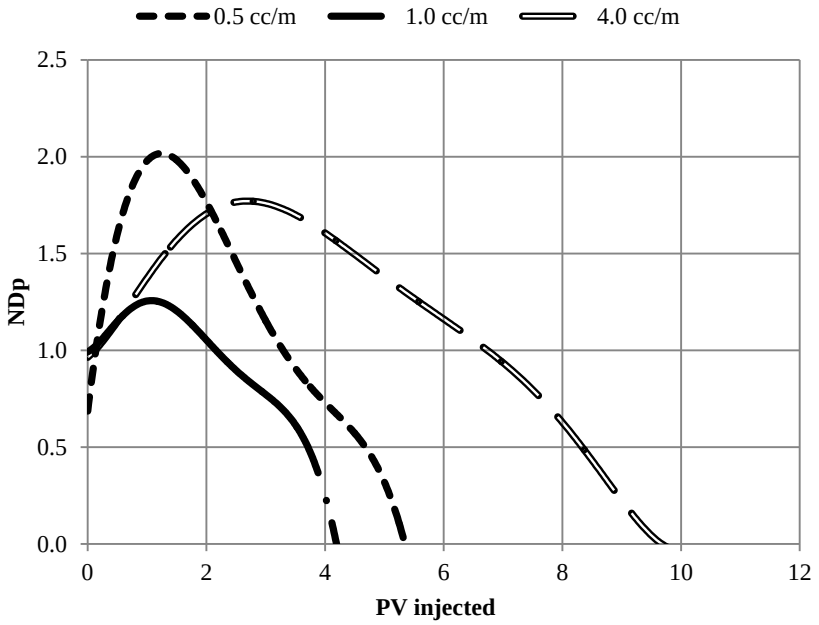

Figure 6.16: Normalized pressure drop versus PV injected for core samples stimulated with HEDTA prepared by DI water at temperature of 250°F

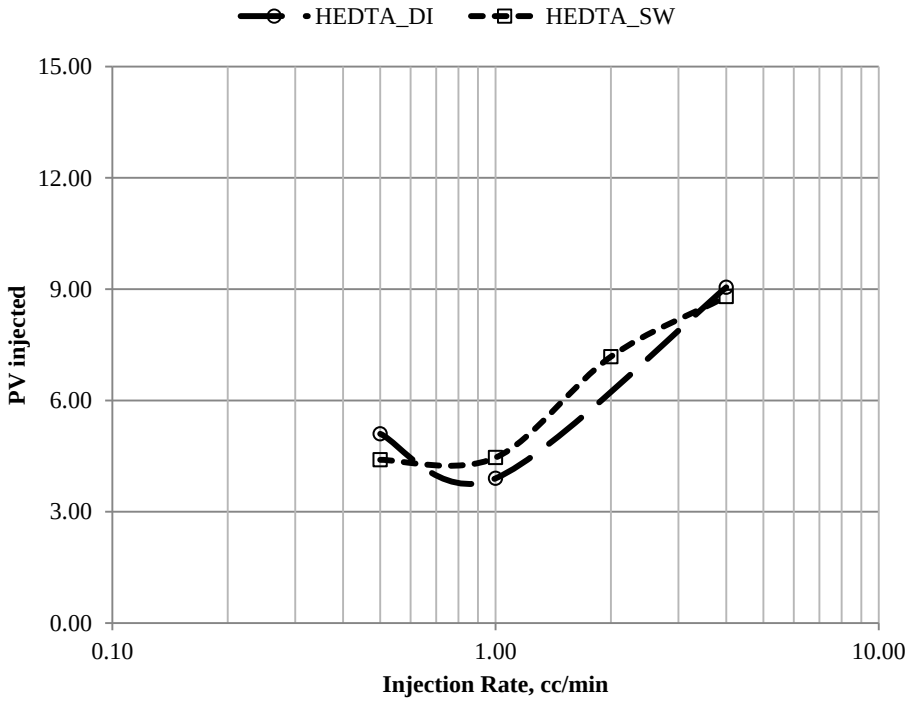

Figure 6.17: Comparison between the experiments conducted using HEDTA prepared by DI water and that prepared by sea water at temperature of 250°F

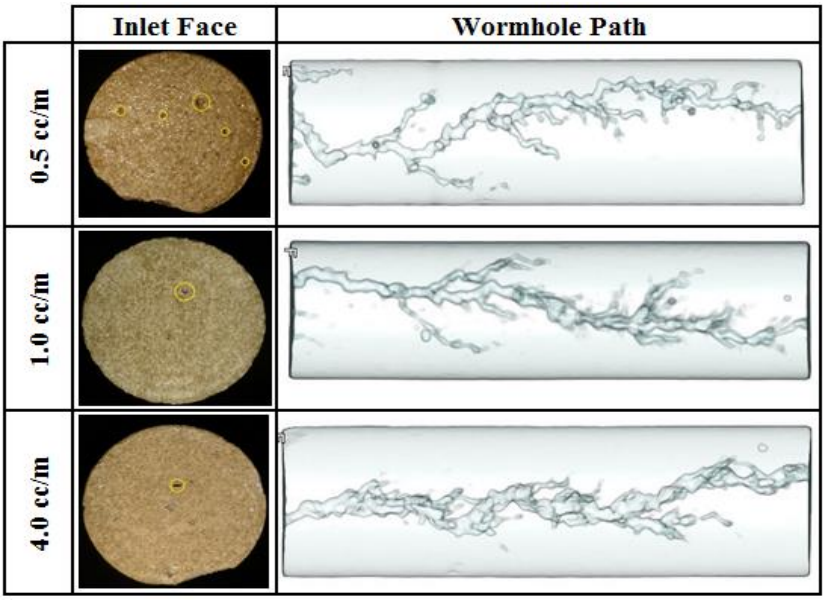

Figure 6.18: Inlet faces and WH paths for core samples stimulated using HEDTA prepared by DI water at temperature of 250^{o}F

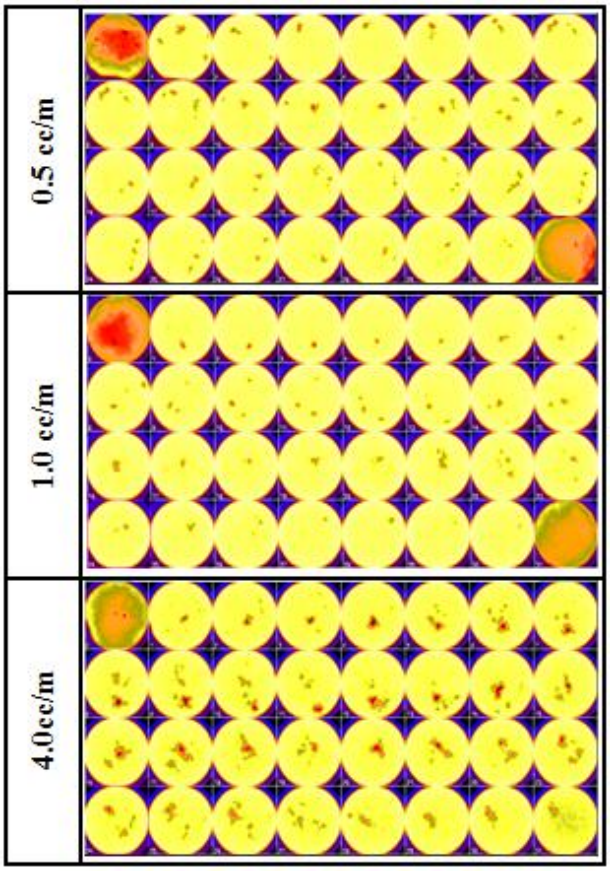

Figure 6. 19: CT scan slices show the WH created using HEDTA prepared by DI water at temperature of 250^{o}F

Table 6.6: Results of experiments conducted using HEDTA prepared by DI water at 250^{o} F

	Units	Exp#1	Exp#2	Exp#3
Injection rate	cc/min	0.5	1.0	4.0
K before	md	0.45	0.45	0.46
K after	md	47	898	560
K increment	Fraction	116	1988	1207
PV injected	Fraction	5.10	3.90	9.05
HEDTA injected	cc	79.1	63.9	154.6

6.2.8 Optimum Conditions for HEDTA Chelating Agent

It is always very important to determine the optimum conditions for any operation in order to be performed in an efficient manner and as low cost as possible. That is why finding the optimum stimulation conditions are very important. Always stimulation treatment should be designed to use the lowest possible volume of stimulation fluid and at the same time perform the treatment at the lowest possible time. Based on the previous experiments, the lowest possible time can be achieved by injecting at high injection rates, but in this case the volume of the stimulation fluid will be high. If we inject the stimulation fluid at low rates, the volume of stimulation fluid will be less, but the time to perform the matrix treatment will be more than that required when high rates are used. So normally economics will be a vital role in the optimum conditions for stimulation treatments. For example, in offshore area where daily operation rates are very high, cost of stimulation fluid may be small as compared to the time required to perform the stimulation.

A method of plotting the normalized volume required to breakthrough and normalized time to breakthrough was proposed to assist in defining the optimum injection rate and optimum HEDTA concentration. The procedure is to plot both normalized parameters against the injection rate or HEDTA concentration, and the point at which both curves

cross will be the optimum condition. Normalized volume to breakthrough is defined as volume required to breakthrough at certain rate or HEDTA concentration divided by the minimum possible volume to create WH for a set of experiments conducted at same condition and only injection rate should be changed. Mathematically:

$$NV_{bt} = \frac{V_{bt}}{V_{bt_{min}}} \tag{6.1}$$

where NV_{bt} is normalized volume to breakthrough, V_{bt} is volume to breakthrough for specific experiment, and V_{bt_min} is minimum volume to breakthrough for set of experiments.

Normalized time to breakthrough is defined as the time required to breakthrough for certain rate or HEDTA concentration divided by the minimum possible time for a set of experiments. Mathematically:

$$Nt_{bt} = \frac{t_{bt}}{t_{bt_{min}}} \tag{6.2}$$

where Nt_{bt} is normalized time to breakthrough, t_{bt} is time to breakthrough for specific experiment, and t_{bt_min} is minimum time to breakthrough for set of experiments.

Minimum volume and time will be selected from set of experiments performed at similar condition and only one parameter will be changed. For example, injection rate will be changed and temperature and stimulation fluid will remain same. Figures 6.20 and 6.21 show the optimum conditions for the experiments conducted at 200^{o}F and 250^{o}F using the same stimulation fluid. These two figures suggested that the optimum injection rates in terms of low volume and time to perform the stimulation are about 2.1 cc/m for temperature of 250^{o}F, and 1.5 cc/m for temperature of 200^{o}F. Figure 6.22 shows the

normalized curves for defining the optimum concentration for HEDTA prepared sea water. The optimum HEDTA concentration was found to be 10% by weight which resulted in low volume as well as time to perform an optimum and efficient matrix stimulation. Figure 6.23 shows the optimum conditions for the experiments conducted at 250^{o}F using 20% HEDTA prepared by deionized water. The figure suggested that the optimum injection rate is about 1.6 cc/m.

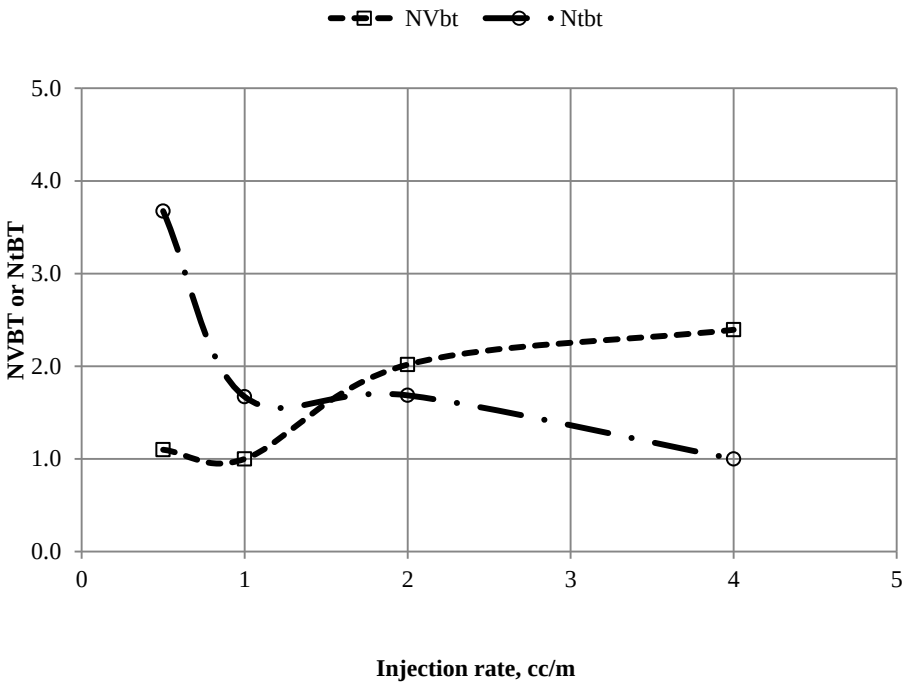

Figure 6.20: Optimum conditions for 20% HEDTA prepared by sea water at 200°F

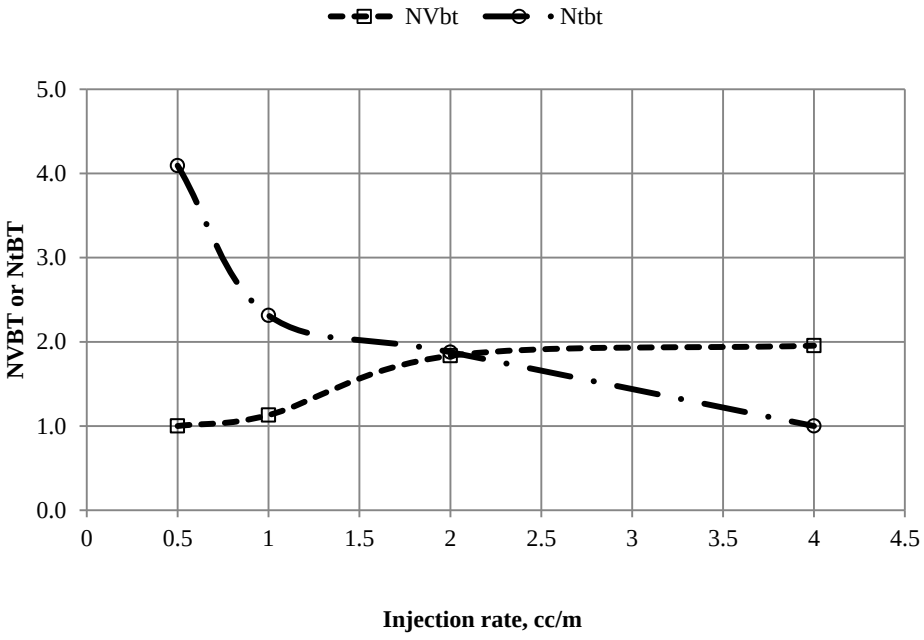

Figure 6.21: Optimum conditions for 20% HEDTA prepared by sea water at 250°F

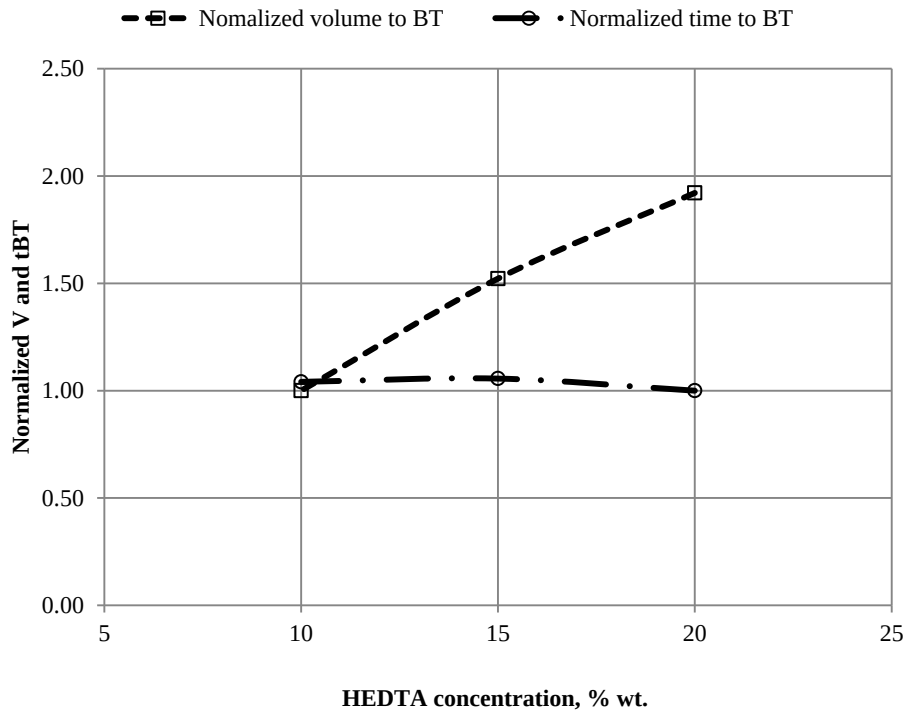

Figure 6.22: Optimum concentration of HEDTA prepared by sea water at 250°F

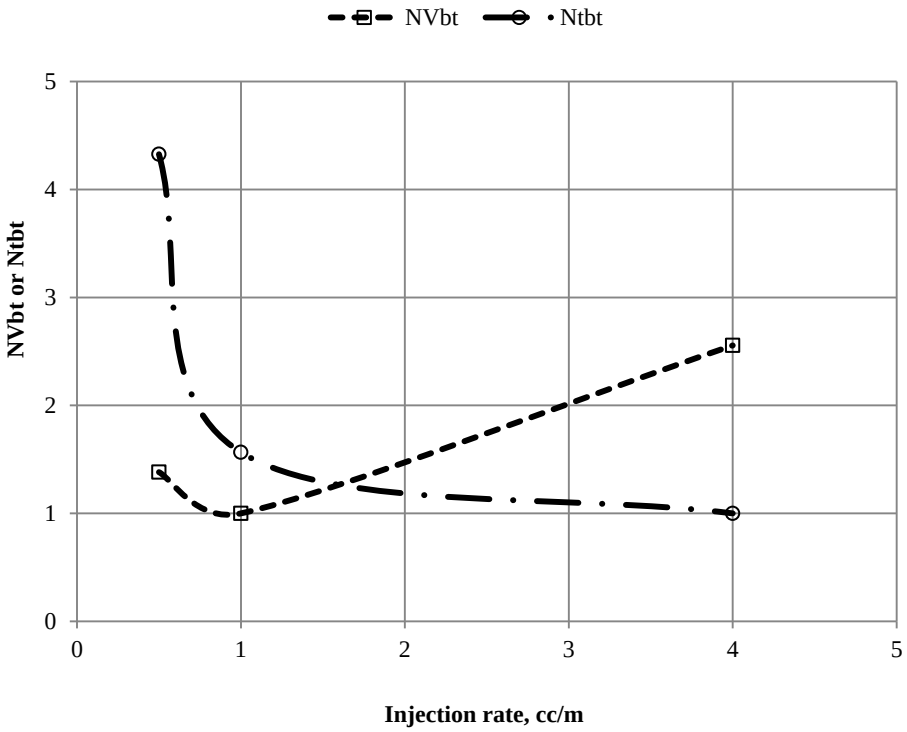

Figure 6.23: Optimum conditions for 20% HEDTA prepared by DI water at 250°F

6.3 Matrix Stimulation using EDTA Chelating Agent

Three fluids of EDTA formulations were prepared by deionized water to be injected inside Austin Chalk core samples as stimulation fluids. All the three core flooding experiments were run at same conditions of 250^{o}F temperature, 1.0 cc/min injection rate, 500 psi net overburden pressure, and 1000 psi back pressure. Another three matrix stimulation treatments were performed using EDTA prepared by sea water and injected inside Indiana Limestone core samples.

6.3.1 Materials used in the Experiments

A 37% EDTA solution having a pH of 8.35 was used to prepare stimulation fluids using DI water and sea water. HCl acid and NaOH were used to adjust the solution pH to the required value. The selected EDTA formulations were 18.5% wt. EDTA 10.0 pH, 9.5%wt. EDTA 10.0 pH and 9.25 %wt. EDTA 4.5 pH. Another 7.0 pH, 18.5% EDTA stimulation fluid was prepared by sea water. All of these fluids were stirred for at least 6 hours to insure their homogeneity.

Austin Chalk core samples of 3.81 cm size and 7.5 cm long and Indiana Limestone core samples of 3.81 cm size and 15.0 cm long were used in these experiments. Austin Chalk porosities were almost similar about 30% while permeabilities were varied from 10 to 15 md, whereas porosities and permeabilities of Indiana Limestone cores were 10.1% - 10.3% and 0.62 – 0.7 md, respectively. CT scan images showed that all of the core samples were looked homogeneous. Table 6.7 shows the properties and experiment condition for each core sample.

Table 6.7: Core samples properties and experiment conditions - EDTA formulations

	Units	Core#1	Core#2	Core#3	Core#4	Core#5	Core#6
Rock Type		Austin Chalk	Austin Chalk	Austin Chalk	Ind. L. stone	Ind. L. stone	Ind. L. stone
Size	cm	3.81	3.81	3.81	3.81	3.81	3.81
Length	cm	7.45	7.50	7.29	15.17	13.40	15.04
Porosity	Fraction	0.29	0.30	0.29	0.102	0.101	0.103
Permeability	md	15.01	13.03	10.34	0.70	0.62	0.69
Pore volume	Fraction	24.61	25.48	24.01	17.76	15.45	17.77
CT number	-	2178	2122	2113	2610	2576	26114
Saturated fluid	-	DI water	DI water	DI water	3% KCl	3% KCl	3% KCl
EDTA Fluid		18.5%DI	9.25%DI	9.25%DI	18.5%SW	18.5%SW	18.5%SW
pH		10.0 pH	10.0 pH	4.5 pH			
Injection rate	cc/min	1.0	1.0	1.0	0.5	1.0	4.0
Temperature	oF	250	250	250	250	250	250
Net ob. pressure	psi	500	500	500	500	500	500
Back pressure	psi	1000	1000	1000	1000	1000	1000

6.3.2 Effect of EDTA Concentration and pH

Three stimulation treatments were conducted at same temperature of 250^{o}F and same injection rate of 1.0 cc/m. The objective of these experiments was to find out the effect of the EDTA concentration and also the solution pH on the pore volume required to create the WHs. Figure 6.24 shows the pore volume to breakthrough for each stimulation fluid. Among the three fluids, 9.25% EDTA of 4.5 pH has the best performance which resulted in the minimum pore volume of about 2.8 PVs. Figure 6.25 shows the normalized pressure drop as the stimulation fluids were injected. 9.25% EDTA of 4.5 pH showed the lowest amount of stimulation fluid amongst the three fluids. Although 18% EDTA is more concentrated than the other two fluids, it needed more volume to create the wormhole. In other words, the non-spent fluid in the concentrated formulation was greater than that for the less concentrated ones. Figures 6.26 and 6.27 show the CT scan, inlet faces and the WH paths for the core samples stimulated by the above fluids.

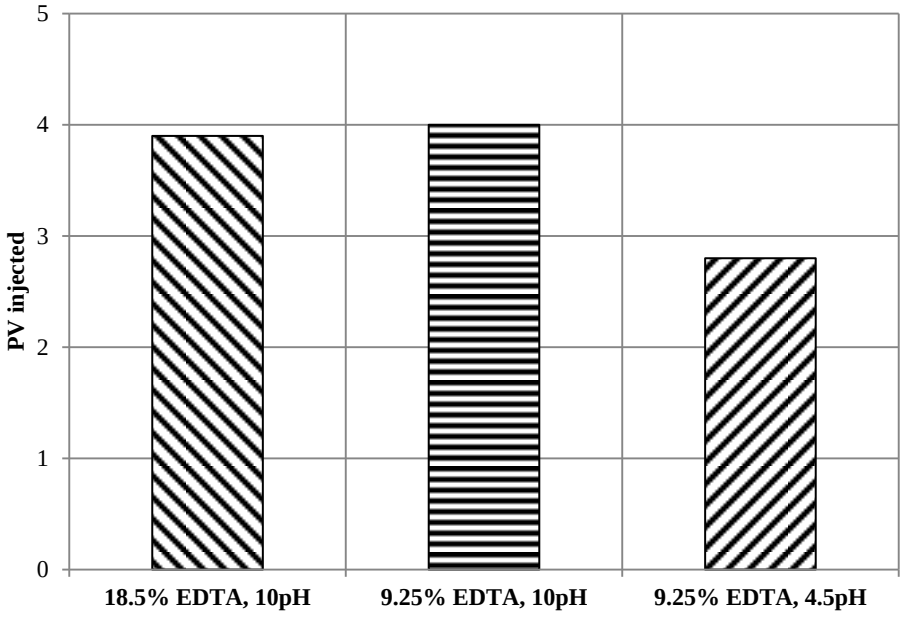

Figure 6.24: Pore volume to breakthrough for different EDTA fluids prepared by DI water at temperature of 250°F

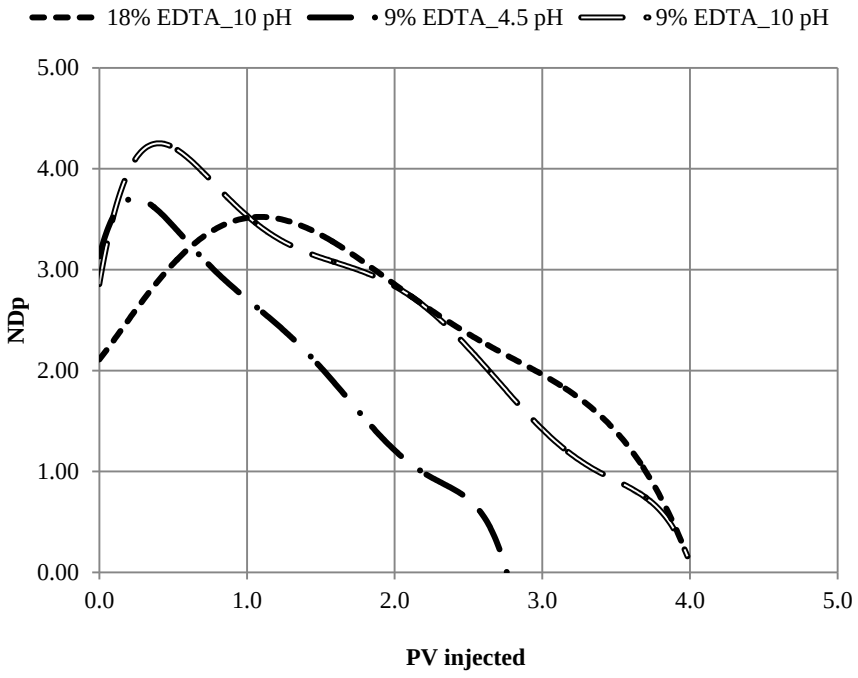

Figure 6.25: normalized pressure drop versus PV injected for core samples stimulated by EDTA at temperature of 250°F

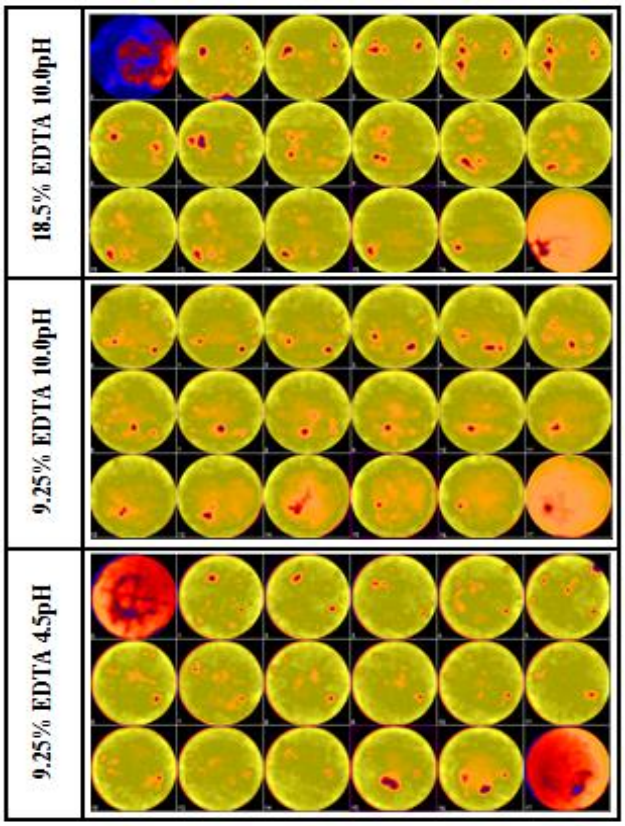

Figure 6.26: CT slices of the core samples stimulated using EDTA prepared by DI water at temperature of 250^{o}F

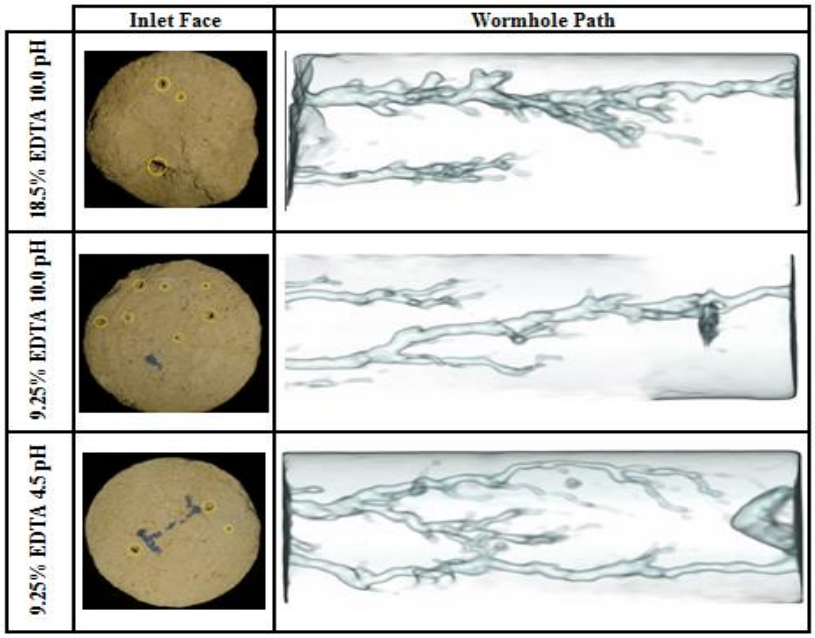

Figure 6.27: Inlet faces and WH paths for the core samples stimulated using EDTA prepared by DI water at temperature of 250^{o}F

6.3.3 Effect of Injection Rate on the Stimulation with EDTA

Three stimulation treatments were conducted at same temperature of 250^{o}F and different injection rates using 7.0 pH, 18.5% EDTA cheating agent prepared by sea water. The objective of these experiments was to find the optimum injection rate. Three injection rates of 0.5, 1.0, and 4.0 cc/m were selected to be used to inject the stimulation fluid. Figure 6.28 shows the normalized pressure drop versus the PV injected for the above three injection rates. Injection rate of 0.5 cc/m was the best rate amongst the three rates, which created dominant WH by injecting only 2.70 PVs. Figure 6.29 shows the relation between the injection rate and the PV to breakthrough. This figure suggested that the optimum injection rate is less than 0.5 cc/m, which can result in PV less than that of 0.5 cc/m.

If the lowest possible volume and time to perform the stimulation treatment were considered in determining the optimum stimulation conditions, the injection rate of nearly 2.0 cc/m will be the optimum injection rate as can be shown in figure 6.30. Figures 6.31 and 6.32 show the CT scans, inlet faces and the WH paths for the core samples stimulated with 18.5% EDTA prepared by sea water.

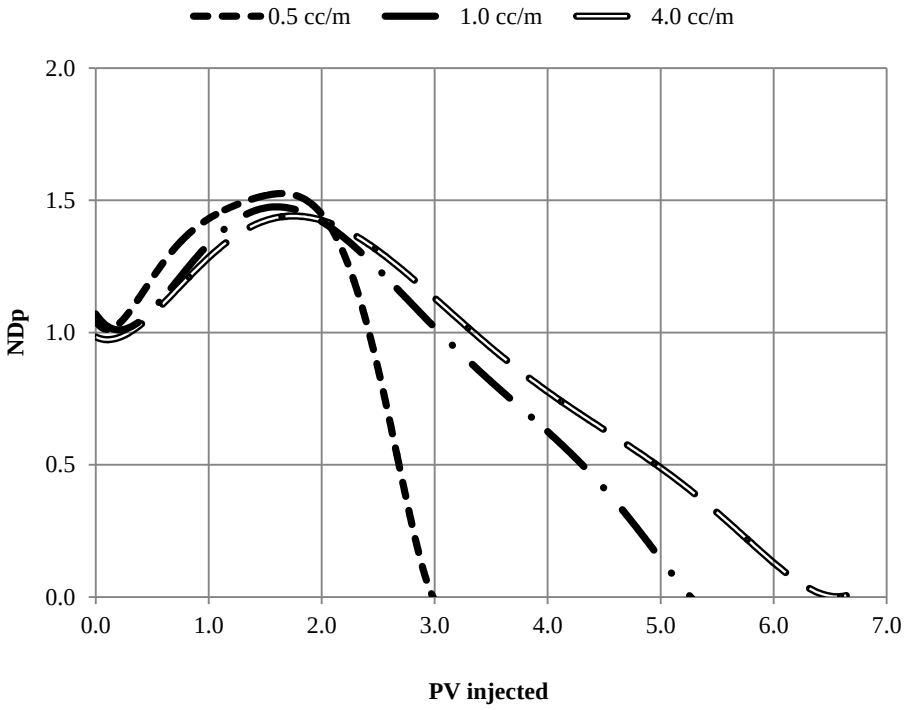

Figure 6.28: Normalized pressure drop versus the PV injected for the core samples stimulated with EDTA prepared by sea water at temperature of 250°F

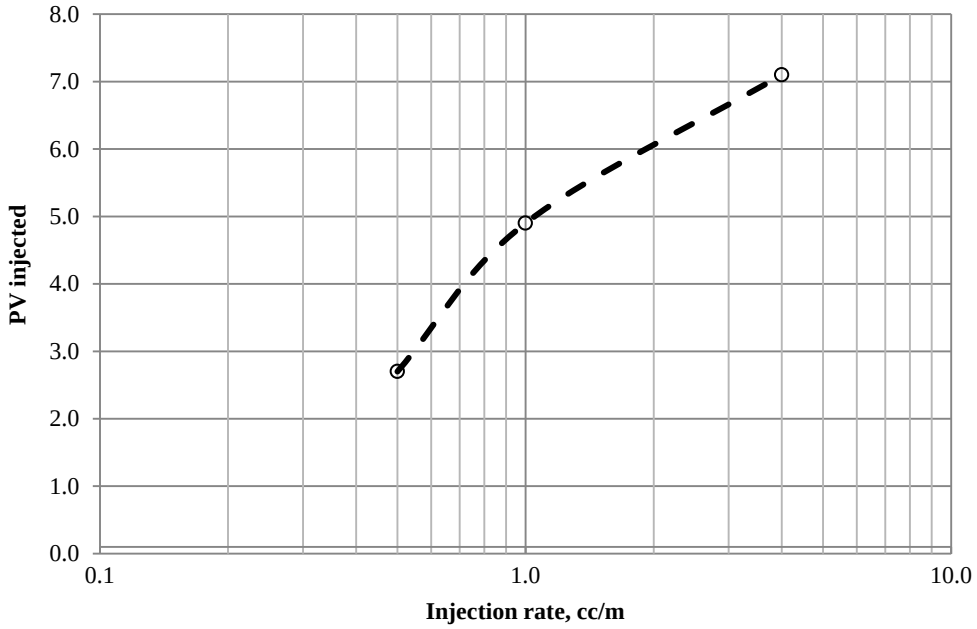

Figure 6.29: Effect of injection rate on PV at breakthrough at temperature of 250°F

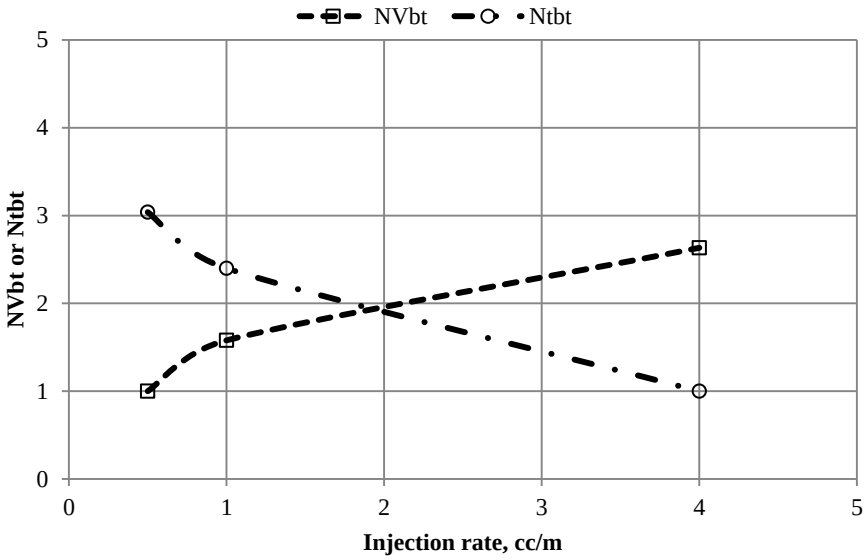

Figure 6.30: Optimum condition for 18.5% EDTA fluid prepared by sea water at temperature of 250°F

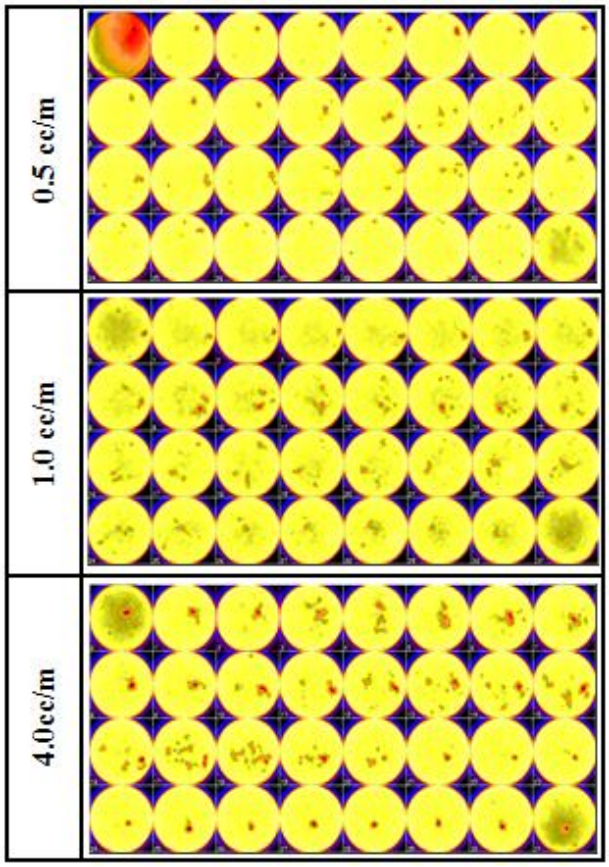

Figure 6.31: CT slices of the core samples stimulated using EDTA prepared by sea water at temperature of 250°F

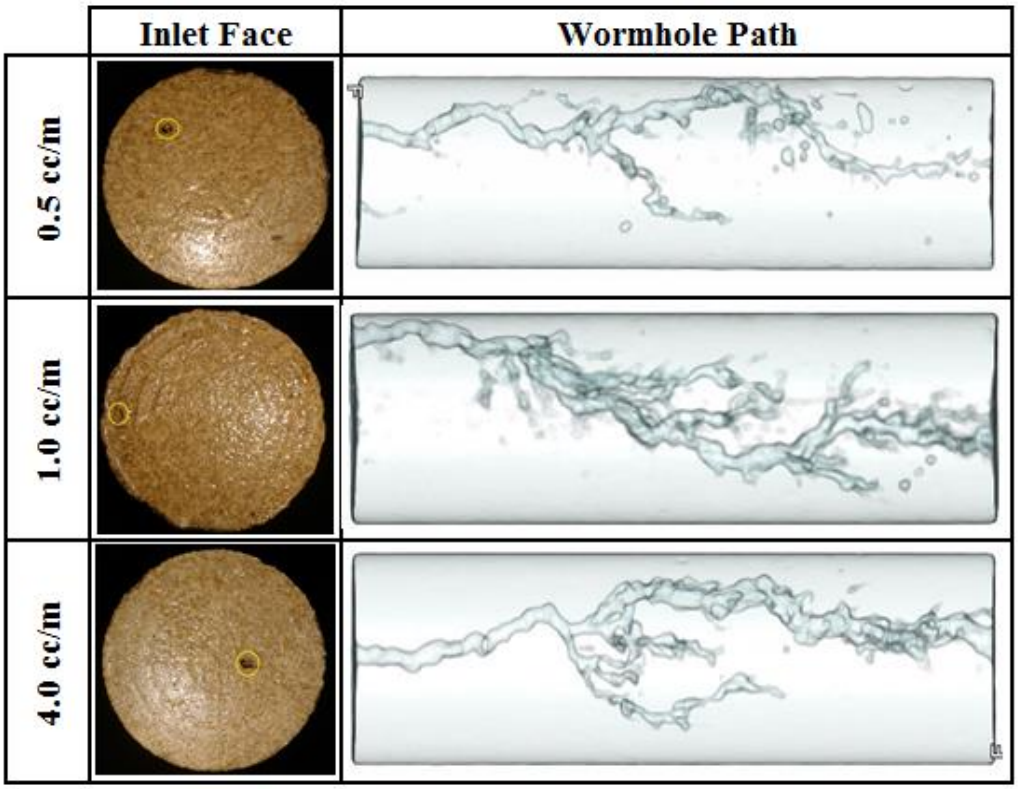

Figure 6.32: Inlet faces and WH paths for the core samples stimulated using EDTA prepared by sea water at temperature of 250^{o}F

6.4 Matrix Stimulation using DTPA Chelating Agent

Five DTPA fluid formulations were prepared to be injected in Austin Chalk core samples as stimulation fluids. All the five core flooding experiments were run at same conditions of 250^{o}F temperature, 1.0 cc/min injection rate, 500 psi net overburden pressure and 1000 psi back pressure. The objective was to determine the optimum DTPA concentration and pH value. All the DTPA solutions were prepared by deionized water.

6.4.1 Materials used in the Experiments

40% DTPA fluid having a pH of 12.0 and deionized water were used to prepare the stimulation fluids formulations. HCl acid was used to adjust the solution pH to the required value. The selected DTPA formulations were 20 %wt. DTPA 12.0 pH, 20 %wt. DTPA 4.5 pH, 10.0 %wt. DTPA 12.0 pH, 10.0 %wt. DTPA 4.5 pH and 4.0 %wt. DTPA 12.0 pH. All of these fluids were stirred for at least 6 hours to insure their homogeneity.

Austin chalk core samples of 3.81 cm size and 7.5 cm long were used in these experiments. Their porosities were almost similar about 30% while permeabilities were varied from 10 to 15 md. CT scan images showed that all of the core samples were looked homogeneous. Table 6.8 shows the properties and experiment condition for each core sample.

Table 6.8: Core samples properties and experiment conditions- DTPA formulations

	Units	Core#1	Core#2	Core#3	Core#4	Core#5
Rock Type		Austin Chalk	Austin Chalk	Austin Chalk	Austin Chalk	Austin Chalk
Size	cm	3.81	3.81	3.81	3.81	3.81
Length	cm	7.40	7.54	7.40	7.5	7.25
Porosity	Fraction	0.28	0.29	0.29	0.29	0.29
Permeability	md	13.15	17.07	15.05	9.48	13.81
Pore volume	Fraction	24.88	24.91	24.40	24.88	23.72
Average CT number	-	2221	2202	2193	2194	2212

	Units	Core#1	Core#2	Core#3	Core#4	Core#5
Saturated fluid	-	DI water	DI water	DI water	DI water	DI water
Stimulated fluid		19% DTPA	19% DTPA	9.5% DTPA	9.5% DTPA	4.0% DTPA
Stimulated fluid's pH		12.3 pH	4.5 pH	12.3 pH	4.5 pH	12.3pH
Injection rate	cc/min	1.0	1.0	1.0	1.0	1.0
Experiment temperature	^{o} F	250	250	250	250	250
Net overburden pressure	psi	500	500	500	500	500
Back pressure	psi	1000	1000	1000	1000	1000

6.4.2 Effect of DTPA pH on Matrix Stimulation

To study the effect of pH of DTPA on matrix stimulation treatment, four experiments were conducted at temperature of 250^{o}F, rate of 1.0 cc/m and four different DTPA fluids have concentrations of 20% and 10%, and pH of 12.0 and 4.5. Figure 6.33 represents the effect of pH of DTPA fluid on the stimulation treatment. The figure shows clearly that higher pH fluids performed better in terms of the minimum pore volume required to form dominant WHs. For example, 20% DTPA of 12.0 pH needed only 3.7 PVs, whereas 20% DTPA of 4.5 pH consumed about 5.3 PVs. Same results were observed for lower concentration DTPA of 10%, where low pH fluid needed 6.3 PVs whereas higher pH fluid needed only 4.6 PVs. Figure 6.34 shows the normalized pressure drop versus the pore volume injected. It was clear from this figure that DTPA fluids with high pH values performed better than that of low values.

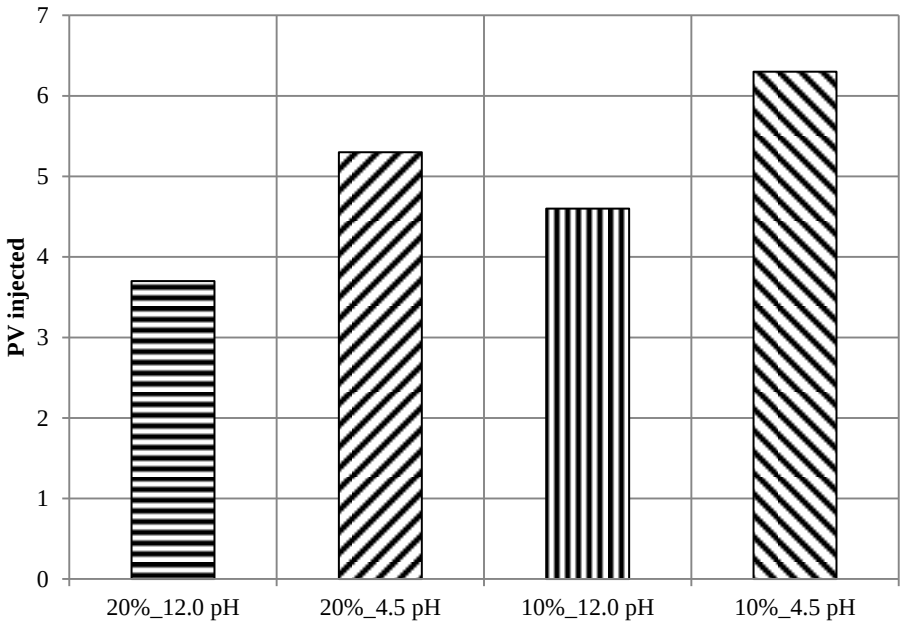

Figure 6.33: Effect of pH fluid on stimulation treatments using DTPA chelating agent at temperature of 250^{o}F

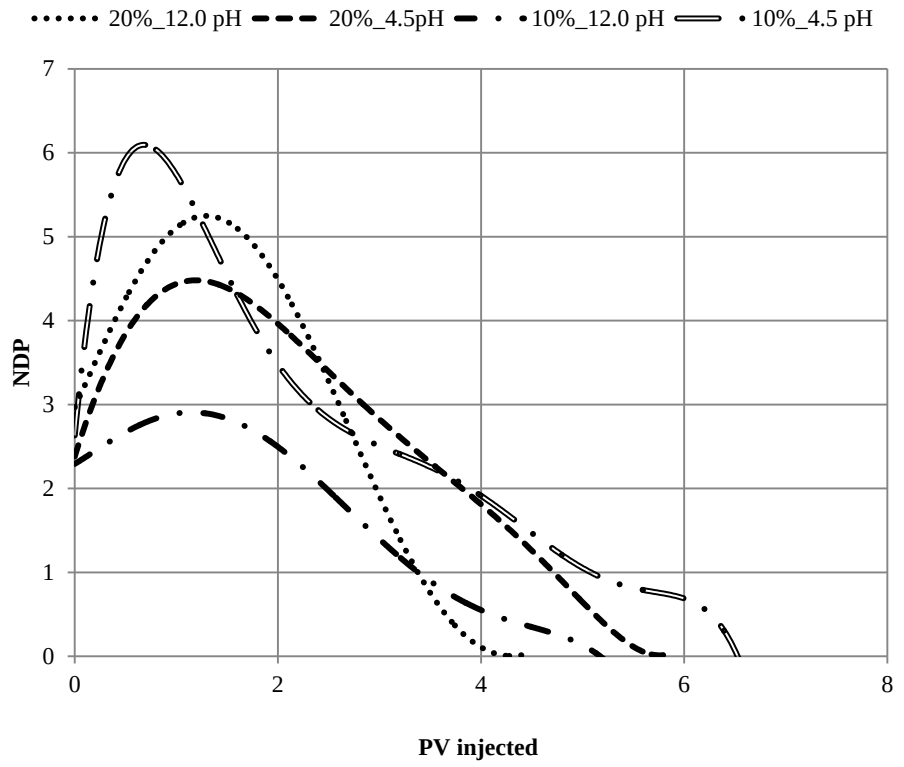

Figure 6.34: Normalized pressure drop versus PV injected for DTPA stimulation fluid at temperature of 250^{o}F

6.4.3 Effect of DTPA Concentration

To study the effect of DTPA concentration on the stimulation process, three experiments were conducted at temperature of 250^{o}F, injection rate of 1.0 cc/m, and DTPA of 12.0 pH and three different concentrations that were 20%, 10% and 4% prepared by deionized water. Figure 6.35 shows the effect of DTPA concentration on stimulation process at high pH value. This figure showed clearly that as DTPA concentration increases, the pore volume to breakthrough decreases. So at constant pH value, the higher the DTPA concentration the lower the PV to breakthrough. This conclusion was confirmed by doing another core flooding experiments at different DTPA concentration and similar and low pH value as can be shown in figure 6.36. Figure 6.37 depicts the relation between DTPA concentration of high pH and PV to breakthrough.

If the lowest volume and time to breakthrough were considered in determining the optimum stimulation concentration, the DTPA concentration of 10% will be the optimum concentration as can be shown in figure 6.38. Figures 6.39 and 6.40 show the CT scans, inlet faces and the WH paths for the core samples stimulated by DTPA

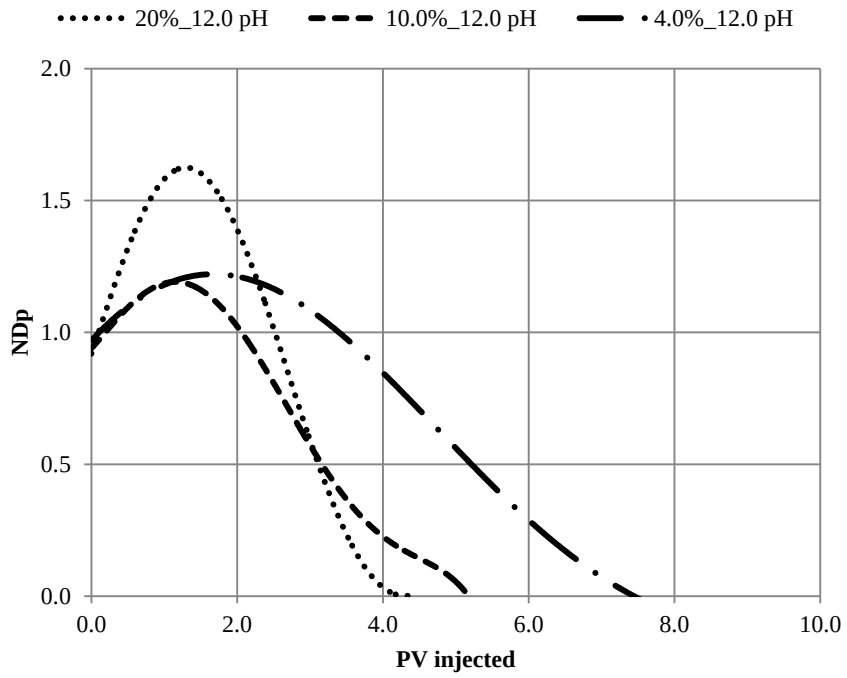

Figure 6.35: DTPA concentration effects on PV to breakthrough_ high pH fluids at temperature of 250°F

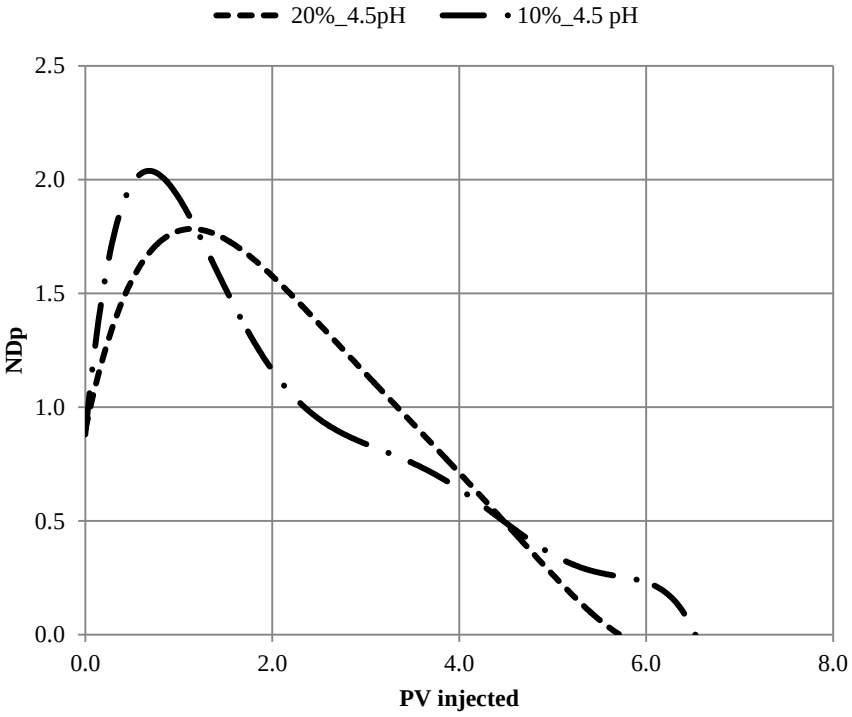

Figure 6.36: DTPA concentration effects on PV to breakthrough_ low pH fluids at temperature of 250°F

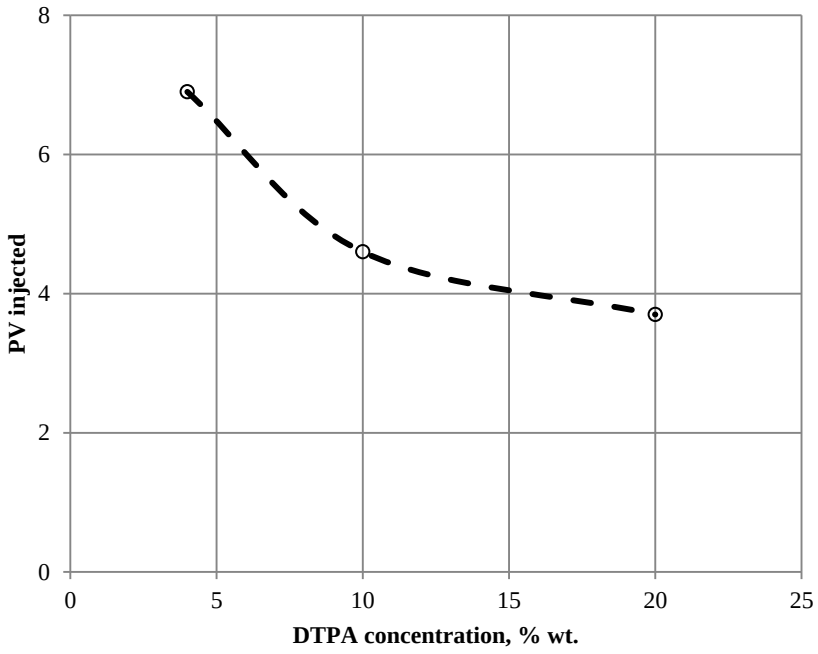

Figure 6.37: DTPA concentration versus PV injected at temperature of 250°F

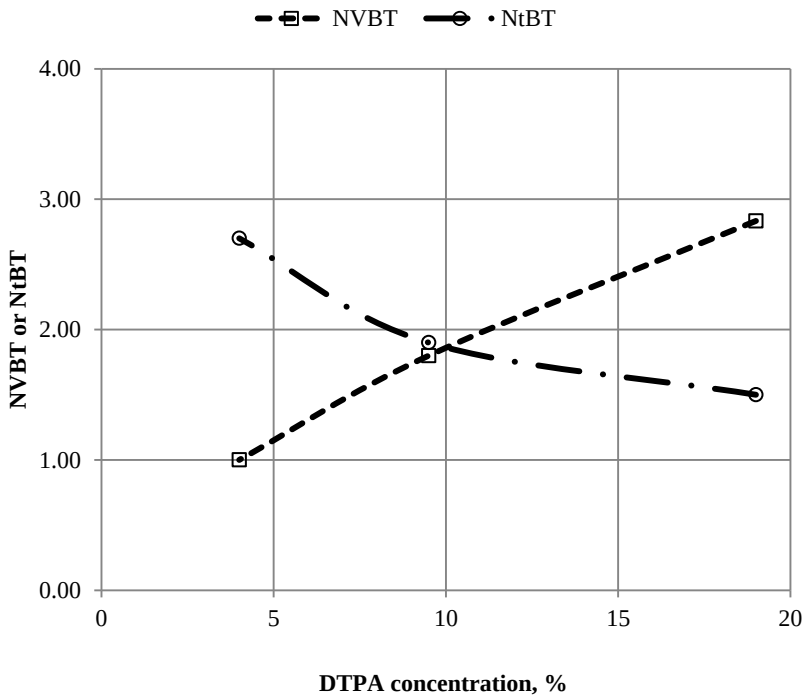

Figure 6.38: Optimum concentration for 12.0 pH DTPA at temperature of 250°F

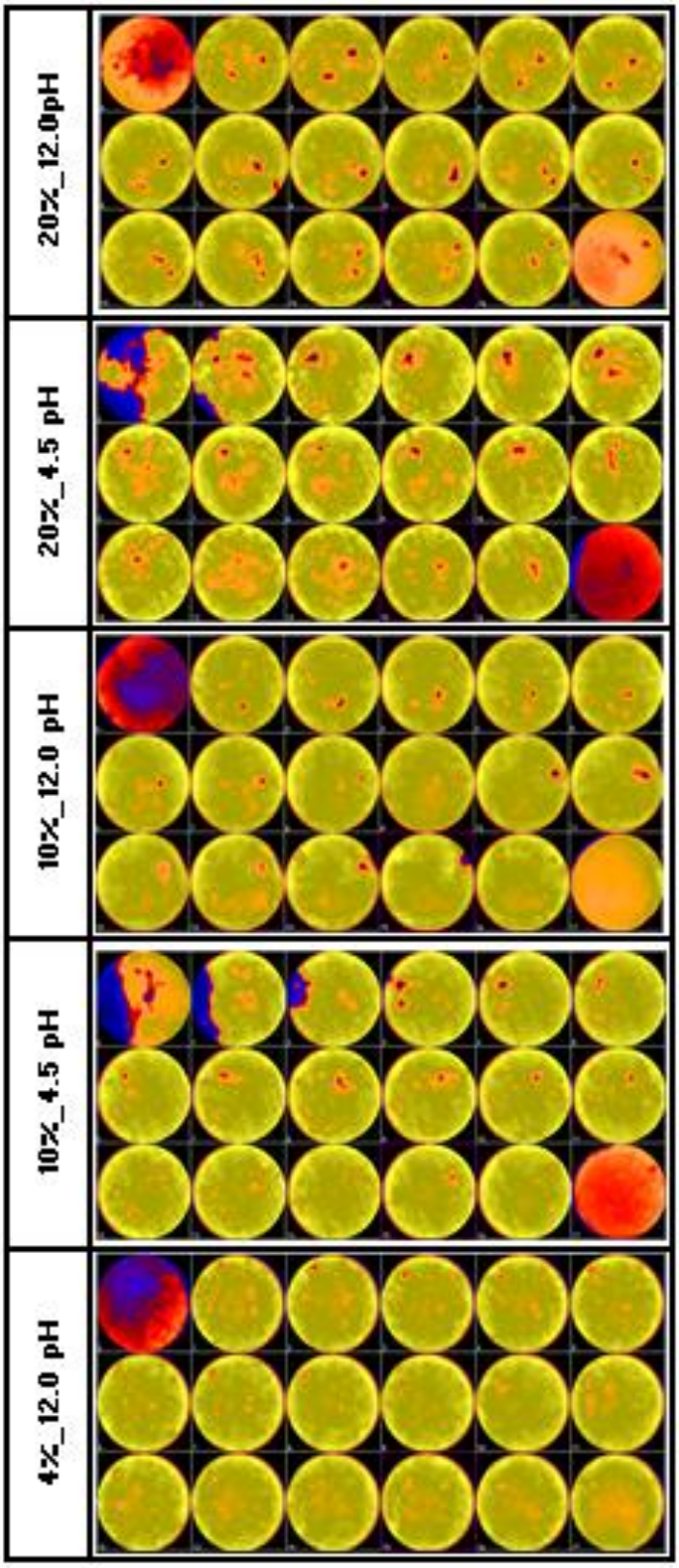

Figure 6.39: CT slices of the core samples stimulated by DTPA at temperature of 250^{o}F

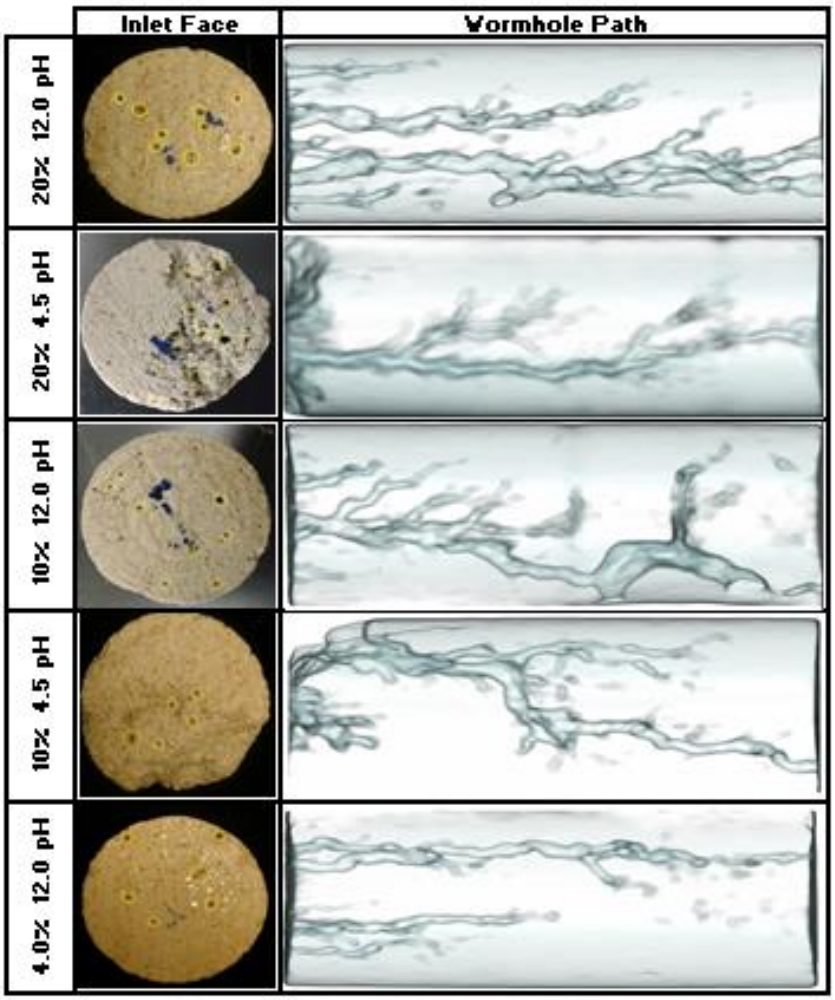

Figure 6.40: Inlet faces and WH paths of the core samples stimulated by DTPA at temperature of 250^{o}F

6.5 Evaluation of Stimulation Treatments using NMR

To study the effectiveness of NMR on evaluating the stimulation process, two stimulation treatments were conducted using 15% HCl acid. The objective of these experiments was to create WHs, and then evaluate the changes occurred to the core sample porosity after the stimulation treatment using NMR. 15% HCl acid with 0.3% corrosion inhibitor was injected in two Austin Chalk core samples at room temperature and 5.0 cc/m and 3.0 cc/m injection rates. Figure 6.41 shows the normalized pressure drop versus the PV injected. Both injection rates managed to create dominant WHs at similar PV, which was 0.45 PV. Figure 6.42 shows the CT number of the wormholes created in both two core samples along their length. It shows clearly creation of wormhole with CT number near zero. Also the curve shows clearly that the wormhole size is decreasing towards the outlet of the core samples. Injecting 15% HCl at 5 cc/min showed creation of wormhole with bigger size than that for 3 cc/min, which indicated by less CT numbers of the WH. Figures 6.43 and 6.44 show the changes in the cumulative and incremental porosity curves for the core samples before and after stimulation. The peak in the incremental porosity versus T_2 relaxation time curves have shifted to the right indicating that the water-filled pores took longer time to relax than what they were before stimulation. The cumulative porosity versus the relaxation time curves was reading higher values of cumulative porosity at higher relaxation time values, which confirmed the creation of the wormholes. Figure 6.45 shows the comparison between the saturation and NMR porosity for the two core samples stimulated with 15% HCl acid. Table 6.9 shows the results of the experiments and the porosity changes before and after the stimulation using the normal saturation procedure and NMR scanning.

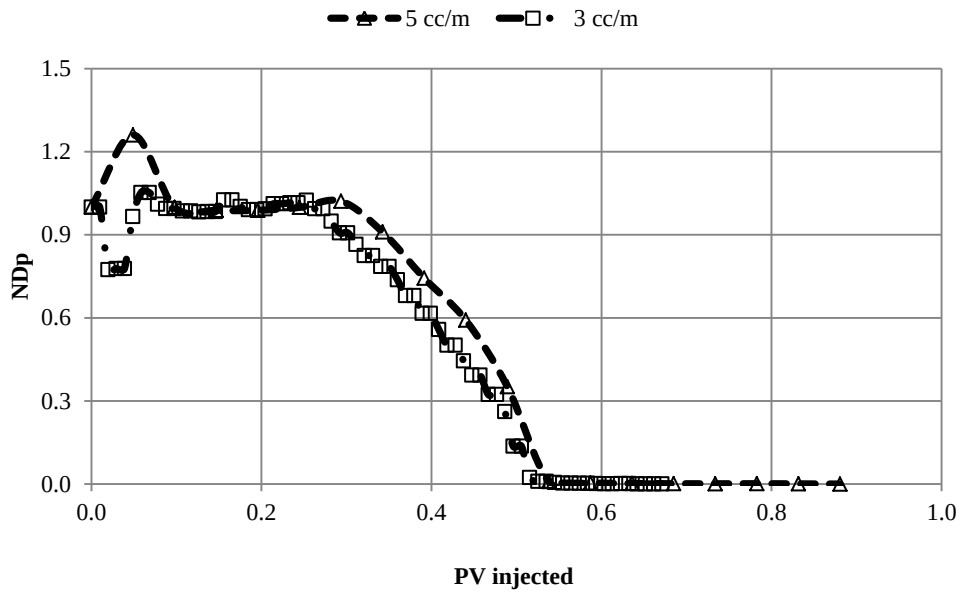

Figure 6.41: Normalized pressure drop versus PV injected for cores stimulated by 15% HCl acid at temperature of 72^{o}F

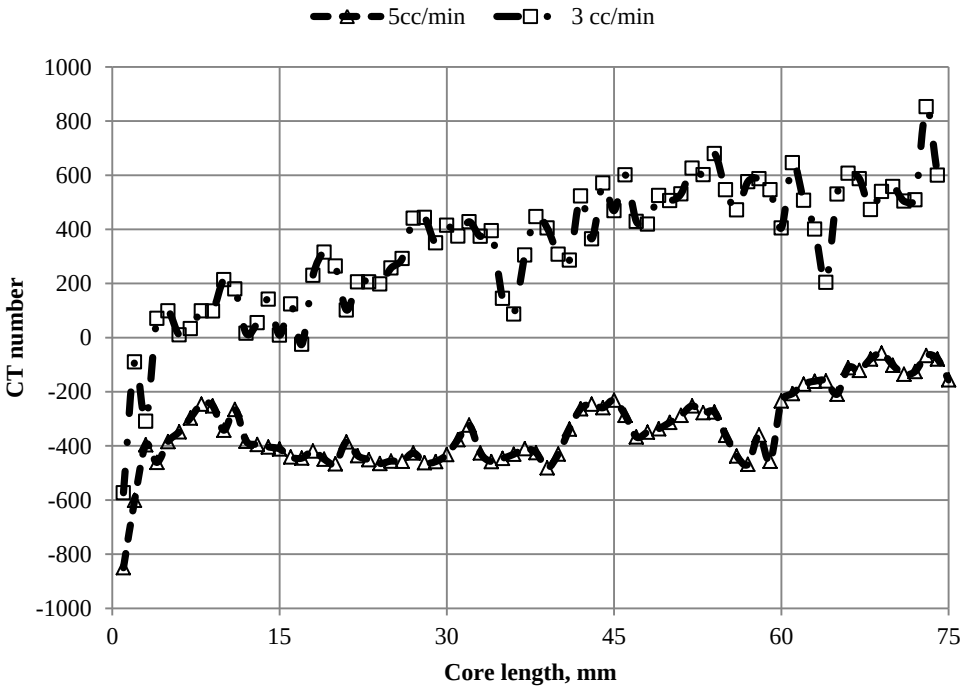

Figure 6.42: CT of the WHs created by 15% HCl injected at different injection rates at temperature of 72^{o}F

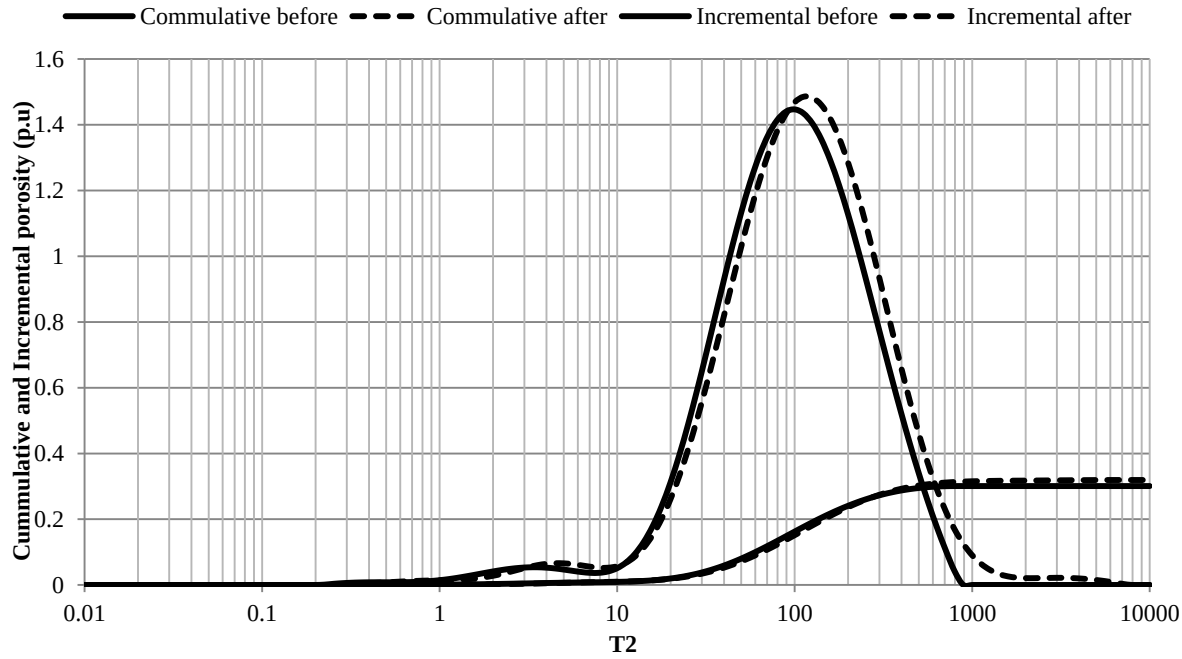

Figure 6.43: NMR before and after the stimulation for the core sample stimulated at 3.0 cc/m HCl acid at temperature of 72^{o}F and atmospheric pressure

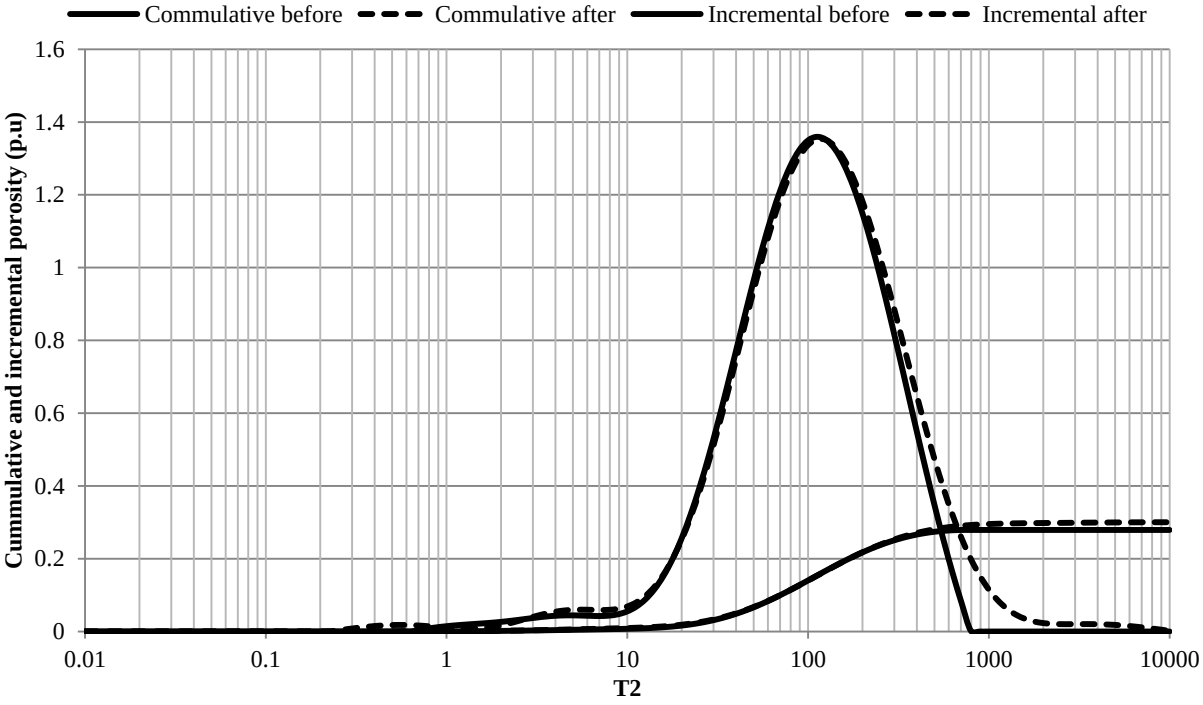

Figure 6.44: NMR before and after the stimulation for the core sample stimulated at 5.0 cc/m HCl acid at temperature of 72^{o}F and atmospheric pressure

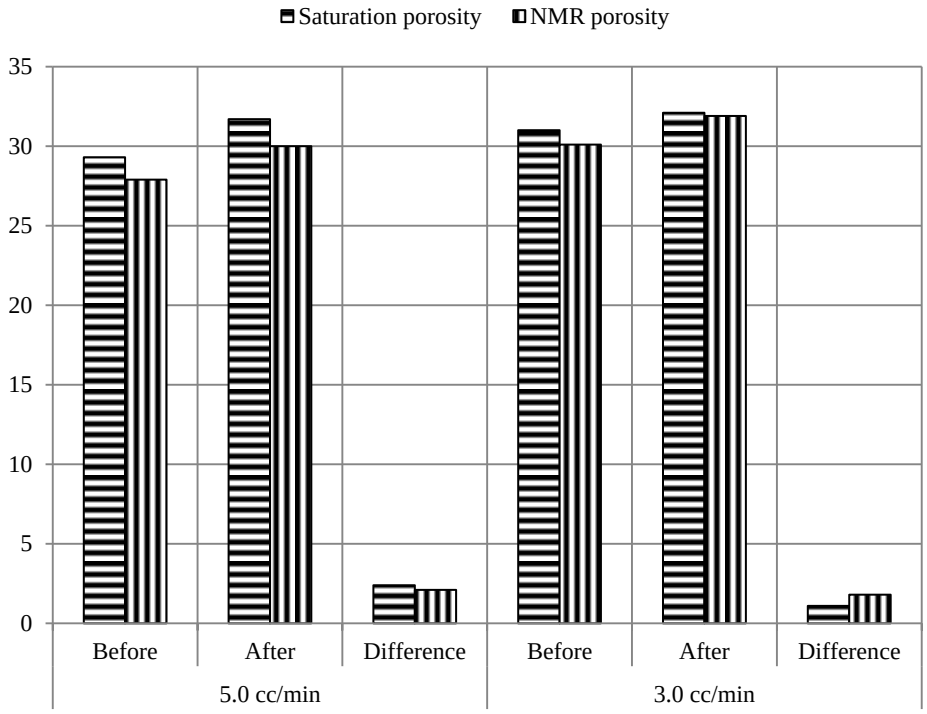

Figure 6.45: Comparison of saturation porosity and NMR porosity at temperature of 72°F and atmospheric pressure

Table 6.9: Results of the experiments conducted using 15% HCl acid

	Units	Core#1	Core#2
Rock Type		Austin Chalk	Austin Chalk
Size	cm	3.81	3.81
Length	cm	7.78	7.32
Saturation porosity before stimulation	%	29.3	31.0
Saturation porosity after stimulation	%	31.7	32.1
NMR porosity before stimulation	%	27.9	30.1
NMR porosity after stimulation	%	30.0	31.9
Saturated fluid	-	DI water	DI water
Stimulated fluid		15% HCl	15% HCl
Injection rate	cc/min	5.0	3.0
PV injected		0.41	0.37
Experiment temperature	°F	72	72
Net overburden pressure	psi	500	500
Back pressure	psi	1000	1000

6.6 Prediction of PV to Breakthrough and Pressure Drop across the Core Sample

Pore volumes required to create wormholes can be predicted using any of the equations stated in chapter 2. In this section, PVs was predicted using Buijse and Glasbern 2005, and Mahmoud and Nasreldin 2011 models. Prediction of PVs assumed that wormhole growth is constant. Table 6.10 shows information of six experiments conducted at temperature of 250^{o} F and injection rate of 1.0 cc/m using different rock types and stimulation fluids. Table 6.11 shows the comparison between the actual PVs and the predicted ones using both models. Both models gave a reasonable prediction of PVs as compared to the actual one. Both models overestimated the volume required to breakthrough. The reason of PVs overestimation could be because Buijse and Glasbern model was developed for strong acids, whereas Mahmoud and Nasreldin model was developed for GLDA chelating agent, which considered stronger than the examined chelating agents. Figure 6.46 and 6.47 show the comparison between the actual and predicted PVs using both Buijse and Glasbern, and Mahmoud and Nasreldin models.

Table 6.10: Experiments conducted at 1.0 cc/m using different stimulation fluids

#	Stim. Fluid	Concentration	pH	Rock type	Porosity	k	Actual PV
		%			%	md	
1	EDTA-DI	18.5	10.0	AC	29.6	16.00	3.90
2	EDTA-SW	18.5	7.0	IL	10.2	0.60	4.90
3	DTPA-DI	20.0	12.0	AC	29.1	18.00	5.30
4	HEDTA-SW	20.0	4.0	IL	10.2	2.60	4.46
5	HEDTA-SW	15.0	4.0	IL	10.1	0.60	5.07
6	HEDTA-DI	20.0	4.0	IL	9.5	0.5	3.90

Table 6.11: Actual and predicted PVs using Buijse & Blasbern, and Mahmoud & Nasr-El-Din models

	Fluid Type	Actual PV	Predicted PV "Buijse & Glasbern"	Predicted PV "Mahmoud & Nasreldin"
1	EDTA-DI 18.5%	3.90	4.10	4.20
2	EDTA-SW 18.5%	4.90	5.08	5.83
3	DTPA-DI 20%	5.30	5.50	6.10
4	HEDTA-SW 20%	4.46	4.63	4.75
5	HEDTA-SW 15%	5.07	5.26	5.32
6	HEDTA-DI 20%	3.90	4.05	4.40

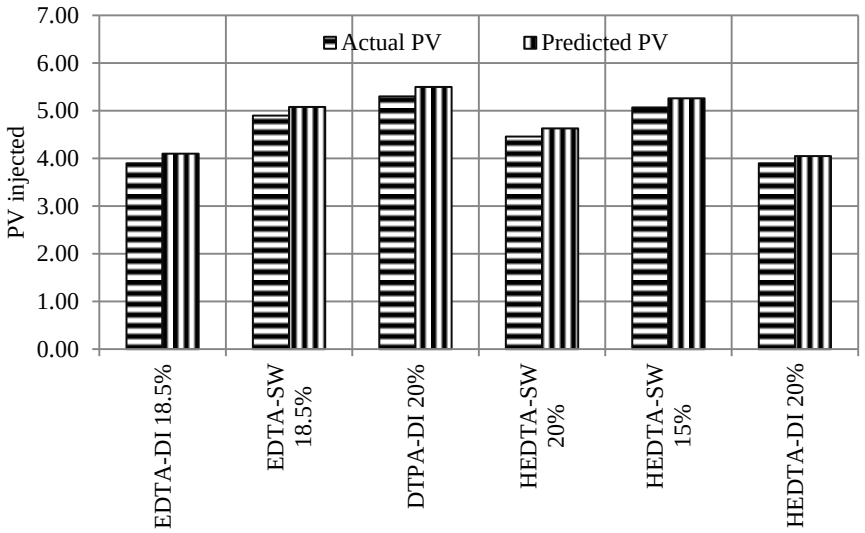

Figure 6.46: Comparison between actual PV and the predicted PV using Buijse and Glasbern (2005) model

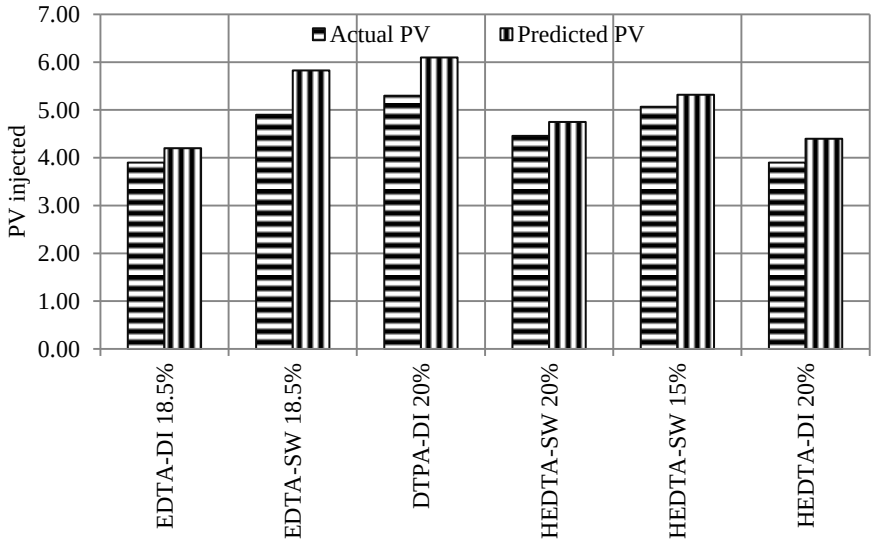

Figure 6.47: Comparison between actual PV and the predicted PV using Mahmoud and Nasreldin (2011) model

The pressure drop across the core sample was predicted using Darcy's equation after arrangement to account for the change in viscosity inside the core while the chelating agents are injected. Viscosity of chelating agent was estimated after measuring the amount of calcium ions in the effluents and with the help of the relations built in chapter 5 for each chelating agent. The pressure drop equation which was used in prediction is:

$$\Delta p = \frac{122.8 Q \mu_{chelate}(L_{chelate} - L_{wh})}{k\, d_{core}^2} + \frac{122.8 Q \mu_{water}(L_{core} - L_{chelate})}{k\, d_{core}^2} \quad \text{.....(6.1)}$$

where Δp is pressure drop, psi, Q is flow rate in cc/min, μ is viscosity in cP, $L_{chelate}$ is length of chelating agent inside the core in inches, L_{wh} is the propagation of wormhole in inches, L_{core} is core length in inches, k is permeability in md, and d_{core} is core diameter in inches. First part of the equation represents the flow of chelating agents inside the core displacing the saturation fluid, which will remain until full creation of wormhole. The second part of the equation represents the displacement of the saturation fluid, and it will die when chelating agents breakthrough at the outlet of the core sample.

The above equation was developed based on the following assumptions:

a. Pressure drop across the wormhole can be neglected.
b. Effect of CO_2 at back pressure of 1000 psi can be neglected.
c. Viscosity of chelating agent at maximum calcium concentration and experiment temperature can be estimated from the correlation developed in chapter 5.
d. Rock permeability is constant.
e. Wormhole propagation is linear and constant.

Figures 6.48 through 6.52 show the prediction of pressure drop for different experiment conducted at different rock and stimulation fluids types. These figures show reasonable match between the actual and predicted pressure drop.

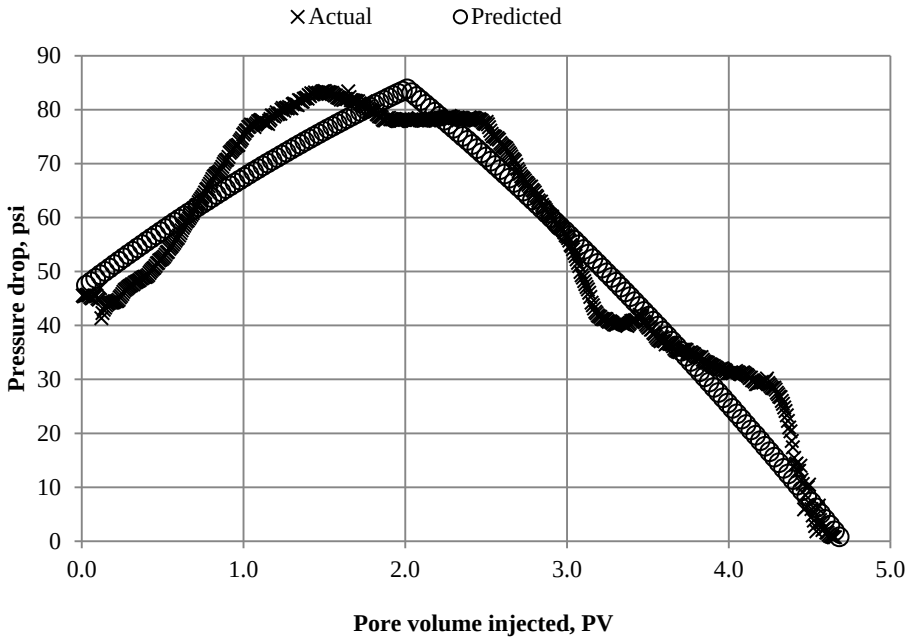

Figure 6.48: Actual and predicted pressure drop of IL core sample stimulated by 4.0 pH, 20% HEDTA prepared by sea water at 0.5 cc/min and 250^{o}F; showing a good match

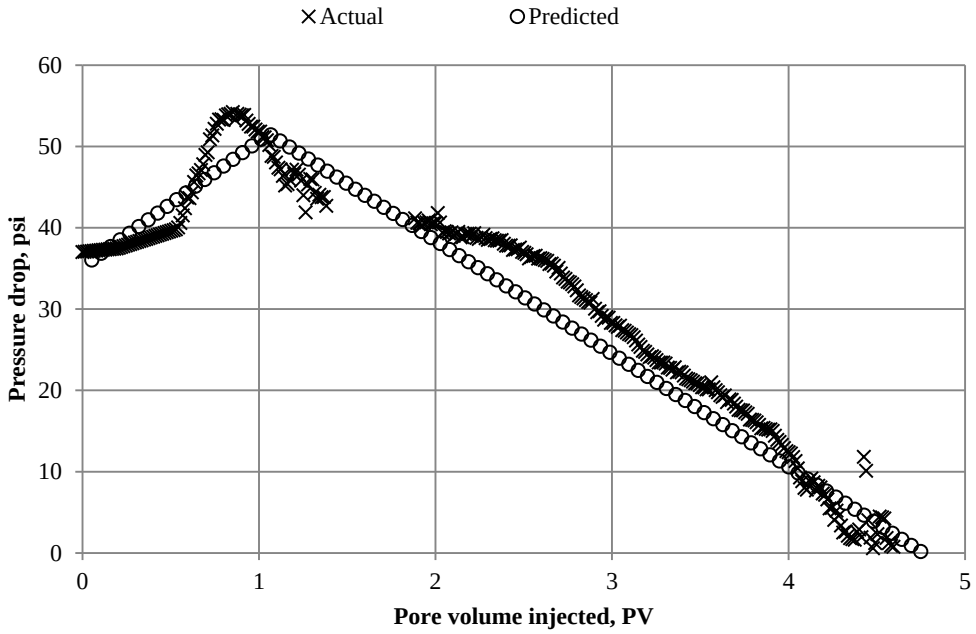

Figure 6.49: Actual and predicted pressure drop of IL core sample stimulated by 4.0 pH, 20% HEDTA prepared by sea water at 1.0 cc/min and 250^{o}F; showing a good match

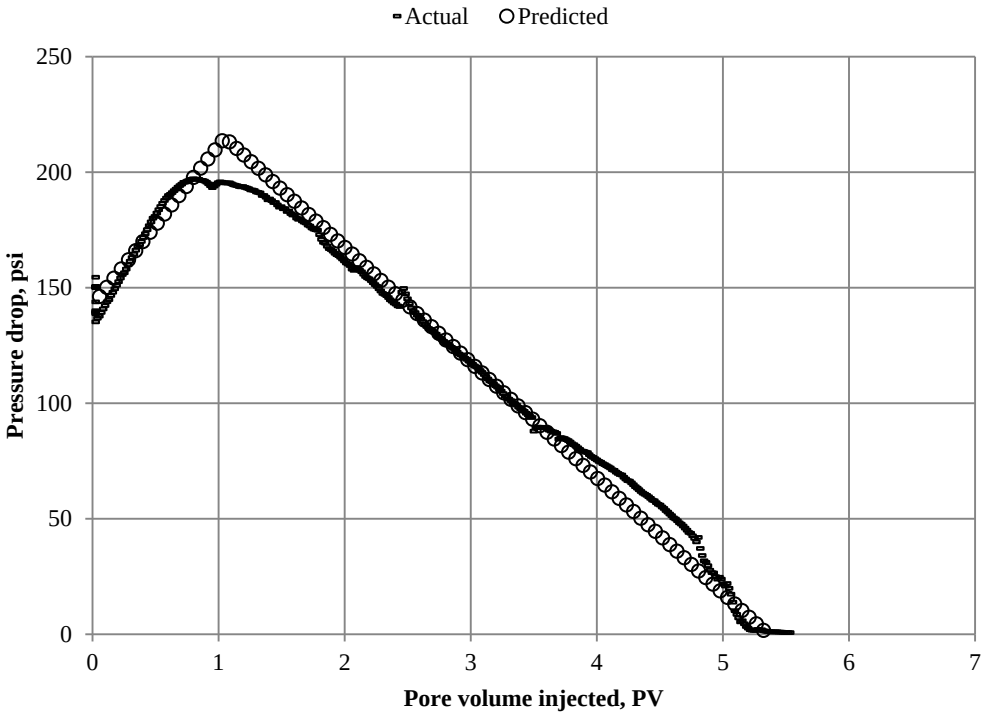

Figure 6.50: Actual and predicted pressure drop of IL core sample stimulated by 4.0 pH, 15% HEDTA prepared by sea water at 1.0 cc/min and 250^{o}F; showing a good match

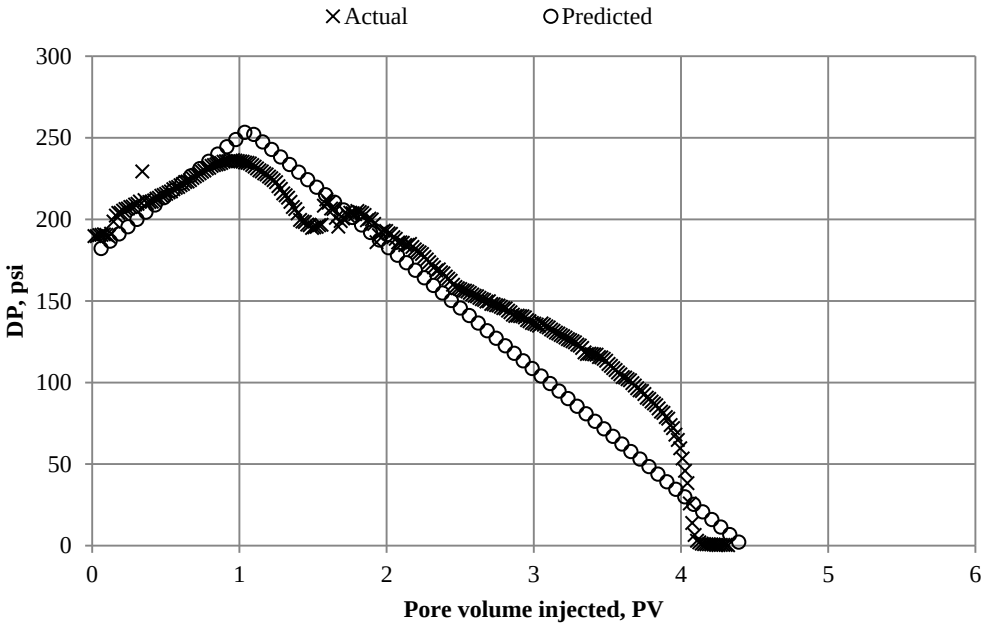

Figure 6.51: Actual and predicted pressure drop of IL core sample stimulated by 4.0 pH, 20% HEDTA prepared by DI water at 1.0 cc/min and 250^{o}F; showing a good match

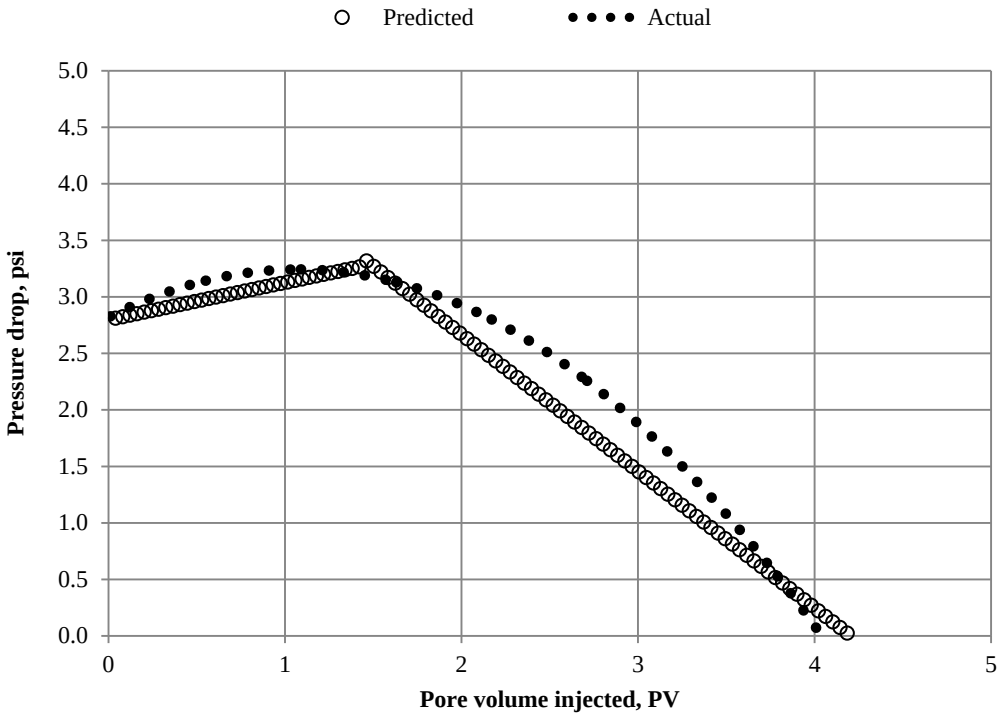

Figure 6.52: Actual and predicted pressure drop of AC core sample stimulated by 10.0 pH, 18.5% EDTA prepared by DI water at 1.0 cc/min and 250^{o} F; showing a good match

CHAPTER 7

EFFECT OF CHELATING AGENTS ON ROCK'S ELASTIC PROPERTIES

7.1 Introduction

Matrix stimulation has being widely used to treat the damaged carbonate formations. It basically removes the near-wellbore damage and also creates channels around the wellbore by means of dissolving some parts of the carbonates. Many stimulation fluids have been used such as HCl acid, acid mud, organic acids, chelating agents, etc. Wormholes created by these fluids are very effective and can decrease the skin factor significantly; and hence results in a noticeable increase in well productivity. Despite the success in creating these wormholes, diffusion of these fluids inside the pores of these rocks can create significant and permanent changes in rock mechanical properties. These changes can eventually lead to weakening the rock strength; which may lead to future formation damage.

In this study, the effect of EDTA and DTPA chelating agents on rock elastic and mechanical properties will be investigated. The focus of the study will be on the effect of wormholes that created by these fluids. CT scan and acoustic tests will be conducted on the core samples before and while stimulation experiments.

7.2 Experimental Methodology

7.2.1 Materials

EDTA and DTPA chelating agents having concentrations and pH of 0.25M and 4.5, respectively for both chelants were used. Four calcite rocks, two from Indiana Limestone and the other two from Austin Chalk rocks having lengths and diameters of approximately 2.0 and 1.5 inches were used. Austin chalk core samples have porosities and permeabilities of 29.1%, 29.0% and 15.5 and 8.4 md; whereas for Indiana Limestone core samples are 13.1, 7.8 and 1.6, 0.08 md, respectively. Core samples were saturated with deionized water

7.2.2 Measurements

Core flooding system was used to conduct the matrix stimulation treatments. 500 psi net overburden pressure was applied on the rock to insure that the fluid is flowing through the core sample. 1,000 psi back pressure on the outlet of the core was applied. Pressures, temperature and injection rates were recorded in the system's monitoring computer during each experiment. CT scanning instrument was used to quantify the changes took place in the core sample during chelant injection. Acoustic measuring instrument from New England Research Inc. was used to evaluate the changes in the elastic properties of the core samples.

7.2.3 Experimental Procedures

Core samples were first weighed dry to measure the dry weight. Core samples were vacuum saturated with deionized water at 2500 psi saturation pressure, then saturated weights were measured to calculate the porosity and pore volume of each core. Core

samples were also CT scanned saturated before injecting the chelants. Elastic properties of the samples were also evaluated at different overburden pressures up to 1500 psi to represent different pressure conditions. Each core sample was stimulated in steps at 250^{o}F temperature, 1000 psi net overburden pressure and 1 cc/min injection rate. About 2 pore volumes were injected in the first step at the above said conditions. Injection was stopped and core sample was removed to do CT scanning and acoustic measurements as well as measuring core porosity and density. Above step was repeated after each 2 pore volumes were injected until breakthrough was reached by having near zero pressure drop across the core sample. Cores 1 and 2 were stimulated using EDTA chelating agent whereas cores 3 and 4 were stimulated using DTPA chelating agent.

7.3 Results and Discussion

7.3.1 Stimulation with Chelating Agents

Both chelating agents were managed to create wormholes in both calcite rock types using a reasonable amount of chelant. 3.1 and 3.3 pore volumes of EDTA; whereas 7.1 and 7.6 pore volumes of DTPA were required to create dominant wormholes in Indiana Limestone and Austin Chalk core samples, respectively. These results agree with the literature where nearly the same PVs were noted .Figure 7.1 and 7.2 show the normalized pressure drop versus the pore volumes injected. Normalized pressure drop was calculated by dividing the pressure drop while injecting chelant by the stabilized pressure drop when injecting deionized water at the same injection rate. Figure 7.3 shows the wormhole propagation inside the core samples as chelants were injected. Many holes were observed for the core samples with relatively high permeability and porosity values, whereas one or two holes were observed for the core sample of low permeability and porosity values.

This is mainly due to high diffusion ability of chelant in the high permeable rocks as compared to low permeable rocks. Changes in porosities and densities were not noticeable as EDTA and DTPA chelating agents dissolved only a small volume of each core sample; and the rest of the core sample was not affected as shown in figure 7.4 and 7.5. As the wormholes were being created, there will be a rapid increase in permeability as a result of forming a wide and long pathway as shown in figure 7.6. Permeability improvement was effective in low permeability cores as compared to high ones.

7.3.2 Changes on CT Number of the Core Samples

Injection of EDTA and DTPA did not affect the average CT number of the cores as can be seen in figure 7.7 which shows negligible decrease in average CT number of each core sample. This is mainly due to small volume dissolved by these chelants, which is not big enough to affect the CT number of the core sample. Instead the area around the wormhole was affected by injection of these fluids. Figure 7.8 shows the changes in the average CT number of the WH as the stimulation fluids were injected.

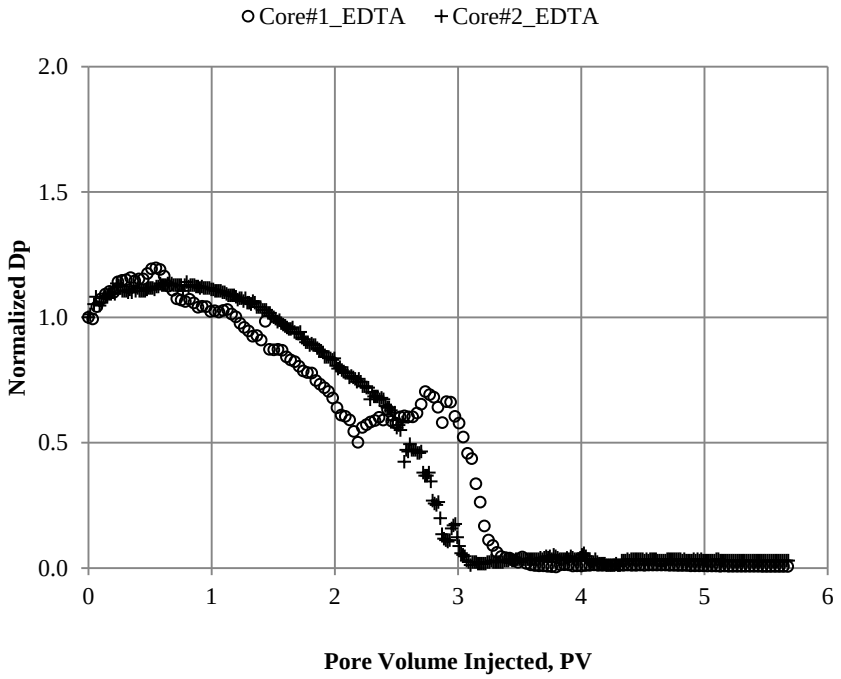

Figure 7.1: Normalized pressure drop versus the PV injected of the cores stimulated by EDTA at temperature of 250°F

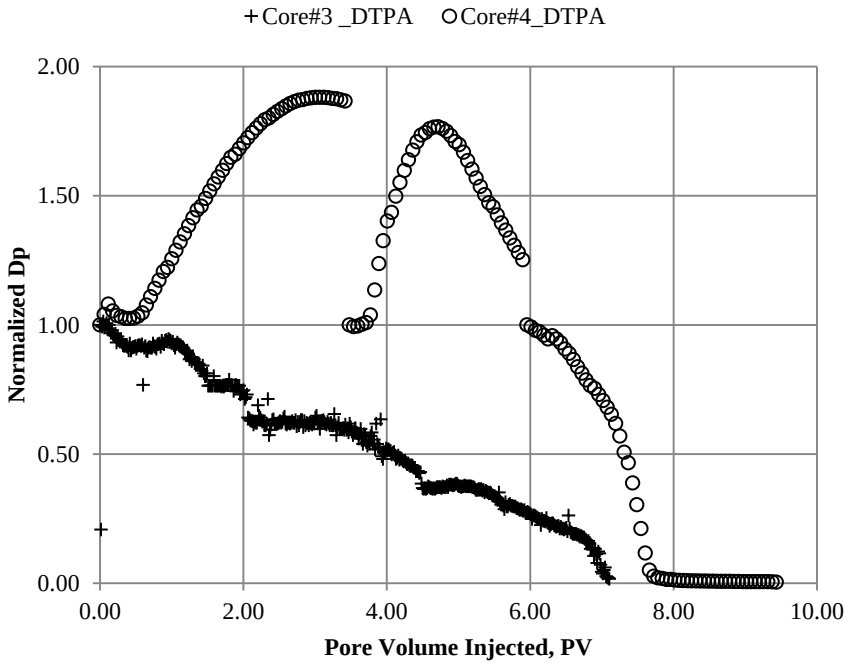

Figure 7.2: Normalized pressure drop versus the PV injected of the cores stimulated by DTPA at temperature of 250°F

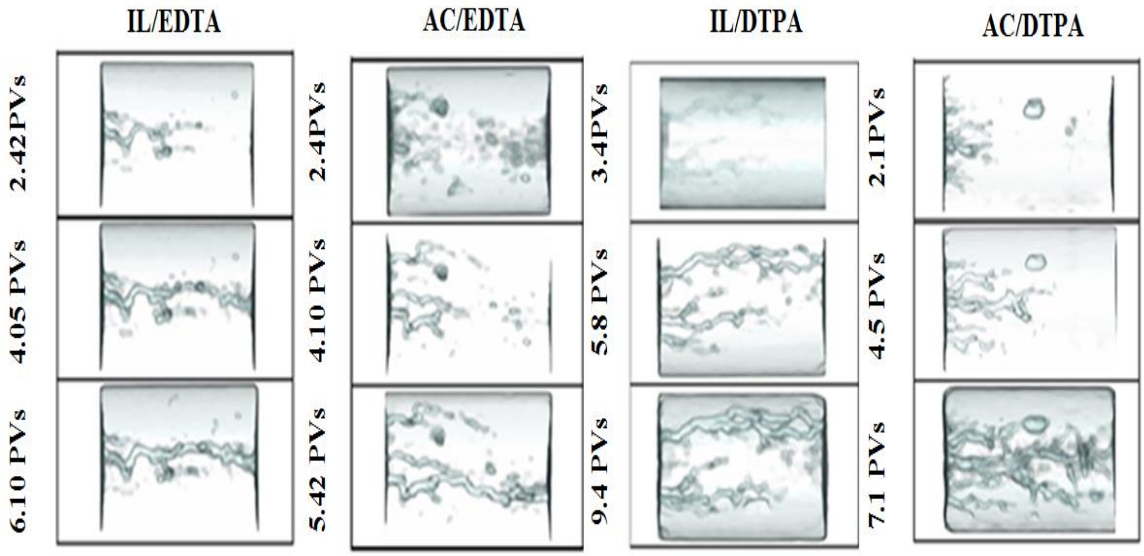

Figure 7.3: Wormhole propagation inside Indiana Limestone and Austin Chalk core samples after injecting them b EDTA and DTPA chelating agents at temperature of 250^{o}F

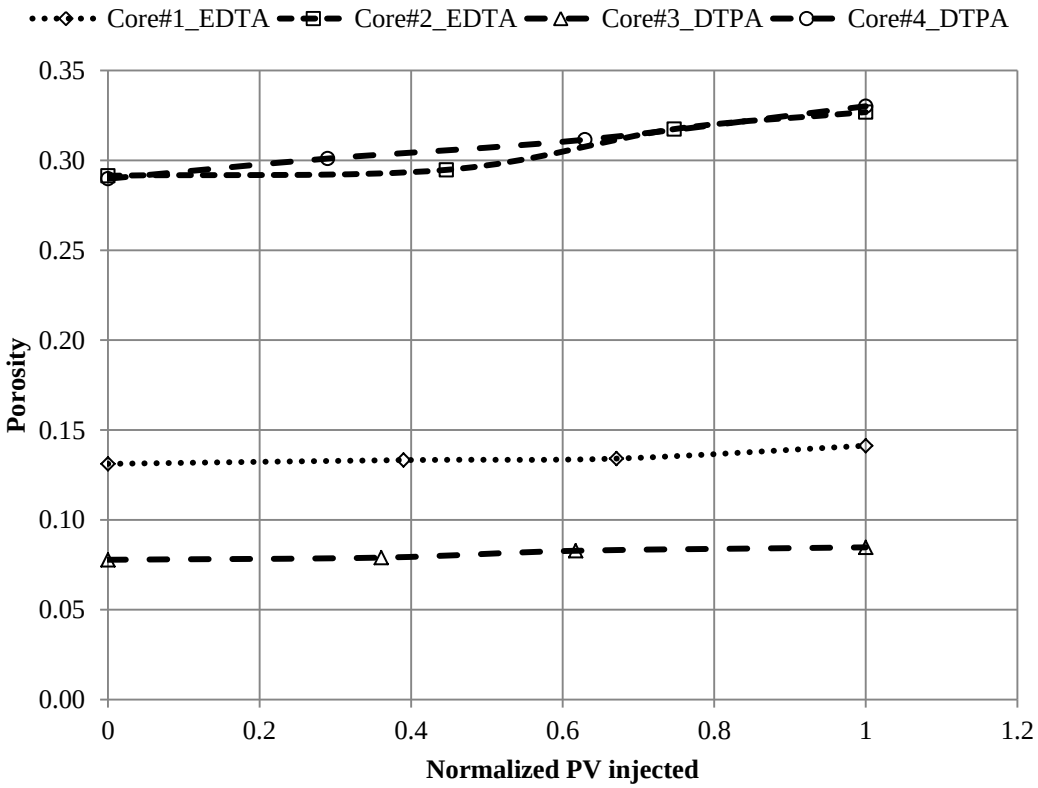

Figure 7.4: Porosity changes while injecting EDTA and DTPA chelating agents at temperature of 250^{o}F

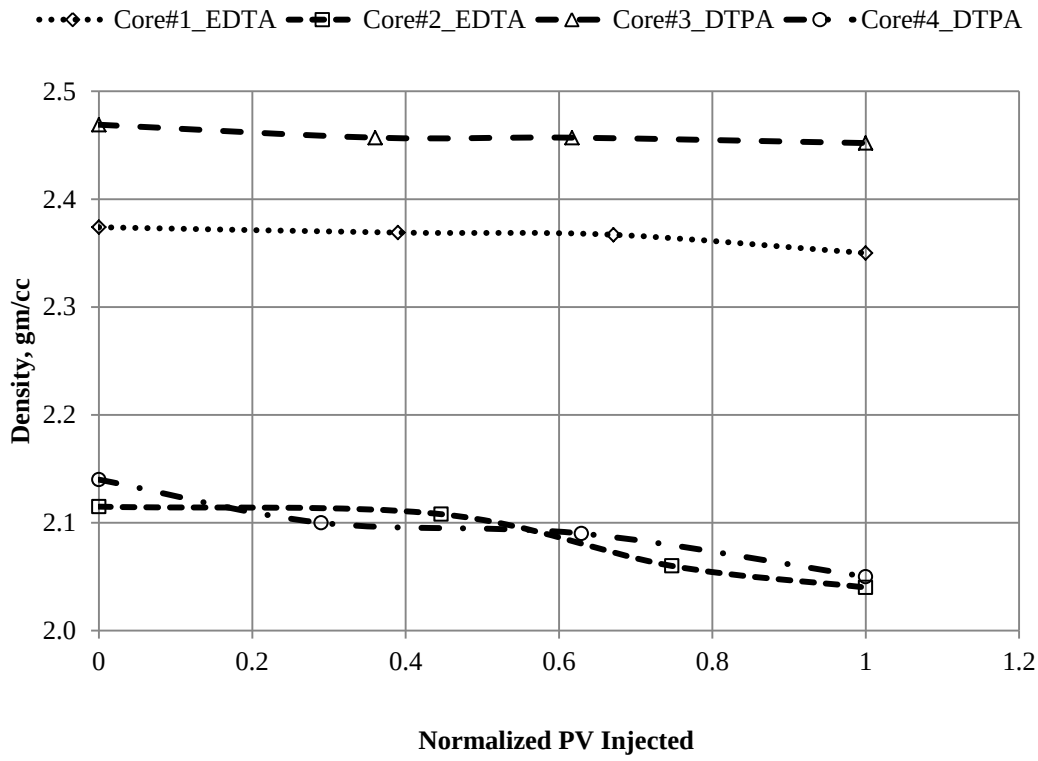

Figure 7.5: Density changes while injecting EDTA and DTPA chelating agents at temperature of 250°F

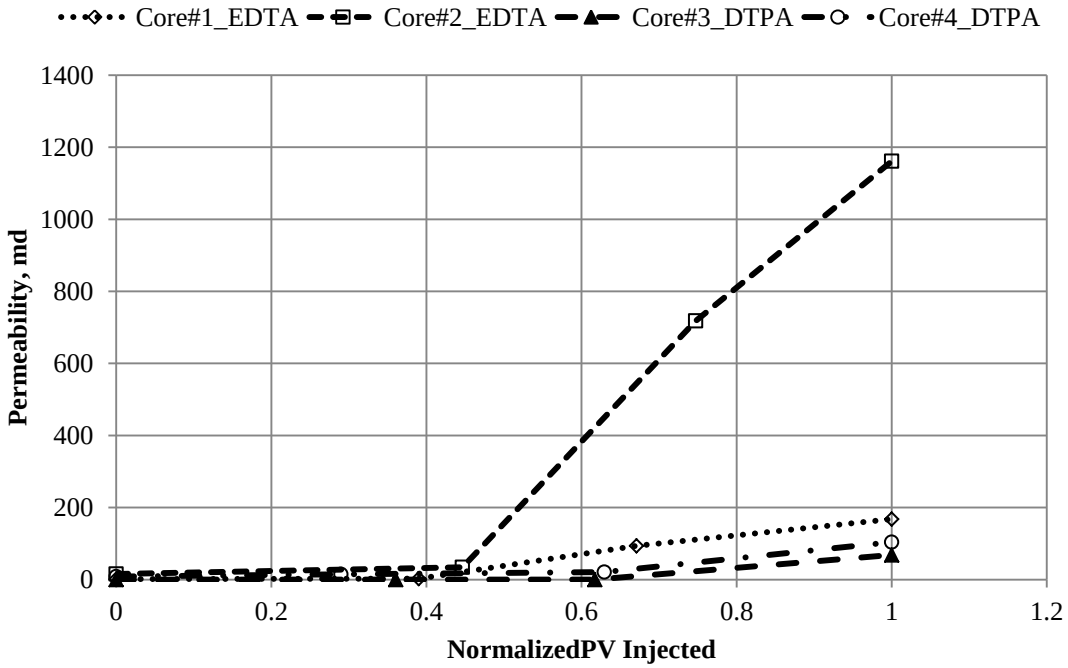

Figure 7.6: Permeability changes while injecting EDTA and DTPA chelating agents at temperature of 250°F

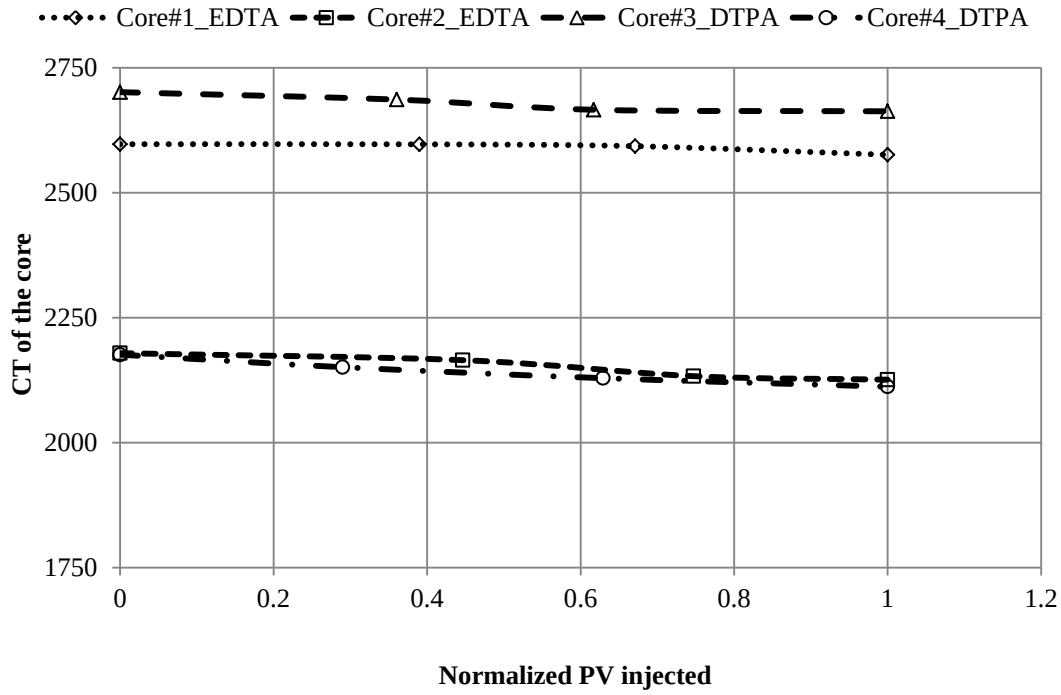

Figure 7.7: Changes on the CT number while injecting EDTA and DTPA chelating agents at temperature of 250°F

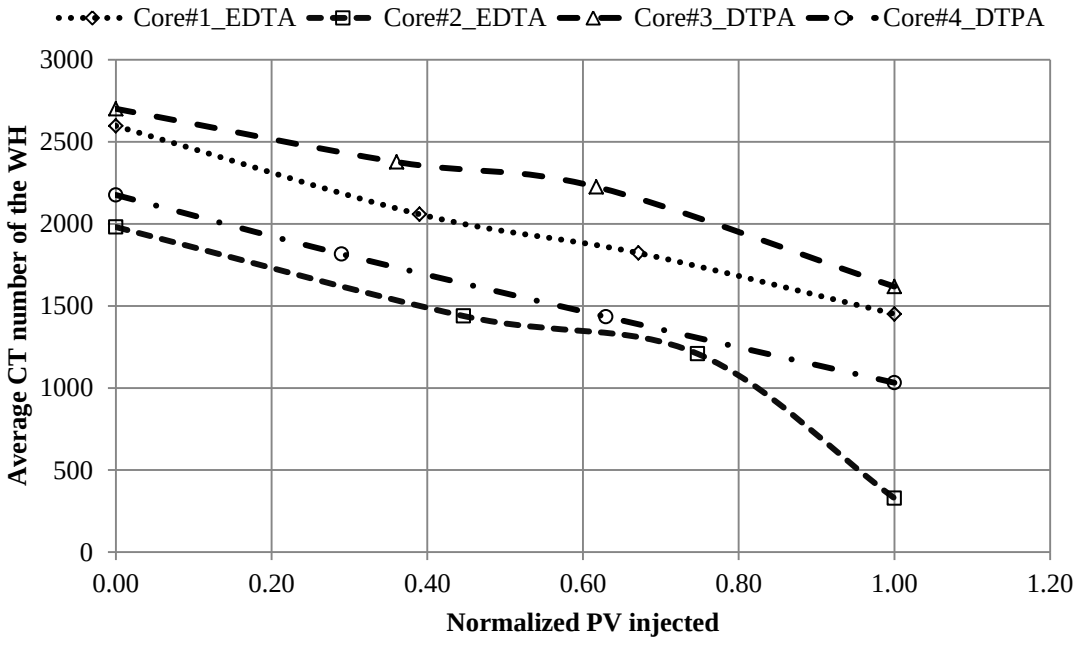

Figure 7.8: Changes on the CT number of the WHs while injecting EDTA and DTPA chelating agents at temperature of 250°F

7.3.3 Effect of Chelating Agents on the Rock's Elastic Properties

As mentioned earlier, the injected fluids dissolve some of the rock material and create wormholes. Creation of wormholes inside the rock will alter the elastic as well as mechanical properties of the rock especially near the walls of the wormholes. Unfortunately, measuring elastic and mechanical properties of the walls of the wormholes were not possible during this study, that is why the changes of elastic and mechanical properties of the whole core sample was considered as an evaluation tool to investigate the changes occurred during injection of stimulation fluid.

Figure 7.9 shows the changes in the compressional wave velocity as the stimulation fluids are injected. The figure shows a negligible effect of the chelant volume injected on the compressional velocity. This mainly because the channels that created by these chelants were narrow enough to have a negligible effect on the plastic wave velocity. Also the water that filled these tunnels will not have a big impact on the compressional wave as the water volume is small as compared to the bulk volume of the core sample.

Figure 7.10 shows the effect of stimulation fluids volume injected on the shear wave velocity. For the case of Indiana Limestone core samples, there were no big effect on the shear velocity due to the negligible volume of rock dissolved by each chelant. That is why shear wave velocity did not affect much by the fluids that filled the wormhole of Indiana Limestone core samples. So there were no noticeable changes in the shear velocity. But for Austin chalk core samples, the increase in the porosity was more than 10% of the original porosity. That is why the shear wave velocity affected much by the fluids that in the WHs as the shear waves do not propagate in fluids. In fact, shear wave lost about 35% of its original velocity.

Acoustic wave velocities can be further used to estimate the rock's elastic moduli as well as Poisson's ratio changes as stimulation fluids are injected. For both chelants, Austin chalk core samples showed significant changes in the elastic moduli as compared to Indiana Limestone core samples. This is mainly because chalk rocks have small rock strengths than that of limestone rocks. On top of that, high values of porosity and reasonable values of permeability let weak stimulation fluids such as EDTA and DTPA to diffuse to a big volume and dissolve high amount of the rock. Thus, elastic properties may alter significantly not like that in low permeability rocks such as Indiana Limestone. For instance, Young's Modulus of Austin Chalk core sample has decreased by more than 55% of its original value, whereas for Indiana Limestone the decrease is only about 5%, as shown in Figure 7.11. The decrease in Young modulus of Austin chalks claims that these rocks became less stiff when stimulation fluids were injected. The more stimulation fluid is injected, the less stiff the chalk rocks will be. Decreasing Young modulus will lead to high potential of rock failure if previous forces are applied to the rock. Figure 7.12 shows similar trend on the shear modulus as compared to Young's modulus for both rock types. For Indiana Limestone samples, changes in shear modulus were negligible and hence the rock did not affect much in terms of rock shear stress. For the case of Austin Chalk rocks, shear modulus decreases indicating that the rock shear potential was increased as a result of injecting these fluids. Figure 7.13 shows the changes on the bulk modulus as the stimulation fluid is injected. Negligible changes were noticed for Indiana Limestone samples, whereas noticeable changes were observed for Austin Chalk samples. The increase in the rock's bulk modulus for the case of Austin Chalk samples was because the rock become weaker and losing the ability of compression without being

deformed. This means it is not possible to apply the same stress and get the same volume compression similar to that before injecting the stimulation fluids. Figure 7.14 shows the relation between Poisson's ratio and stimulation fluid volumes injected. No changes were noticed for the case of Indiana Limestone, whereas there was noticeable increase in the Poisson's ratio as the stimulation fluids were injected. The increase in Poisson's ratio suggested that these core samples behaved more ductile than what they were before injecting the stimulation fluids. Table 7.1 shows the original properties of all the core samples before injecting the stimulation fluid.

Table 7.1: Properties of the core samples

#	Property	Unit	Core#1	Core#2	Core#3	Core#4
1	**Rock Type**	-	Indiana Limestone	Austin Chalk	Indiana Limestone	Austin Chalk
2	**Porosity**	-	0.13	0.29	0.078	0.290
3	**Permeability**	md	1.60	15.00	0.08	8.40
4	**Saturated density**	gm/cc	2.37	2.12	2.469	2.140
5	**Average CT number**	-	2597	2179	2701	2176
6	**Compressional velocity**	m/sec	4771.00	3294.00	5177	3314
7	**Shear velocity**	m/sec	2329.00	1662.00	2508	1596
8	**Poisson's Ratio**	-	0.34	0.33	0.347	0.349
9	**young's Modulus**	GPa	34.60	15.50	41.83	14.49
10	**Bulk Modulus**	GPa	36.97	15.14	45.57	15.99
11	**Shear Modulus**	GPa	12.87	5.84	15.53	5.37

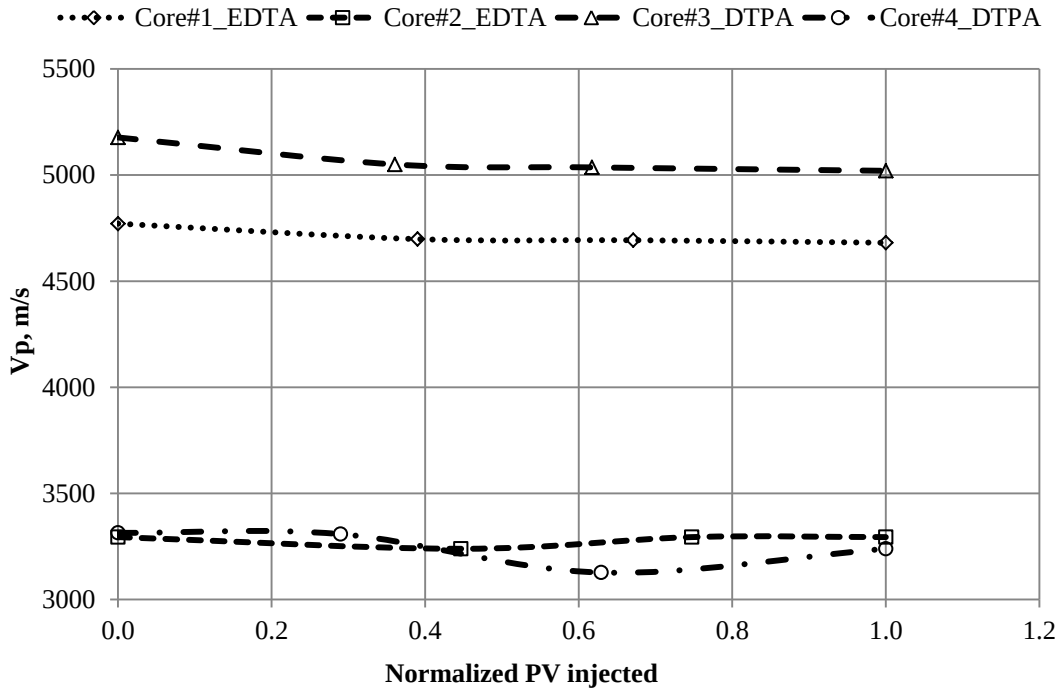

Figure 7.9: Plastic wave velocity changes while injecting EDTA and DTPA chelating agents at temperature of 250°F

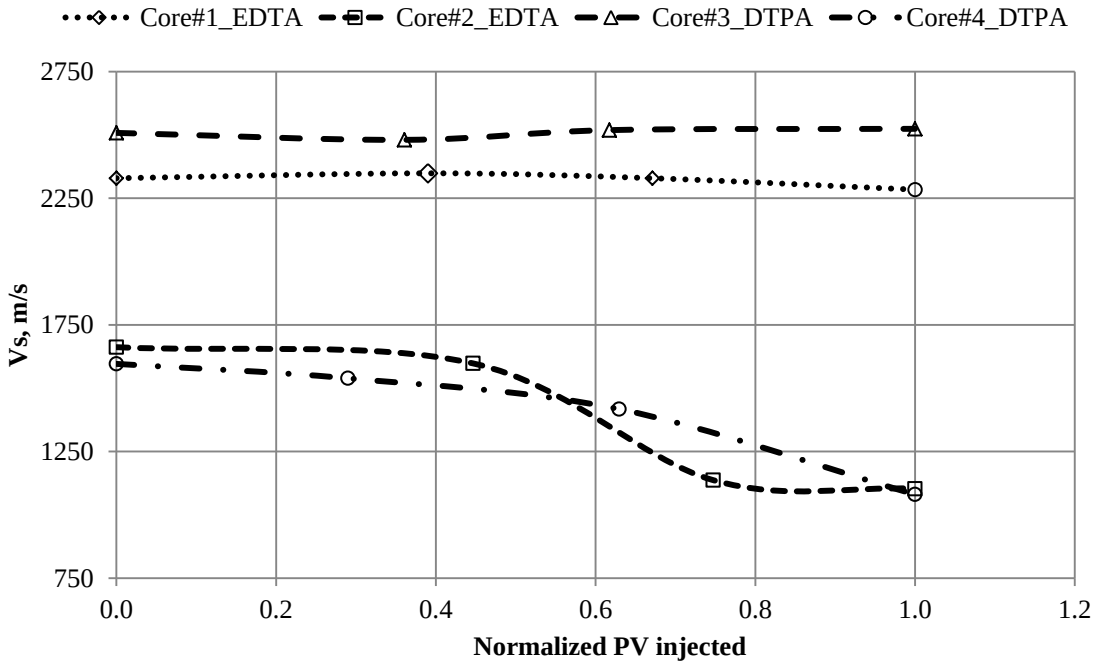

Figure 7.10: Plastic wave velocity changes while injecting EDTA and DTPA chelating agents at temperature of 250°F

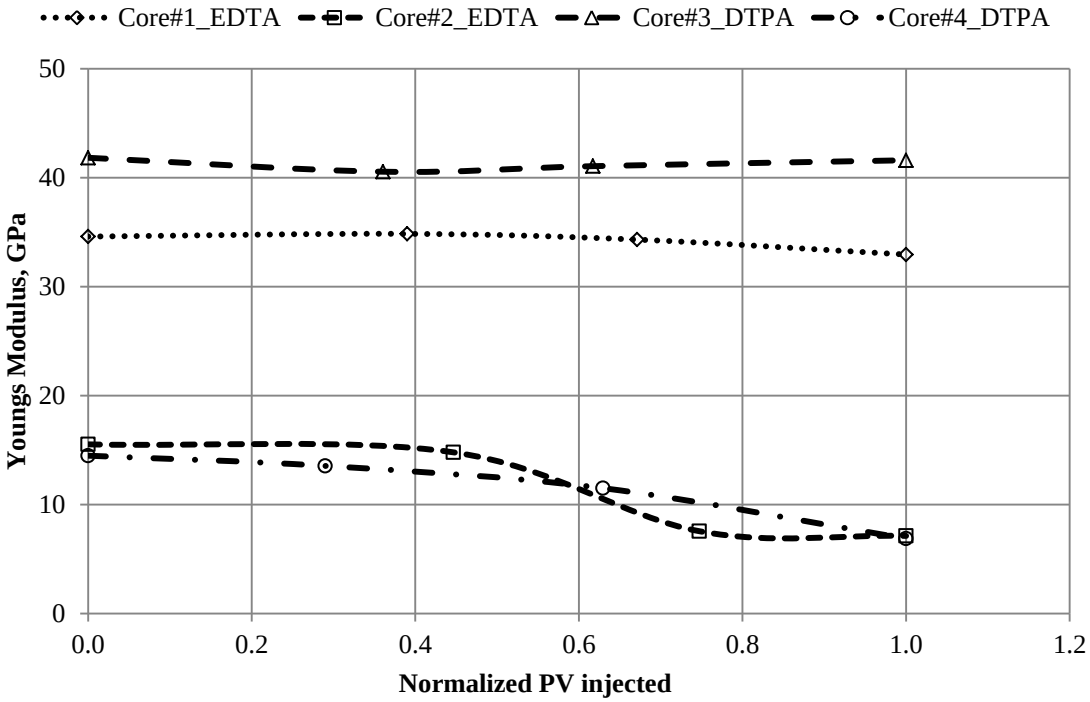

Figure 7.11: Changes in the Young modulus while injecting EDTA and DTPA chelating agents at temperature of 250°F

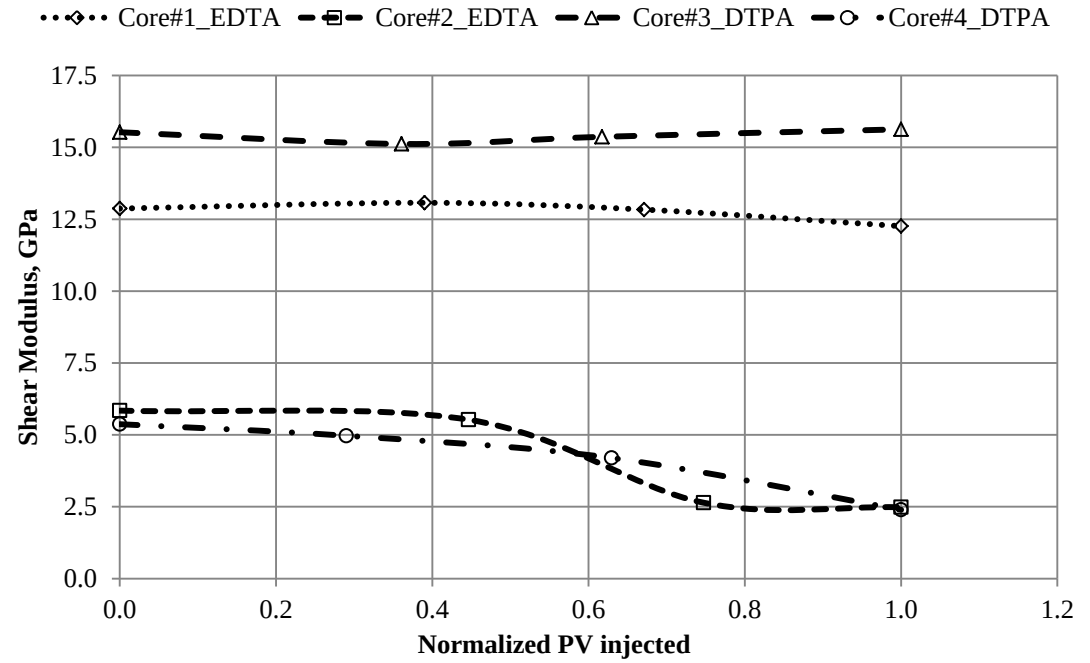

Figure 7.12: Changes in the Shear modulus while injecting EDTA and DTPA chelating agents at temperature of 250°F

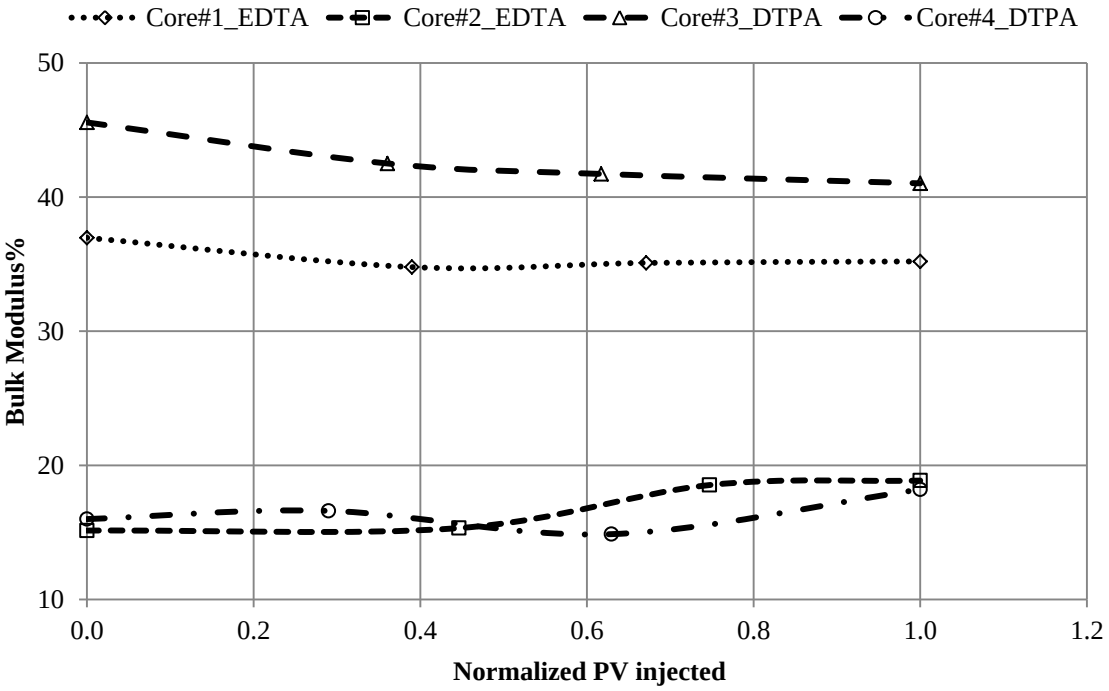

Figure 7.13: Changes in the Bulk modulus while injecting EDTA and DTPA chelating agents at temperature of 250°F

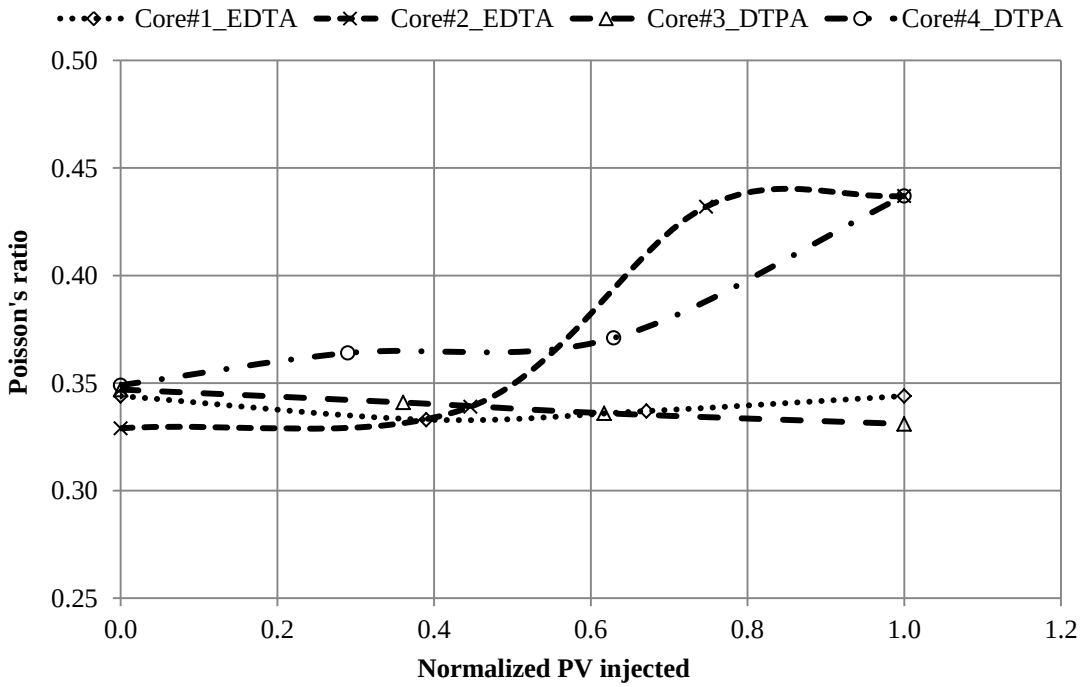

Figure 7.14: Changes in the Poisson's ratio while injecting EDTA and DTPA chelating agents at temperature of 250°F

CHAPTER 8

CONCLUSIONS AND RECOMMEDNATIONS

8.1 Conclusions

Comprehensive matrix stimulation studies using chelating agents were performed. Solubility screening studies were conducted on these chelating agents to investigate their solubilities at different conditions and different pH environments. Matrix stimulation treatments were performed at different conditions and different rock types to determine the optimum conditions for the selected chelating agents. Many laboratory instruments were used throughout this research to achieve the agreed objective. The following conclusions can be drawn from the interpretation of the results of this research:

- Solubility studies showed that DTPA, HEDTA and GLDA chelating agents were soluble at lower pH environment for higher and lower chelant concentrations. In fact the pH of these chelating agents can be decreased to 2.0 or even less without any precipitations. Preparing the chelating solution of any of the above chelating agents by sea water does not affect its solubility.
- EDTA chelating agent was not soluble in all pH at any concentration. As EDTA concentration increases, minimum pH increases to reach about 7.5 for EDTA concentration of 40%. Lower pH of 3.0 was achieved by decreasing EDTA concentration to 3.7%. Preparing EDTA by sea water decreased the solubility of EDTA, and it was found that the minimum pH value was 5.45 at EDTA concentration of 5.0%.

- Studies on HEDTA, DTPA and GLDA chelating agents as well as acetic and citric acids as iron control agents concluded that:
    - None of the studied cheating agents were soluble in 28% wt. HCl acid.
    - HEDTA and GLDA were soluble in 20% HCl acid at concentration of 5.0%, whereas DTPA was soluble at concentration of 7.5% wt.
    - All of the chelating agents have no solubility issues in 15% wt. HCl acid, as they were soluble at concentration as high as 20%.
    - Using sea water instead of deionized water in mixing decreased the solubility of chelating agents in 28% and even 20% HCl acid. In fact none of the studied chelating agents was soluble at HCl concentrations higher than 20% expect DTPA which was soluble in 20% HCl acid at concentration of 2.5%. No solubility issues for the case of 15% HCl. Based on that, it is not recommended to prepare HCl acid by sea water for concentrations higher than 20%.
    - Acetic acid does not have solubility issues in all HCl concentrations up to 28% when prepared by deionized water, as up to 10% acetic acid was mixed by HCl at different concentrations without any solubility issues. For 28% HCl acid prepared by sea water, acetic acid was not soluble at any concentration. For HCl acid concentrations of 20% and less, acetic acid was soluble.
    - Citric acid was soluble in HCl concentrations up to 28% at concentration of 10%. Also citric acid solubility does not affected when HCl acid prepared by sea water.

- No improvement in chelating agents solubility in 28% HCl acid was observed when acetic and citric acids were mixed with the chelant/HCl formulations.
- Adding 5% of DTPA or HEDTA chelating agents to 20% HCl acid managed to keep 3000 ppm of ferric ions in solution at pH up to 4.4, whereas adding 5% of GLDA managed to prevent 3000 ppm ferric ions precipitations for pH up to 2.75 only.
- Adding 2.5%/2.5% of acetic/citric acids managed to prevent ferric ions precipitations for pH up to 4.0.

- Density and viscosity of different chelating agent formulations were measured at different temperatures and pH values. Also the above physical properties were re-measured at different temperatures and pH values after adding specified amount of calcium ions to the chelating agents.
- Surface tension between EDTA, HEDTA and GLDA chelating agents at low pH value and crude oils of different API gravities were measured at room conditions. It was found that surface tension increases with the increase in the chelating agent's concentration and decreases with the increase in the crude oil API gravity. Similar trend was observed for the spent EDTA chelating agent.
- Comprehensive core flooding experiment were conducted using different chelating agents at different concentrations and pH values and different treatment conditions of temperature and injection rates. The following were the main conclusions of these experiments:

- There exist an optimum injection rate between 0.5 and 1.0 cc/m for 4.0 pH 20% HEDTA chelating agent prepared by sea water. This optimum range was confirmed by conducting two sets of treatments at different temperatures. But when taking both the time and volume to breakthrough into consideration, the optimum injection rate lies between 1.5 – 2.0 cc/m.
- Pore volume to breakthrough was increased as the experiment temperature decreased when 4.0 pH 20% HEDTA was used as a stimulation fluid.
- Experiments conducted at different HEDTA concentrations showed that 4.0 pH 10% HEDTA is the optimum HEDTA concentration which resulted in the lowest time and raw HEDTA volume to create the wormholes.
- Sea water did not affect the performance of HEDTA chelating agents as similar results were observed for both HEDTA fluid prepared by deionized water and sea water.
- Studies conducted for EDTA chelating agents showed that solution pH has a significant effect on the stimulation treatment. Low pH EDTA solutions require less amount of stimulation fluid to achieve better stimulation as compared to higher pH solutions.
- 4.5 pH 9.25% EDTA fluid performed better than 10.0 pH 18.5% EDTA fluid in terms of volume to breakthrough. This is mainly due to acidity nature of the first fluid which stimulate by de-protonation and chelation at the same time.

- DTPA chelating agent worked better in alkaline environment rather than acidic environment. This was confirmed by conducting stimulation experiment using DTPA solutions at low and high pH values. The high pH solutions required less amount of stimulation fluid as compared to low pH solutions.
- The optimum DTPA concentration was found to be 10% when taking both the time and volume to breakthrough into considerations.

- Separate stimulation treatments were conducted using EDTA and DTPA chelating agents to investigate the effect of chelating agents on the rock's elastic properties. The following are the mains conclusions of these experiments:
  - A 0.25 M 4.5pH EDTA and DTPA chelating agents were managed to create dominant wormholes for both calcite rock types that are Indiana Limestone ad Austin Chalk. Less than 3.5 PVs of EDTA was consumed to create the wormholes, whereas more than 7.0 PVs of DTPA was required.
  - A noticeable change in rock porosity and saturated density were observed after creating the WH, which is the indication of WH diameter enlargement.
  - Changes of elastic properties of denser calcite rocks such as limestone were negligible as chelating agents created narrow tunnels.
  - Lighter calcite rocks such as chalks demonstrated strong alteration on the elastic properties during injection of EDTA and DTPA chelating agents.
  - Austin Chalk core samples observed changes of rock behavior from elastic to ductile as the stimulation fluid is injected.

- In general, stimulation with chelating agents will not have a severe effect on the rock's mechanical properties in terms of rock strength especially in hard, low permeability rocks; which in turn make chelating agents one of the good stimulation fluids.

8.2 Recommendations

- More studies can be performed to investigate the effect of solution pH on the stimulation treatments for the fluids prepared by sea water.
- Effect of rock properties such as porosity and permeability as well as core length can further be investigated for the stimulation fluids prepared by sea water.
- Effect of chelating agents on the rock's elastic properties can be further investigated at different solution pH and concentrations. Also the effect of the injection rate and experiment's temperature can be assessed.

References

1. Hoefner, M.L., et al., Role of acid diffusion in matrix acidizing of carbonates. Journal of petroleum technology, 1987. **39**(2): p. 203-208.
2. Rae, P. and G. Di Lullo. Matrix acid stimulation-a review of the state-of-the-art. in SPE European Formation Damage Conference. 2003. Society of Petroleum Engineers.
3. Muskat, M., Physical principles of oil production. 1981.
4. Mahmoud, M.A., et al., Optimum Injection Rate of A New Chelate That Can Be Used To Stimulate Carbonate Reservoirs. SPE Journal, 2011. **16**(04): p. 968-980.
5. Maheshwari, P. and V. Balakotaiah. 3D Simulation of Carbonate Acidization with HCl: Comparison with Experiments. in SPE Production and Operations Symposium. 2013. Society of Petroleum Engineers.
6. Metcalf, A., C. Parker, and J. Boles, Acetic acid demonstrates greater carbonate dissolution than typically expected. Journal of Canadian Petroleum Technology, 2005. **44**(12): p. 22-24.
7. Blauch, M., et al. Novel carbonate well production enhancement application for encapsulated acid technology: first-use case history. in SPE Annual Technical Conference and Exhibition. 2003. Society of Petroleum Engineers.
8. Qiu, X., et al. Revisiting Reaction Kinetics and Wormholing Phenomena During Carbonate Acidising. in IPTC 2014: International Petroleum Technology Conference. 2014.
9. Qiu, X., et al. Quantitative Modeling of Acid Wormholing in Carbonates-What Are the Gaps to Bridge. in SPE Middle East Oil and Gas Show and Conference. 2013. Society of Petroleum Engineers.
10. Huang, T., L. Ostensen, and A. Hill. Carbonate matrix acidizing with acetic acid. in SPE international symposium on formation damage control. 2000.
11. Frenier, W., C. Fredd, and F. Chang. Hydroxyaminocarboxylic acids produce superior formulations for matrix stimulation of carbonates at high temperatures. in SPE Annual Technical Conference and Exhibition. 2001. Society of Petroleum Engineers.
12. Fredd, C. and H.S. Fogler, Alternative stimulation fluids and their impact on carbonate acidizing. SPE J, 1998. **13**(1): p. 34.
13. Jacobs, I. Chemical systems for the control of asphaltene sludge during oilwell acidizing treatments. in SPE International Symposium on Oilfield Chemistry. 1989. Society of Petroleum Engineers.
14. Fredd, C. and H. Fogler. Chelating agents as effective matrix stimulation fluids for carbonate formations. in SPE international symposium on oilfield chemistry. 1997.
15. Nasr-El-Din, H., et al. Stimulation of Deep Gas Wells Using HCl/Formic Acid System: Lab Studies and Field Application. in Canadian International Petroleum Conference. 2002. Petroleum Society of Canada.

16. He, J., I.M. Mohamed, and H.A. Nasr-El-Din. Mixing Hydrochloric Acid and Seawater for Matrix Acidizing: Is It a Good Practice? in SPE European Formation Damage Conference. 2011. Society of Petroleum Engineers.
17. Dill, R.W. and B.R. Keeney. Optimizing HCl-Formic Acid Mixtures for High Temperature Stimulation. in SPE Annual Fall Technical Conference and Exhibition. 1978. Society of Petroleum Engineers.
18. Al-Katheeri, M., et al. Determination and Fate of Formic Acid in High Temperature Acid Stimulation Fluids. in International Symposium and Exhibition on Formation Damage Control. 2002. Society of Petroleum Engineers.
19. Buijse, M., et al., Organic acids in carbonate acidizing. SPE production & facilities, 2004. **19**(03): p. 128-134.
20. Chang, F.F., et al. Matrix Acidizing of Carbonate Reservoirs Using Organic Acids and Mixture of HCl and Organic Acids. in SPE Annual Technical Conference and Exhibition. 2008. Society of Petroleum Engineers.
21. Martell, A.E. and M. Calvin, Chemistry of the metal chelate compounds. Soil Science, 1952. **74**(5): p. 403.
22. Furui, K., et al. A comprehensive model of high-rate matrix acid stimulation for long horizontal wells in carbonate reservoirs. in SPE Annual Technical Conference and Exhibition. 2010. Society of Petroleum Engineers.
23. Nasr-El-Din, H., J. Lynn, and K. Taylor. Lab Testing and Field Application of a Large-Scale Acetic Acid-Based Treatment in a Newly Developed Carbonate Reservoir. in SPE International Symposium on Oilfield Chemistry. 2001. Society of Petroleum Engineers.
24. Alkhaldi, M.H., H. Nasr-El-Din, and H.K. Sarma. Application of citric acid in acid stimulation treatments. in Canadian International Petroleum Conference. 2009. Petroleum Society of Canada.
25. Robert, J. and C. Crowe, Carbonate Acidizing Design. Reservoir Stimulation, 2000: p. 17-11.
26. Rabie, A.I., D.C. Shedd, and H.A. Nasr-El-Din, Measuring the Reaction Rate of Lactic Acid with Calcite and Dolomite by Use of the Rotating-Disk Apparatus. SPE Journal, 2014(Preprint).
27. Broaddus, G., Well-and formation-damage removal with nonacid fluids. Journal of petroleum technology, 1988. **40**(06): p. 685-687.
28. Cikes, M., et al., A successful treatment of formation damage caused by high-density brine. SPE Production Engineering, 1990. **5**(02): p. 175-179.
29. Clemmit, A., D. Ballance, and A. Hunton, The dissolution of scales in oilfield systems. Offshore Europe, 1985.
30. Paul, J. and E. Fieler. A new solvent for oilfield scales. in SPE Annual Technical Conference and Exhibition. 1992. Society of Petroleum Engineers.
31. Vetter, O., Oilfield Scale---Can We Handle It? Journal of petroleum technology, 1976. **28**(12): p. 1,402-1,408.
32. Fredd, C.N. and H.S. Fogler, The influence of chelating agents on the kinetics of calcite dissolution. Journal of colloid and interface science, 1998. **204**(1): p. 187-197.

33. Mahmoud, M.A., et al. An Effective Stimulation Fluid for Deep Carbonate Reservoirs: A Core Flood Study. in International Oil and Gas Conference and Exhibition in China. 2010. Society of Petroleum Engineers.
34. Fredd, C. and H. Fogler, Optimum conditions for wormhole formation in carbonate porous media: Influence of transport and reaction. SPE Journal, 1999. **4**(03): p. 196-205.
35. Husen, A., et al., Chelating Agent-Based Fluid for Optimal Stimulation of High-Temperature Wells. Paper SPE 77366 presented at the Annual Technical Conference and Exhibition, San Antonio, Texas, USA, 29 September–2 October, 2002.
36. LePage, J., et al., An Environmentally Friendly Stimulation Fluid for High-Temperature Applications. SPE Journal, 2011. **16**(01): p. 104-110.
37. Mahmoud, M., et al. When Should We Use Chelating Agents in Carbonate Stimulation? in SPE/DGS Saudi Arabia Section Technical Symposium and Exhibition. 2011. Society of Petroleum Engineers.
38. Mahmoud, M.A. and H.A. Nasr-El-Din. Challenges during shallow and deep carbonate resevoirs stimulation. in International Petroleum Technology Conference. 2011. International Petroleum Technology Conference.
39. Mahmoud, M.A. and H.A. Nasr-El-Din. Modeling of the Flow of Chelating Agents in Porous Media in Carbonate Reservoirs Stimulation. in North Africa Technical Conference and Exhibition. 2012. Society of Petroleum Engineers.
40. Mahmoud, M.A., et al. Effect of lithology on the flow of chelating agents in porous media during matrix acid treatments. in SPE Production and Operations Symposium. 2011. Society of Petroleum Engineers.
41. Eberli, G.P., et al., Factors controlling elastic properties in carbonate sediments and rocks. The Leading Edge, 2003. **22**(7): p. 654-660.
42. Sokhanvarian, K., et al. Thermal Stability of Various Chelates That Are Used In The Oilfield And Potential Damage Due To Their Decomposition Products. in SPE International Production and Operations Conference & Exhibition. 2012. Society of Petroleum Engineers.
43. Wang, Y., A. Hill, and R. Schechter. The optimum injection rate for matrix acidizing of carbonate formations. in SPE Annual Technical Conference and Exhibition. 1993. Society of Petroleum Engineers.
44. Brandås, L.T., Relating acoustic wave velocities to formation mechanical properties. 2012.
45. Fjar, E., et al., Petroleum related rock mechanics. Vol. 53. 2008: Elsevier.
46. Mokhtar, E.A., et al. Rock Physics Characterization Using Acoustic Velocity Measurements On Late Cretaceous Carbonate Rocks From the Middle East. in Abu Dhabi International Petroleum Exhibition and Conference. 2010. Society of Petroleum Engineers.
47. Nguyen, M., E. Bemer, and L. Dormieux. Micromechanical modeling of carbonate geomechanical properties evolution during acid gas injection. in 45th US Rock Mechanics/Geomechanics Symposium. 2011. American Rock Mechanics Association.

48. Li, L., et al. Reaction of Simple Organic Acids and Chelating Agents with Calcite. in International Petroleum Technology Conference. 2008. International Petroleum Technology Conference.
49. Gong, M. and A. El-Rabaa, Quantitative model of wormholing process in carbonate acidizing. paper SPE, 1999. **52165**.
50. Huang, T., D. Zhu, and A. Hill, Prediction of Wormhole Population Density in Carbonate Matrix Acidizing. Paper SPE 54723 presented at the SPE European Formation Damage Conference, The Hague, 31 May–1 June, 1999.
51. Hung, K., A. Hill, and K. Sepehrnoori, A Mechanistic Model of Wormhole Growth in Carbonate Matrix Acidizing and Acid Fracturing. JPT 41 (1): 59-66. Trans., AIME, 1989. **287**.
52. Panga, M.K., et al. A new model for predicting wormhole structure and formation in acid stimulation of carbonates. in SPE International Symposium and Exhibition on Formation Damage Control. 2004. Society of Petroleum Engineers.
53. Mahmoud, M. and H. Nasr-El-Din, Modeling Flow of Chelating Agents During Stimulation of Carbonate Reservoirs. Arabian Journal for Science and Engineering, 2014. **39**(12): p. 9239-9248.
54. Assem, A., H. Nasr-El-Din, and A. De Wolf. Formation Damage Due To Iron Precipitation In Carbonate Rocks. in SPE European Formation Damage Conference & Exhibition. 2013. Society of Petroleum Engineers.
55. Dill, W. and P. Smolarchuk, Iron control in fracturing and acidizing operations. Journal of Canadian Petroleum Technology, 1988. **27**(03).
56. Taylor, K.C., H. Nasr-El-Din, and M. Al-Alawi, Systematic study of iron control chemicals used during well stimulation. SPE Journal, 1999. **4**(01): p. 19-24.
57. Walker, M.L., W.R. Dill, and M.R. Besler, Iron Control Provides Sustained Production Increase in Wells Containing Sour Gas. Journal of Canadian Petroleum Technology, 1990. **29**(06).
58. Crowe, C., Evaluation of agents for preventing precipitation of ferric hydroxide from spent treating acid. Journal of petroleum technology, 1985. **37**(04): p. 691-695.
59. Legemah, M., et al. Successful Acidizing Treatment of Four Offshore Wells with High Bottomhole Temperatures in Mobile Bay, Gulf of Mexico: Laboratory and Field Case Studies. in SPE Annual Technical Conference and Exhibition. 2014. Society of Petroleum Engineers.
60. Taylor, K., et al., Laboratory evaluation of iron-control chemicals for high-temperature sour-gas wells. Paper No. SPE65010, 2001.
61. BE, H., Iron Control Additives for Limestone and Sandstone Sweet and Sour Wells. 1988.
62. Dabbousi, B., H. Nasr-El-Din, and A. Al-Muhaish. Influence of oilfield chemicals on the surface tension of stimulating fluids. in Paper SPE 50732, Presented at the 1999 SPE International Symposium on Oilfield Chemistry Held in Houston, Texas, February. 1999.

Vitae

Name	:Assad Ahmed Abdallah Barri
Nationality	:Sudanese
Date of Birth	:11/27/1979
Email	:assadbarri@hotmail.com
Address	:KFUPM-Petroleum Engineering Department
Academic Background	:Petroleum Engineer
Publications	:SPE-172194 paper presented in SPE SAS in 2015
	:SPE-172709 paper presented in SPE MEOS in 2015
Patents	:USPTO, serial number 14/174467